5153

Babcock & Wilcox

MAGNESIA BASE WET SCRUBBING OF PULVERIZED COAL GENERATED FLUE GAS - PILOT DEMONSTRATION

RESEARCH AND DEVELOPMENT DIVISION
RESEARCH CENTER ALLIANCE, OHIO

MAGNESIA BASE WET SCRUBBING OF PULVERIZED COAL GENERATED FLUE GAS - PILOT DEMONSTRATION

PROJECT SPONSORED BY NATIONAL AIR POLLUTION CONTROL ADMINISTRATION

ORDER 4152-01

RESEARCH CENTER REPORT 5153

BY: W. DOWNS

A. J. KUBASCO

SEPTEMBER 28, 1970

THE BABCOCK & WILCOX COMPANY
RESEARCH AND DEVELOPMENT DIVISION
RESEARCH CENTER
ALLIANCE, OHIO

COPY NO. 93

THE BABCOCK & WILCOX COMPANY
RESEARCH AND DEVELOPMENT DIVISION
RESEARCH CENTER
ALLIANCE, OHIO

MAGNESIA BASE WET SCRUBBING OF PULVERIZED COAL GENERATED FLUE GAS - PILOT DEMONSTRATION

By: W. Downs
A. J. Kubasco

ABSTRACT

Purpose

The purpose of this project was to demonstrate the adequacy of magnesia base wet scrubbing to remove essentially all of the particulates (99^+%) and most of the sulfur dioxide (97^+%) from pulverized coal fired furnaces. Side effects such as sulfate formation, NO_x absorption, and scrubber operability were to be determined.

Summary

A wet scrubbing pilot plant consisting of three scrubbers was designed and constructed. An existing test furnace was modified to burn pulverized coal at a rate of 500 pounds per hour. These three scrubbers consisted of a venturi-type particulate scrubber, a venturi-type absorber, and a tray-type absorber (floating bed absorber). Over 100 short-term tests were performed to determine the most satisfactory operating conditions for each scrubber. Following this, several extended tests were performed.

Results

Sulfur dioxide absorption in the floating bed absorber was a maximum at about 99.2% at 6.5 inches w.g. The venturi absorber performed at 95.5% for the same pressure drop. SO_2 absorption in both absorbers was sensitive to slurry composition including pH and sulfate concentration. For an average 7 inches w.g. pressure drop, the particulate scrubber collected 99.5^+%, the venturi absorber 99.1%, and the floating bed absorber 97.7% of the fly ash. Sulfate formation averaged between 4 and 8% of the absorbed SO_2 in both absorbers. Deposition of $MgSO_3 \cdot 6H_2O$ in the piping was prevalent under some operating conditions but did not form when fly ash was present in the absorber slurry.

Conclusions

The magnesia base wet scrubbing process has been demonstrated to be superior to other wet processes known to be under development for abatement of both particulates and SO_2 from coal-fired furnaces. The process as demonstrated is compatible with the B&W regeneration concept.

Research Center Report 5153
Order 4152-01
September 28, 1970
Magnesia Base Wet Scrubbing
Project Sponsored by National Air
Pollution Control Administration

ABSTRACT (Cont'd)

Recommendations

A regeneration facility should be added to the present pilot plant to demonstrate its capability to regenerate magnesia for reuse and to produce a usable sulfur product.

SUMMARY

The magnesia base wet scrubbing and regeneration process offers a potential solution to the problem of sulfur and particulate pollution from large stationary sources. This process is illustrated in simplest form as:

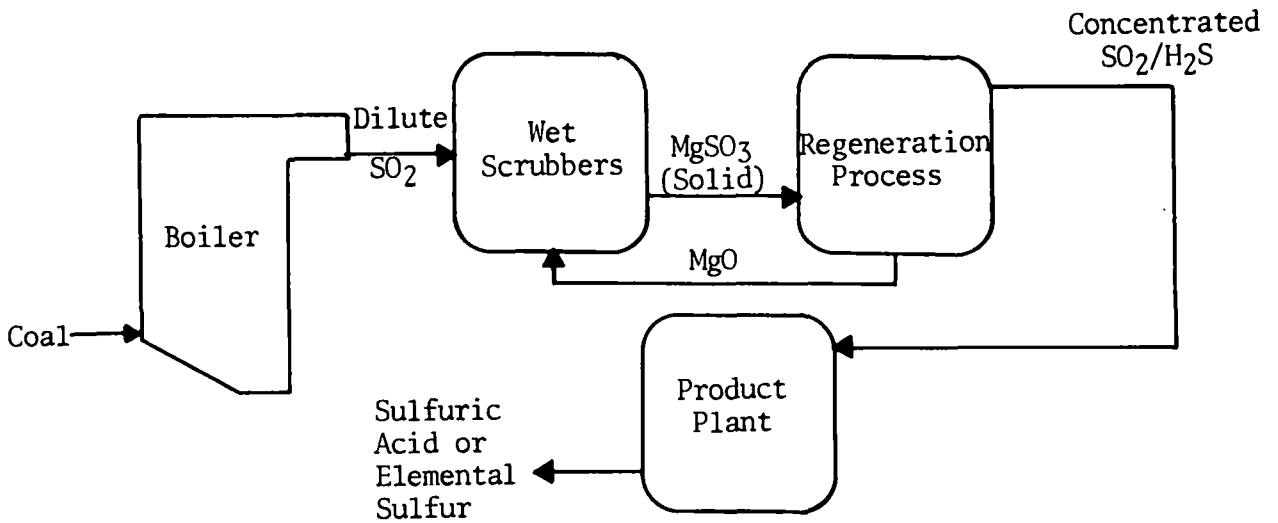

As a first step in the evaluation of this process, the National Air Pollution Control Administration has sponsored the subject project for a demonstration of the wet scrubbing of pulverized coal generated flue gas with a magnesia base slurry. Regeneration of the products was not included. This work sponsored under contract CPA 22-69-162 called for the fabrication of a wet scrubbing pilot plant behind an existing pilot-scale fossil fuel burning facility. The furnace, which was designed for burning gas, oil, and special waste liquors, was converted to accommodate pulverized coal. This coal was prepared and stored in existing facilities. The furnace burns approximately 500 pounds of coal per hour, which is roughly the firing rate of a 1/2 megawatt (electrical) power boiler.

The wet scrubbing pilot plant handled all of the flue gas from the furnace (5400 pounds/hour). This plant included a venturi-type fly ash scrubber, two gas absorbers (a venturi type and a tray type), chemical makeup and disposal systems, and auxiliary piping and pumps.

The test specifications called for an investigation of the following parameters:

SO_2 absorption as a function of absorber type, chemical composition of the spray slurry, chemical composition of the makeup slurry, sump residence time, and sulfate level.

Sulfate formation rate as a function of furnace excess air, scrubber arrangement, and combustion air temperature.

Particulate collection in all three scrubbers.

NO_x absorption in all three scrubbers under normal and special conditions.

SO_3 formation as a function of furnace operation.

In addition to the above parameters, deposition and the means for its prevention or reduction became an integral part of this program.

The test program was divided into two phases: parameter studies and extended tests for as long as 4 days. Over 200 tests, of which about 1/3 were short-term parameter studies, were performed. The results demonstrated that this wet scrubbing process is capable of removing 99^+% of both particulates and sulfur dioxide from the flue gas. The maximum sulfation rate was shown to be less than 8% at 15% excess air, and it was also shown that deposition can be prevented by proper design and operation.

SO_2 absorption in the floating bed absorber (FBA) was found to be superior to that in the venturi absorber for comparable energy levels. In the FBA only, SO_2 absorption increased substantially with increasing liquid flow rate and increasing pH up to about 7.0. At lower pH's, and at high sulfate concentrations in the absorbing slurry, the SO_2 absorption was adversely affected in both absorbers. The presence of fly ash in the absorbing slurry had no adverse effects upon SO_2 absorption.

Sulfate formation was found to be a function of furnace excess air. The presence of fly ash in the absorbing slurry contributed substantially to the sulfate formation rate. The floating bed absorber and venturi absorber were not substantially different in their sulfate formation rates.

Deposition of magnesium sulfite was a recurring problem. This deposition was believed to result from the neutralization reaction between bisulfite and magnesia. Temperature cycling of the scrubbing slurry was also found to contribute

to this deposition. The deposition was prevented by fly ash in the slurry. Nonwettable materials also reduced the tendency to receive deposits.

Deposition at the wet-dry line in the gas-liquid contacting zone was not a problem in the particulate scrubber under any condition and was not a problem in the gas absorbers when the gas was first attemperated by the particulate scrubber. However, deposition at that point was severe when the gas absorbers were in direct contact with the hot furnace gases. Evidently, deposition occurs only if the spray slurry contains solubles which plate out upon evaporation.

Particulate collection of furnace exit flue gas was excellent in all three scrubbers. Amongst these, the particulate scrubber was best, and the floating bed absorber was least effective. Neither absorber, however, collected a measurable quantity of fly ash leaving the particulate scrubber. Evidently, this fly ash was much too fine to be collected by the relatively low energy absorbers.

Absorption of oxides of nitrogen was negligible across all three scrubbers under all operating conditions tested. Injection Of NO_2 into the gas stream was designed to promote total NO_x absorption. However, injection did not increase NO_x absorption. In fact, it significantly increased the sulfate formation rate.

With proper design and operation, this wet scrubbing process will remove both dust and sulfur gases more effectively than most systems presently proposed.

TABLE OF CONTENTS

		Page
1.0	INTRODUCTION	1-1
2.0	PILOT PLANT EQUIPMENT	2-1
2.1	Pulverizer	2-2
2.2	Coal Separation Apparatus and Bunker	2-2
2.3	Coal Feed System	2-3
2.4	Burner and Furnace	2-4
2.5	Fuel	2-7
2.6	Wet Scrubbing Apparatus	2-8
2.6.1	Particulate Scrubbing System	2-8
2.6.2	Venturi Absorber System	2-11
2.6.3	Floating Bed Absorber	2-12
2.7	Flue Gas Exhaust Section	2-14
2.8	Pilot Plant Monitoring System	2-14
2.9	MgO Makeup and Product Disposal	2-14
2.10	Chemical Analysis Lab	2-16
2.11	Overall Pilot Plant Schematic	2-16
3.0	TEST APPARATUS AND PROCEDURES	3-1
3.1	Test Procedure for 1-Day Operation	3-1
3.2	Test Procedure for Extended Operation	3-2
3.3	Special Tests	3-2
3.3.1	High Sulfate Concentration Tests	3-2
3.3.2	NO_X Absorption Tests	3-2
3.4	Sulfur Dioxide Sampling and Analysis	3-3
3.4.1	Barton Titrator	3-3
3.4.2	Reich Method for SO_2 Analysis	3-5
3.5	Sulfur Trioxide Sampling	3-6
3.6	NO_X Sampling and Analysis	3-7
3.7	Dust Loading	3-8
3.8	Cascade Impactor	3-10
3.9	Orsat Analyzer	3-11
3.10	Magnesium Sulfite-Bisulfite Analysis	3-11
3.11	Sulfate Analysis	3-12
3.11.1	Titration Method	3-12
3.11.2	Sulfate Sample for Chemistry Lab Analysis	3-13
3.12	Particulate Solids Sampling	3-13
3.13	Magnesium Sulfite Solids Sampling	3-14
3.14	MgO Makeup Slurry Titration	3-14
3.15	Other Measurements	3-15

TABLE OF CONTENTS CONT'D

		Page
4.0	RESULTS	4-1
4.1	SO_2 Absorption - Particulate Scrubber	4-1
4.2	SO_2 Absorption - Floating Bed Absorber	4-1
4.2.1	Parameter Study	4-1
4.2.2	Floating Bed Absorber - Absorption Correlation	4-2
4.3	SO_2 Absorption - Venturi Absorber	4-4
4.3.1	Parameter Study	4-4
4.3.2	Venturi Absorber Absorption Correlations	4-5
4.4	Crystalline Deposition	4-7
4.4.1	Parameters Affecting Deposition	4-8
4.5	Deposition at Wet-Dry Lines	4-10
4.6	Sulfate Formation	4-11
4.6.1	Floating Bed Absorber	4-11
4.6.2	Venturi Absorber	4-12
4.7	Particulate Collection	4-13
4.7.1	Particulate Venturi Scrubber	4-13
4.7.2	Floating Bed Absorber With Prescrubber	4-14
4.7.3	Floating Bed Absorber Without Prescrubber	4-14
4.7.4	Venturi Absorber With Prescrubber	4-15
4.7.5	Venturi Absorber Without Prescrubber	4-16
4.8	NO_x Absorption	4-16
4.9	NO_x Injection Test	4-17
4.10	SO_3 Formation	4-17
4.11	The Floating Bed Absorber Tray Hydraulics	4-18
5.0	DISCUSSION OF RESULTS	5-1
5.1	Data Analysis	5-1
5.2	Error Analysis	5-1
5.3	SO_2 Absorption	5-1
5.3.1	Comparison Between Absorbers	5-1
5.3.2	Mathematical Models of SO_2 Absorption	5-2
5.3.3	SO_2 Vapor Pressure from Literature	5-6
5.3.4	Effect of Sulfates Upon SO_2 Absorption	5-6
5.3.5	Comparison of Absorber Performance with Literature	5-7
5.4	Chemistry of Absorbing Slurry	5-8
5.5	Deposition	5-11
5.5.1	Deposition Mechanisms	5-11
5.5.2	Method of Deposit Elimination	5-15
5.6	Sulfate Formation	5-15
5.7	NO_x Absorption	5-18

TABLE OF CONTENTS CONT'D

	Page
6.0 CONCLUSIONS	6-1
6.1 SO_2 Absorption	6-1
6.2 Sulfate Formation	6-1
6.3 Deposition Within Absorber	6-2
6.4 Others	6-2
7.0 RECOMMENDATIONS	7-1
7.1 Particulate Scrubber Operation and Design	7-1
7.2 SO_2 Absorber Operation and Design	7-1
7.3 Future Work	7-1
8.0 ACKNOWLEDGEMENTS	8-1
REFERENCES	R-1
APPENDIX A, DETAILS OF ANALYSIS TECHNIQUES	A-1
A.1 Sulfur Dioxide Sampling	A-1
A.2 SO_3 Sampling Apparatus & Procedure	A-5
A.3 Dust Loading Apparatus and Procedure	A-10
A.4 Modified Palmrose Analysis	A-12
A.5 Determination of Sulfate Ion in $Mg\text{-}SO_2\text{-}H_2O$ System	A-15
A.6 Particulate Solids Apparatus and Procedure	A-19
A.7 MgO Makeup Slurry Titration Procedure	A-19
A.8 Magnesia Hydration Analysis	A-20
APPENDIX B, CORRELATION COEFFICIENTS	B-1
APPENDIX C, ERROR ANALYSIS	C-1
C.1 General Technique	C-1
C.2 Gas Sampling Errors	C-2
C.3 Chemical Analysis Errors - Liquid	C-11
C.4 Flow Rate Error Analysis	C-14
C.5 Material Balances	C-19

List of Tables

Table		
2.1	Pulverized Coal and Gas Analysis	2-8
4.1	MgO Conversion to $Mg(OH)_2$	4-4
4.2	X-Ray Diffraction Analysis of Crystalline Deposits	4-8
4.3	Degree of Deposition at Various Locations During Periods of Rapid Formation	4-10

TABLE OF CONTENTS CONT'D

List of Tables Cont'd

		Page
4.4	Average Sulfate Formation in FBA for Individual Test Series	4-12
4.5	Average Sulfate Formation in Venturi Absorber for Individual Test Series	4-13
4.6	Particulate Collection Performance of Particulate Scrubber	4-15
4.7	Particulate Collection Across FBA With Prescrubber	4-16
4.8	Particulate Collection Across FBA Without Prescrubber	4-16
4.9	Particulate Collection Across Venturi Absorber With Prescrubber	4-17
4.10	Particulate Collection in Venturi Absorber (Without Prescrubber)	4-17
4.11	Average NO_x Concentrations Throughout Pilot Plant	4-18
4.12	Summary of NO_x Results	4-18
4.13	NO_2 Injection Test Results	4-18
4.14	Sulfur Trioxide Concentration at Furnace Exit	4-19
4.15	Effect of Bed Height on Dry Pressure Drop Across FBA	4-19
4.16	FBA Packing Attrition After 270 Hours	4-19

List of Figures

Figure		
2.1	Magnesia Base Wet Scrubbing Pilot Plant	2-1
2.2	Coal Pulverizer	2-2
2.3	Coal Handling System	2-2
2.4	Coal Storage Facilities	2-3
2.5	Pulverized Coal Sizing Plot	2-3
2.6	Coal Screw Feeder	2-4
2.7	Coal Screw Feeder	2-4
2.8	Pulverized Coal Burner	2-5
2.9	Pulverized Coal Burner	2-5
2.10	Basic Combustion Test Furnace	2-6
2.11	Furnace Sectional View	2-6
2.12	Furnace Relief Valve - Open Position	2-6
2.13	Furnace Relief Valve - Closed Position	2-6
2.14	Steam Lances	2-7
2.15	Furnace Control Panel	2-7

TABLE OF CONTENTS COND'D

List of Figures Cont'd

		Page
2.16	Particulate Scrubbing System	2-8
2.17	Particulate Scrubbing System	2-9
2.18	Particulate System Dimensions	2-9
2.19	Product Discharge Nozzle	2-10
2.20	Venturi Absorber Flow Control System	2-10
2.21	Venturi Absorber System	2-11
2.22	Venturi Absorber System Dimensions	2-11
2.23	Floating Bed Absorber	2-12
2.24	Floating Bed Absorber	2-12
2.25	Plastic "Wiffle" Balls Deformed	2-13
2.26	Floating Bed Absorber Dimensions	2-13
2.27	Top of Floating Bed Absorber	2-14
2.28	Moisture Disengagement Region - Sectional View	2-14
2.29	Measurement Locations	2-15
2.30	Makeup System	2-15
2.31	Product Disposal Leach Beds	2-16
2.32	Pilot Plant Analysis Lab	2-16
2.33	Schematic Arrangement of Test Facilities	2-17
3.1	NO_2 Injection Apparatus	3-3
3.2	SO_2 Sampling System	3-3
3.3	Barton Titrators	3-4
3.4	Barton Electrical Circuit	3-5
3.5	Reich Board	3-5
3.6	SO_3 Collection Apparatus	3-6
3.7	SO_3 Collection Apparatus	3-6
3.8	Particulate Sampling Nozzle	3-8
3.9	Particulate Sampling Apparatus	3-8
3.10	Particulate Sampling Apparatus	3-9
3.11	Thorston Dust Sampler	3-9
3.12	Cascade Impactor	3-10
3.13	Impactor Stage	3-10
3.14	Orsat Apparatus	3-11
3.15	Syringe Filter Holder	3-12
3.16	Syringe in Septum	3-12

TABLE OF CONTENTS CONT'D

List of Figures Cont'd

		Page
3.17	Palmrose Titration Apparatus	3-13
3.18	Sulfate Sample Preparation Apparatus	3-13
3.19	Sulfate Titration Apparatus	3-14
3-20	MgO Makeup Titration Curve	3-14
4.1	SO_2 Absorption - FBA	4-2
4.2	SO_2 Absorption - FBA	4-2
4.3	Correlation for Equation 4-1, SO_2 Absorption - FBA	4-3
4.4	Pressure Drop - FBA	4-3
4.5	SO_2 Absorption - FBA Without Prescrubber	4-4
4.6	Comparison of Effect of High Sulfates Upon SO_2 Absorption - FBA	4-4
4.7	SO_2 Absorption - Venturi Absorber	4-5
4.8	SO_2 Absorption - Venturi Absorber	4-6
4.9	Pressure Drop Effect Upon SO_2 Absorption - Venturi Absorber	4-6
4.10	SO_2 Absorption Correlation for Venturi Absorber	4-7
4.11	Comparison of Effect of High Sulfates Upon SO_2 Absorption - Venturi Absorber	4-7
4.12	The Effect of Fly Ash Upon Deposits Formation	4-8
4.13	Particulate Scrubber - Inside View	4-10
4.14	Sulfate Formation - FBA With Prescrubber	4-11
4.15	Sulfate Formation - FBA Without Prescrubber	4-11
4.16	Sulfate Formation - Venturi Absorber With Prescrubber	4-12
4.17	Sulfate Formation - Venturi Absorber Without Prescrubber	4-13
4.18	Dust Collection Performance Particulate Scrubber	4-14
4.19	Dust Collection Performance Particulate Scrubber	4-14
4.20	Pressure Drop - Particulate Scrubber	4-15
4.21	Dust Collection Performance - FBA	4-16
4.22	Dust Collection Performance - Venturi Absorber	4-17
5.1	Computer Results	5-1
5.2	Comparison of SO_2 Absorption in the Venturi Absorber With Literature	5-8
5.3	Solubility of Magnesium Sulfite	5-10
5.4	Relationship Between Bisulfite Concentration and Slurry pH	5-10
5.5	Example of Coarse Deposit	5-11
5.6	Equilibrium Constants for NO_x-SO_x-H_2O Systems	5-19
5.7	SO_2-NO_x Absorption Process	5-20

TABLE OF CONTENTS CONT'D

List of Figures Cont'd

		Page
A.1	Spinning Syringe Apparatus	A-3
A.2	SO_3 Collector	A-5
C.1	Barton SO_2 Analysis Error Potential	C-3
C.2	Comparison Between Barton and Reich Methods	C-4
C.3	Velocity Profile Downstream of Flow Straightener	C-11
C.4	Maximum Probable Error in Palmrose Analysis	C-12
C.5	Comparison of Slurry Strength by Two Techniques	C-12
C.6	Comparison Between Gravimetric and Titrametric Sulfate Analyses	C-13
C.7	Flue Gas Material Balance	C-17
C.8	Sulfur Material Balance	C-20

NOMENCLATURE

Test Series	Purpose	Dates
A-xxx	Final Shakedown Tests	11/18/69-12/5/69
B-xxx	Parameter Study, Particulate Scrubber and Venturi Absorber, Faulty Gas Analysis	12/4/69-12/9/69
C-xxx	Parameter Study, Particulate Scrubber and Venturi Absorber	12/12/69-12/19/69
D-xxx	Parameter Study, Particulate Scrubber and Floating Bed Absorber	1/9/70-1/26/70
E-xxx	Parameter Study, Particulate Scrubber and Venturi Absorber	2/2/70-2/6/70
F-xxx	Extended Test, Particulate Scrubber and Venturi Absorber	3/9/70-3/10/70
G-xxx	Parameter Study, Particulate Scrubber and Venturi Absorber, Elevated Sulfates	3/18/70
H-xxx	Extended Test, Particulate Scrubber and Venturi Absorber	3/23/70-3/24/70
I-xxx	Extended Test, Particulate Scrubber and Venturi Absorber	3/31/70-4/2/70
J-xxx	Extended Test, Venturi Absorber Only (Particulate Scrubber Bypassed)	4/14/70-4/16/70
K-xxx	NO_2 Injection Tests	4/9/70
L-xxx	Extended Test, Particulate Scrubber and Floating Bed Absorber	4/27/70-4/30/70
M-xxx	Extended Test, Floating Bed Absorber Only, (Particulate Scrubber Bypassed)	5/12/70-5/15/70
N-xxx	Parameter Study, Particulate Scrubber and Floating Bed Absorber, Elevated Sulfates	5/27/70
O-xxx	Parameter Study, Particulate Scrubber and Floating Bed Absorber, Elevated Sulfates	7/21/70

1.0 INTRODUCTION

Abatement of pollution from large stationary sources such as power plants is a primary goal of government, industry, and an aroused public. However, the magnitude of this abatement task is reflected by the huge disposal problem with which the power industry is confronted. For example, an 800 MW power plant burning pulverized coal, which produces electricity for roughly one million people, creates the following yearly emissions: 65 billion pounds of combustion gases, of which about 15% can be considered alien to the atmosphere, 635 million pounds of solid noncombustibles (fly ash), and 36,500 billion Btu of waste heat. In a conventional boiler cycle, the carbon dioxide emissions and the waste heat are not amenable to treatment. The fly ash disposal is presently accomplished through landfill. The major emissions which constitute an immediate hazard include the oxides of sulfur and the oxides of nitrogen. These emissions presently are being discharged to the atmosphere with only minor treatment. From the above 800 MW power plant sulfur dioxide is emitted at a rate of 300 million pounds per year (based on 3% sulfur coal) and nitric oxide (assuming 1000 ppm at the stack) amounts to 65 million pounds per year. To put the sulfur dioxide emission in perspective, the rate of sulfur emission per customer serviced by this power plant is roughly three times the per capita rate of sulfur mined in the United States.

The major problem in removing sulfur dioxide from flue gases is not the technical problem of sulfur dioxide absorption or adsorption itself but is how to do this economically without adversely affecting the business of electric power production. Handling the volumes of flue gases required by standard chemical engineering unit operations such as fixed bed reactors or spray absorption towers constitutes a completely new engineering problem. Thus, a primary task of the Division of Process Control Engineering of the National Air Pollution Control Administration, under which this contract was sponsored, has been to investigate a broad range of research and development processes potentially amenable to this problem.

Wet scrubbing of flue gases by various aqueous absorbents capable of reacting with SO_2 has been one of the most vigorously investigated approaches. The obvious technical advantage of wet scrubbing is the well-established unit operation of particulate collection and gas absorption by aqueous sprays.

The most widely applied wet process has been the calcium base or limestone process. This is technically simple and cheapest to install among potential wet processes. However, this nonregenerative process has two liabilities that make other wet processes such as magnesia more attractive. First, no sulfur products can be produced to defray the cost of the process, and secondly, the solid disposal load is more than doubled.

The B&W Magnesia Base Wet Scrubbing and Regeneration Process has the potential of avoiding both of the above liabilities. Obviously, in order to justify a regeneration plant, the production cost of the sulfur product must be less than the saleable price of that product. Secondly, the regenerated magnesia must be reusable because it is expensive compared to limestone and its disposal would constitute a pollution problem itself. Without a regeneration process, however, magnesia has no economic validity in spite of any potential technical advantages from a wet scrubbing standpoint.

The object of this contract was to demonstrate the capability of only the wet scrubbing portion of the magnesia base system on pulverized coal generated flue gas. The technical program was based upon no specific regeneration process. Potential interactions between the wet scrubbing and regeneration steps were not explicitly investigated. The major technical areas studied were:

SO_2 Absorption
Sulfate Formation
Deposition
Particulate Collection

All of these except deposition were in the original plan. Solution of the deposition problem was, however, an absolute necessity.

The following pages report the results of over 200 tests under this contract, CPA-22-69-162.

2.0 PILOT PLANT EQUIPMENT

Tests were carried out on a pilot plant using a 1/2-megawatt (electrical) pulverized coal-burning furnace to generate flue gas. A water tube section was used to cool the gases to a temperature typical of a boiler stack gases.

The coal handling facilities included a pulverizer, dilute phase transport system, and a coal storage bunker. The pulverized coal-burning furnace was part of an existing combustion test as were the coal handling facilities. The gas cleanup equipment consisted of a particulate scrubber venturi, a venturi absorber, and a floating bed absorber; the latter two absorbers were used for sulfur dioxide removal. This section covers a general description of the pilot plant equipment and related facilities. A pictorial drawing of the pilot plant showing equipment layout is shown in Figure 2.1.

FIGURE 2.1 MAGNESIA BASE WET SCRUBBING PILOT PLANT

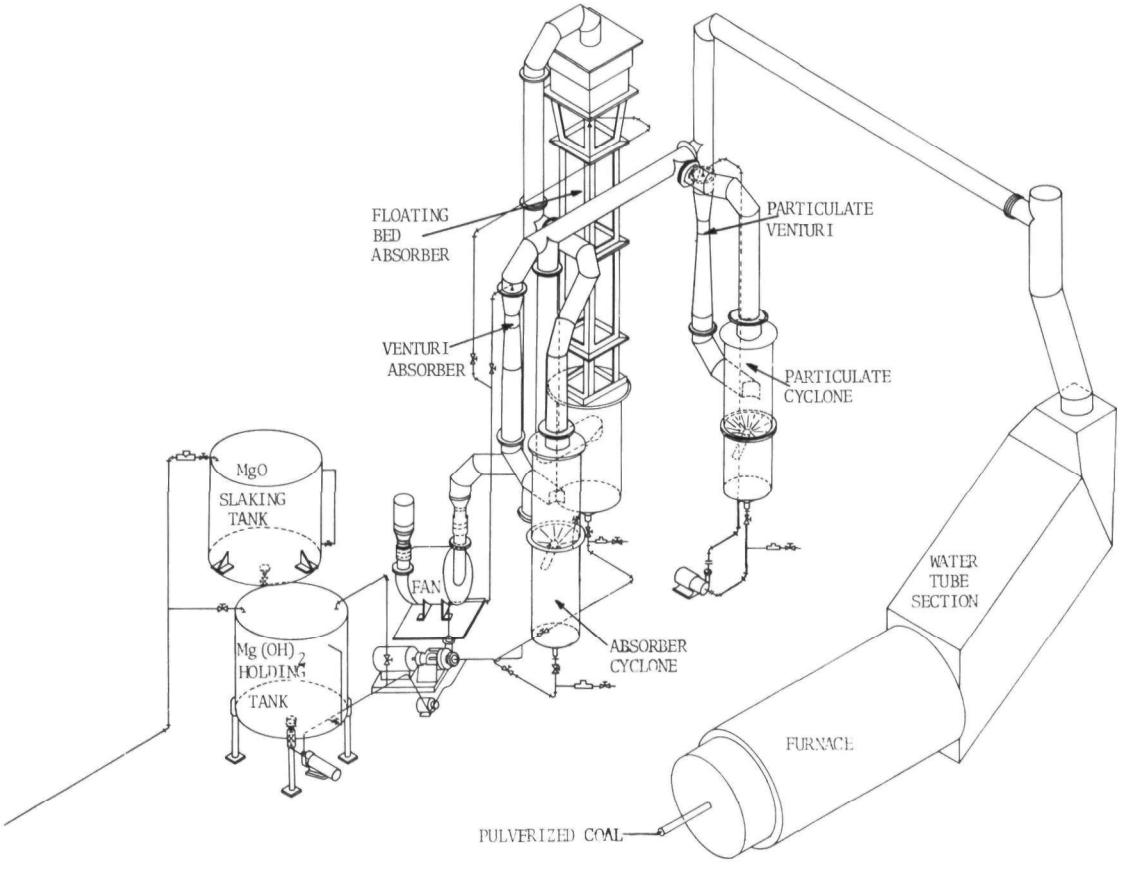

2.1 PULVERIZER

The coal pulverizer, Figure 2.2, is a B&W B 200 Series with a maximum capacity of about 10 tons/hr. This is a double row ball-and-race pulverizer where an intermediate revolving grinding ring is interposed with two sets of balls between the races of two stationary rings. Raw coal is fed inside the grinding ring. As it passes through the top row of balls, the coal is partially pulverized. The coarse particles fall behind the lower row of balls and are further pulverized. A primary air blower supplies heated air, which entrains, dries, and carries the coal over to the separation and storage facility. The coal is transported by dilute phase with 1 pound of coal requiring about 1-1/2 pounds of air.

FIGURE 2.2 COAL PULVERIZER

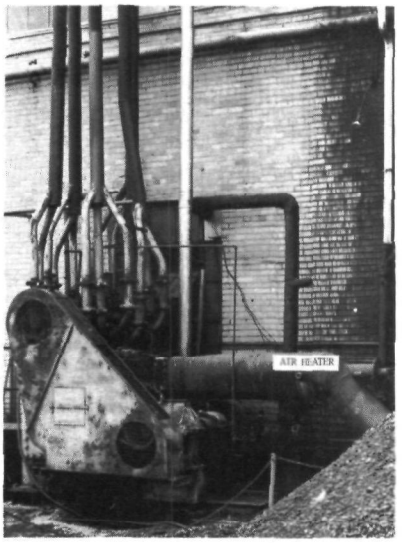

2.2 COAL SEPARATION APPARATUS AND BUNKER

The pulverized coal leaving the pulverizer travels about 200 feet to a cyclone, which separates the conveying air from the coal; see Figure 2.3. Some of the very fine coal remains entrained in the air after leaving the cyclone. This coal is scrubbed out by a venturi after which the air is vented to the atmosphere. Thus some of the coal fines is lost by this separation process. The separated coal leaves the bottom of the cyclone and passes into the coal bunker; see Figure 2.4. The bunker has a capacity for 30 tons of pulverized coal.

FIGURE 2.3 COAL HANDLING SYSTEM

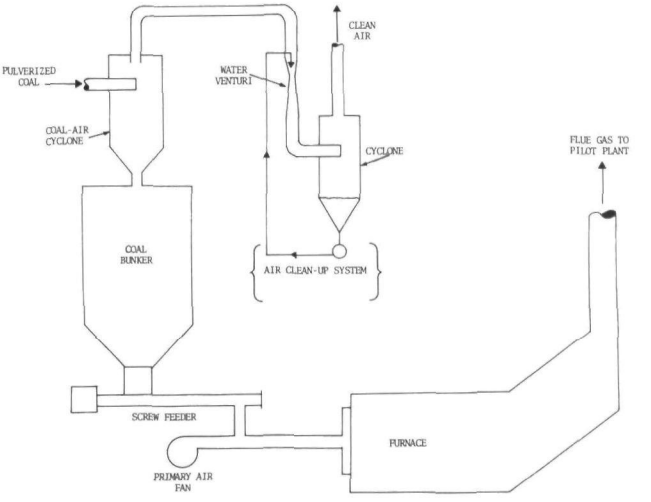

FIGURE 2.4 COAL STORAGE FACILITIES

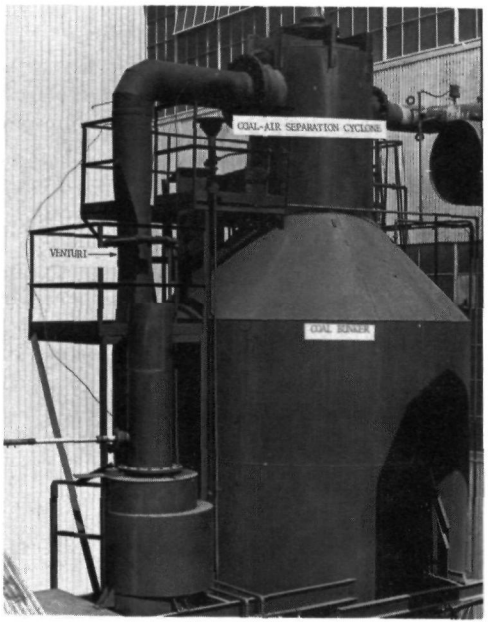

FIGURE 2.5 PULVERIZED COAL SIZING PLOT

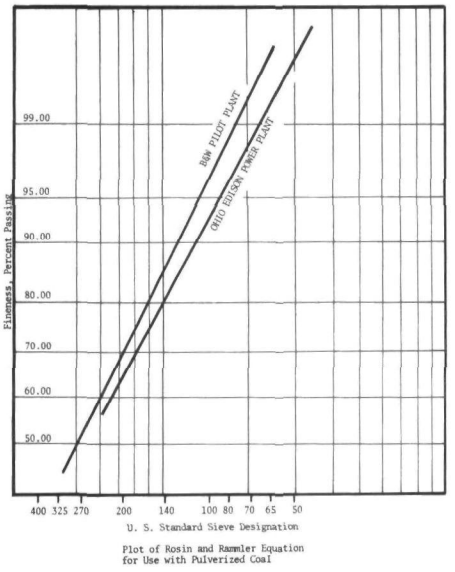

Since a part of the coal fines is lost in the coal-air separation process, a coal sizing analysis was performed on a sample from the bunker to determine whether this coal was typical of pulverized coals. Figure 2.5 shows a plot of the coal sizing analysis. Typical pulverized coal passes about 70% through a #200 U. S. standard sieve. This plot showed that the coal used in this test, designated B&W, was similar to the "typical" pulverized coal from the Ohio Edison Edgewater Station.

2.3 COAL FEED SYSTEM

The pulverized coal feed system, Figures 2.6 and 2.7, uses a screw feeder and conveying air. The screw transports the coal from the bottom of the hopper to the feed pipe, where it is partially fluidized with compressed air. The coal falls a few inches and is entrained by the primary air, which carries it to the burner. Approximately 500 lb/hr of primary air, measured by an orifice meter, is used to transport about 500 lb/hr of coal.

2.4 BURNER AND FURNACE

The pulverized coal burner is a B&W cell-type circular burner with a natural gas lighter. This lighter is operated continuously during coal firing to help maintain stable ignition. A sectional view of the burner is shown in Figure 2.8 and a photograph in Figure 2.9.

The furnace, Figure 2.10, consists of a horizontal cylinder 8 feet in length by 4-1/2 feet in diameter. This forms the actual combustion chamber. The walls of the furnace are formed by a water jacket, which dissipated heat by the production of nonpressurized steam. See Figure 2.11. The inside walls were originally covered with refractory. However, prior to running extended tests, the refractory was removed from all walls except the front. This was necessary to prevent excessive slagging of the tube banks. The furnace continually grows hotter as it operates because of slag buildup on the walls, which act as a refractory. When extended tests were attempted with refractory in place, molten slag froze onto the cold tube banks, thereby causing furnace plugging. Removing the refractory permitted the furnace to run cooler, thus allowing the slag to solidify to an ash before contacting the tubes.

FIGURE 2.6 COAL SCREW FEEDER

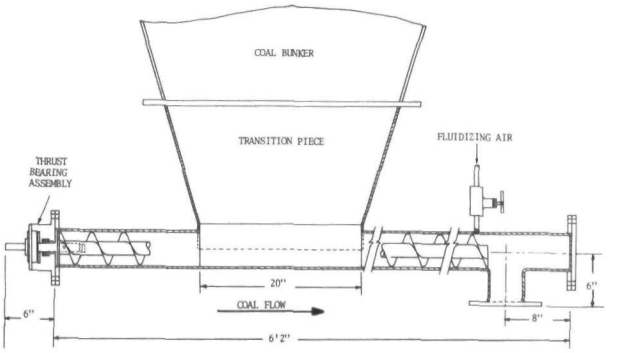

FIGURE 2.7 COAL SCREW FEEDER

FIGURE 2.8 PULVERIZED COAL BURNER

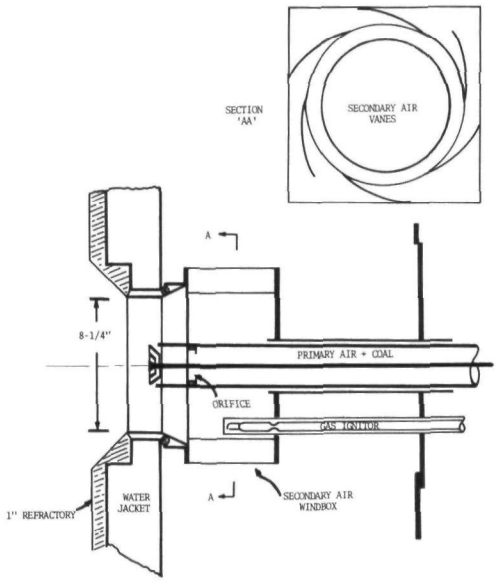

FIGURE 2.9 PULVERIZED COAL BURNER

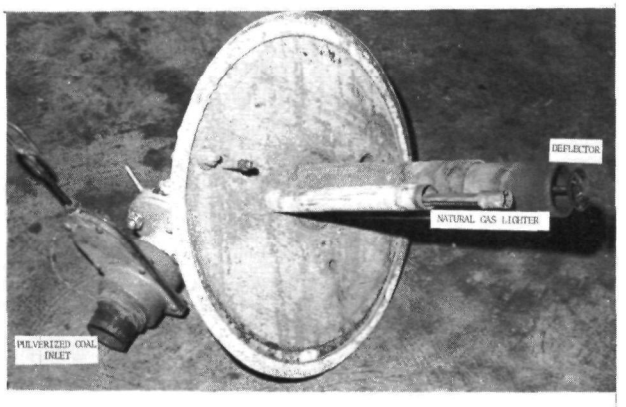

To maintain stable ignition, the pulverized coal must be fired with preheated air. This air is supplied by a forced draft fan and preheated by two direct fired air heaters capable of heating 10,000 lb/hr air to a temperature of 1000 F. The heat release rate of the furnace averages about six million Btu/hr.

Combustion gases pass from the furnace proper through three tube banks that cool the flue gas to approximately 450 F. All tubes are 1-1/2-inch O.D. on 2-1/2-inch centers with exception of the first six rows of tubes which are on 5-inch centers. Behind each tube bank is a duct permitting flue gas recirculation to the burner. This feature, however, was not used during the tests. Flue gas leaving the tube bank passes through a transition piece to a 15-inch-diameter vertical stack. Gas flow to the scrubbing system is taken from the side of this stack. The vertical stack ends at a relief valve. The relief valve is pneumatically operated and is automatically activated during a test if furnace pressure becomes too great. The relief valve can also be operated manually from the control panel and is used during startup and shutdown operations; see Figures 2.12 and 2.13.

FIGURE 2.10 BASIC COMBUSTION TEST FURNACE

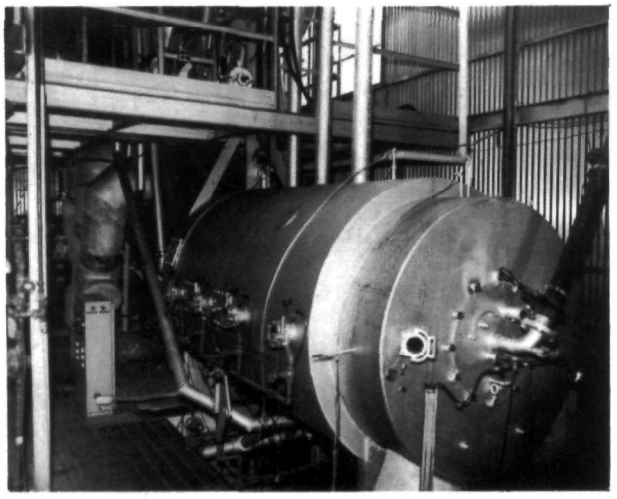

FIGURE 2.12 FURNACE RELIEF VALVE - OPEN POSITION

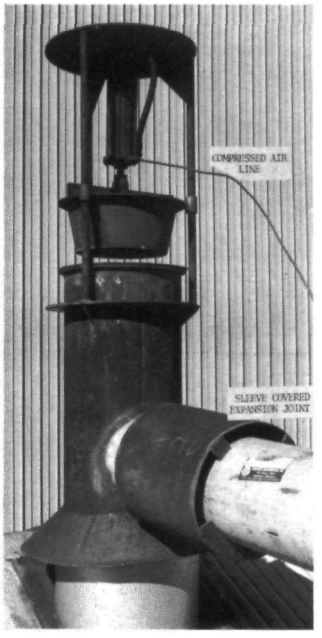

FIGURE 2.11 FURNACE SECTIONAL VIEW

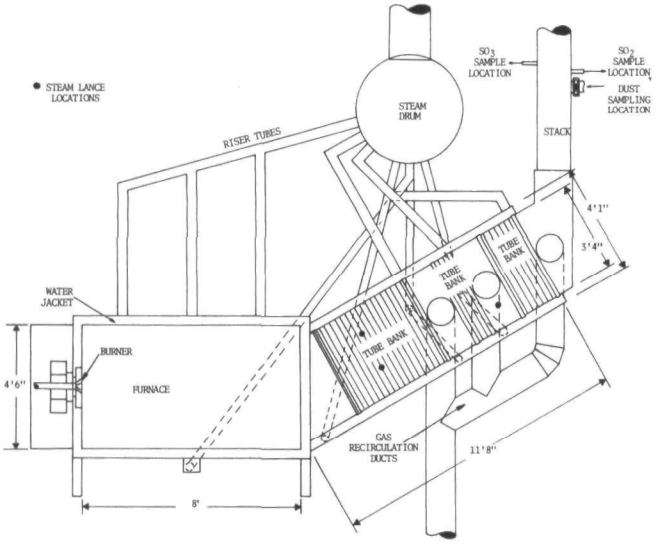

FIGURE 2.13 FURNACE RELIEF VALVE - CLOSED POSITION

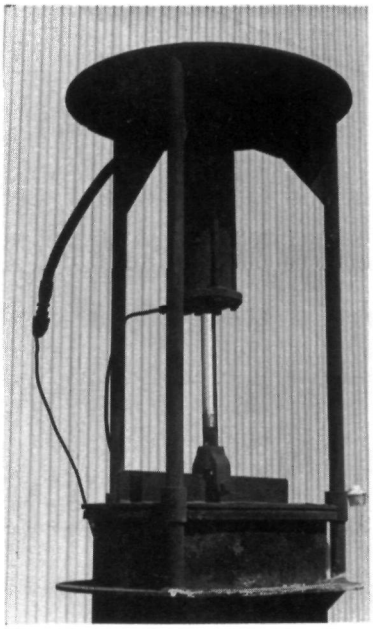

FIGURE 2.14 STEAM LANCES

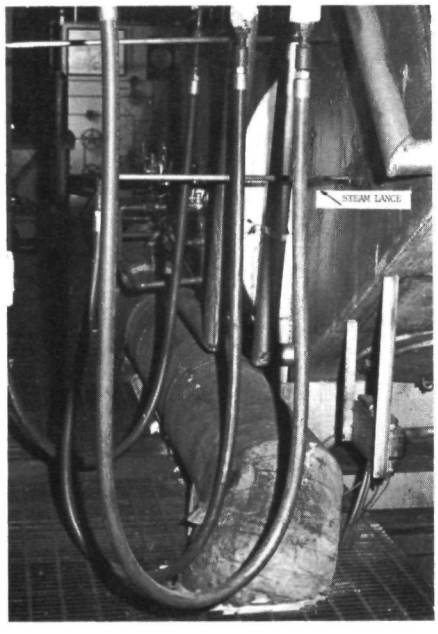

FIGURE 2.15 FURNACE CONTROL PANEL

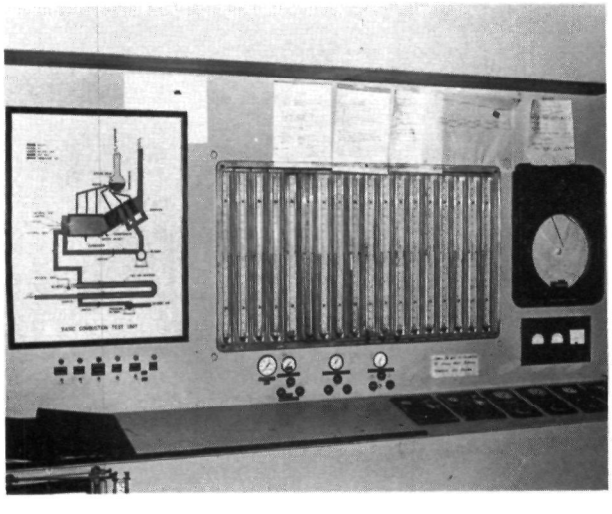

To prevent buildup of slag and ash deposits in the tube banks, three steam lances were installed; see Figure 2.14. During extended tests the tubes were lanced about every 6 hours. This succeeded in keeping the tubes free of ash buildup.

The furnace control panel, shown in Figure 2.15, is fully equipped to monitor and control the furnace pressures. A 12-point Speedomax recorder provides a continuous check of the temperatures within the furnace and ancillary components. Oxygen concentration of the flue gas is continuously monitored by a Bailey O_2 Analyzer Model A57. From time to time the Bailey Analyzer was checked by Orsat analysis and also by a Bailey electrochemical O_2 analyzer.

Located on top of the furnace, Figure 2.11 is the steam drum, a steel cylinder 4-ft. diameter by 6-ft. long. This drum supplies water to the furnace water jacket and acts as a steam-water separator for venting the steam to atmosphere.

2.5 FUEL

Two types of fuel were used during the tests, pulverized coal and natural gas. Pulverized coal was

the main fuel while natural gas was used in the lighter and accounted for about 4% (thermal) of the fuel used. A number of coal analyses were run and the results reported in Table 2.1. A typical natural gas analysis obtained from the Ohio Fuel Company is also shown in Table 2.1.

2.6 WET SCRUBBING APPARATUS

2.6.1 Particulate Scrubbing System

Flue gas leaving the furnace passed through the water tube section to the particulate venturi and cyclone, see Figures 2.16 and 2.17. The ducts were arranged in such a way that by changing blanks the particulate scrubber could be bypassed. As the gas entered the venturi throat, its velocity was greatly increased. It is here that the fly ash slurry spray was introduced, just slightly ahead of the throat. The fly ash particles traveling at high velocity impacted upon the slower moving slurry droplets and were thereby trapped.

The fly ash slurry was separated from the cleansed flue gas in the cyclone separator; see Figure 2.16. The flue gas and slurry entered the cyclone tangentially, spinning the slurry to the walls while the gases moved toward the center and out the top. The slurry moved from the cyclone into the sump located immediately below.

TABLE 2.1 PULVERIZED COAL AND GAS ANALYSIS

PULVERIZED COAL ANALYSES

Lab. Serial No.	C-13425	C-13426	C-13427
Sample Description	Coal from BCTU Hopper 3-9-70 2200 hrs.	Coal from BCTU Hopper 3-10-70 1000 hrs.	Coal
Ash (Dry) %	9.6	9.2	--
Sulphur (Dry) %	3.8	4.1	4.5
Carbon (Ult.)%	--	--	--

Lab. Serial No.	C-13260	C-13386	C-13377
Sample Description	Pulv. Coal Sample N. Industry Strip	Pulverized Coal Ohio Seam #5&6	Pulverized Coal Ohio Seam #5&6
Total Moisture, %	3.0	4.2	
Ash, %	8.1	--	7.4
Sulphur, %	4.1	3.8	3.7
Btu per lb. (Dry)	12730	12700	
Btu per lb. (M&A Free)	13850		

NATURAL GAS ANALYSES

Sulphur Compounds	
Hydrogen Sulfide, gr/100 cf	0.017
H_2S Sulphur Equiv., gr/100 cf	0.018
Mercaptans - S - Equiv.	0.007
Sulfide Sulphur, gr/100 cf	0.007
Residual Sulphur, gr/100 cf	0.004
Total Sulphur, gr/100 cf	0.034

	Tennessee Guernsey
Date of Sample	2/12/69
Components:	Mol %
Nitrogen	0.44
Carbon Dioxide	0.65
Methane	95.40
Ethane	2.86
Propane	0.49
Iso-Butane	0.07
N-Butane	0.06
Iso-Pentane	0.02
N-Pentane	0.01
Total	100.00

FIGURE 2.16 PARTICULATE SCRUBBING SYSTEM

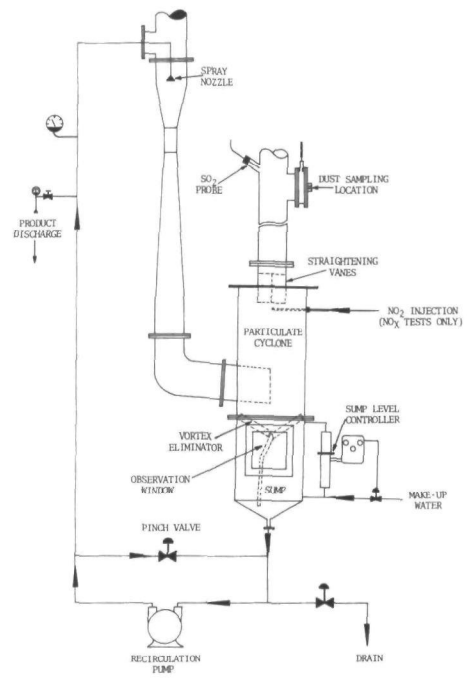

FIGURE 2.17 PARTICULATE SCRUBBING SYSTEM

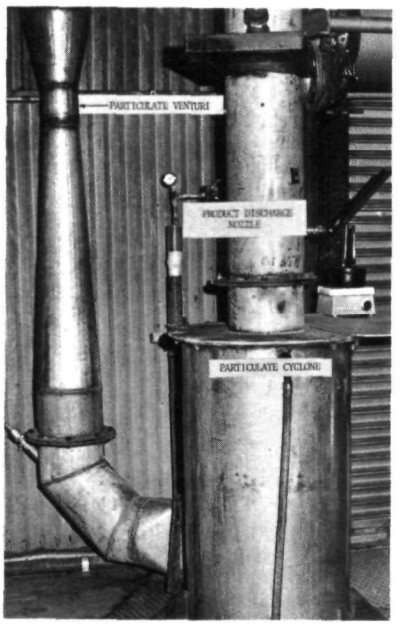

FIGURE 2.18 PARTICULATE SYSTEM DIMENSIONS

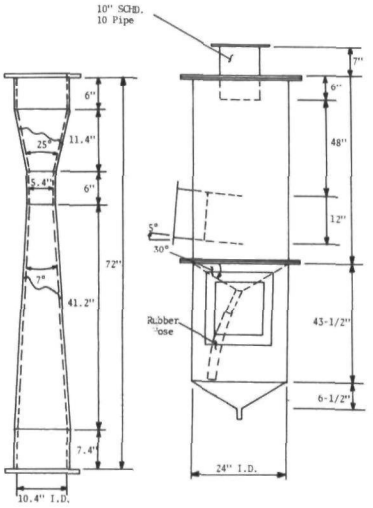

The slurry was pumped from the sump and recirculated back to the venturi spray nozzle. To maintain the desired composition, part of the slurry was discarded. Fresh water previously treated by a zeolite bed was added directly to the sump. Approximately 23 gal/min of slurry were recirculated through the spray nozzle, and about 5 gal/min were discarded as particulate product. The overall diminsion of the venturi and cyclone is shown in Figure 2.18.

During shakedown (November 1969) of the venturi and cyclone an unexpected development occurred. The pressure drop across the cyclone was about 14 inches of water. This was 10 inches more than expected. Observation of the cyclone operating with the top removed showed a large vortex action indicated by excessive liquid spinning. To break up the vortex a series of baffles (vortex eliminators) was installed on the bottom cone of the cyclone; see Figure 2.16. This reduced the pressure drop to a normal 4 inches of water.

The particulate venturi spray nozzle flow was controlled by a pump and pinch valve. A pneumatically controlled pinch valve (Red Valve Co.) controlled the amount of "short circuit" recirculation through the pump and valve loop. Closing the pinch valve

forced more slurry through the spray nozzle. This arrangement was used instead of the normal control method via a gate or glove valve, because solids tend to collect behind the seat, thereby restricting flow. The product nozzle takeoff, shown in Figure 2.19 is merely an orifice calibrated versus pressure.

At the gas outlet from the particulate cyclone, the vortex spin was eliminated by a flow straightener. This cross-shaped member 10 inches long by 10 inches in diameter was placed in the cyclone gas exit duct.

A 5-inch slide valve located in the particulate cyclone exit duct is part of the dust sampling apparatus. With the valve closed, particulate sampling probe bolts to the slide valve. The valve is then opened so that the probe can be inserted into the gas stream. This procedure eliminates sudden pressure upsets in the furnace.

A gas sampling probe used for both NO_x sampling and SO_2 sampling is positioned 4 inches downstream from the dust sampling connection. The probe includes a 6-inch long 1-3/4-inch pipe welded flush to the duct wall and a 1/8-inch glass tube located concentrically in this pipe. The pipe provides a "quiescent" zone in which the gas flow to the glass probe is relatively slow. This minimizes the possibility of slurry carryover from the cyclone entering into the glass tubing

FIGURE 2.19 PRODUCT DISCHARGE NOZZLE

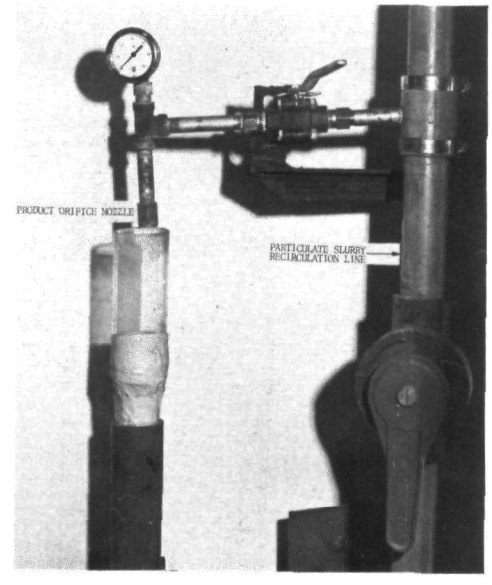

FIGURE 2.20 VENTURI ABSORBER FLOW CONTROL SYSTEM

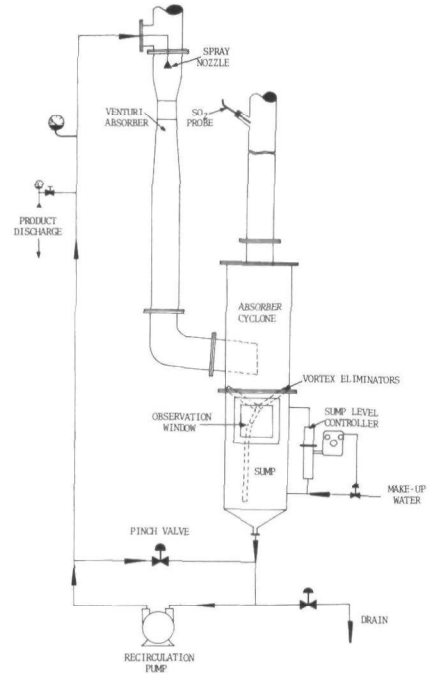

FIGURE 2.21 VENTURI ABSORBER SYSTEM

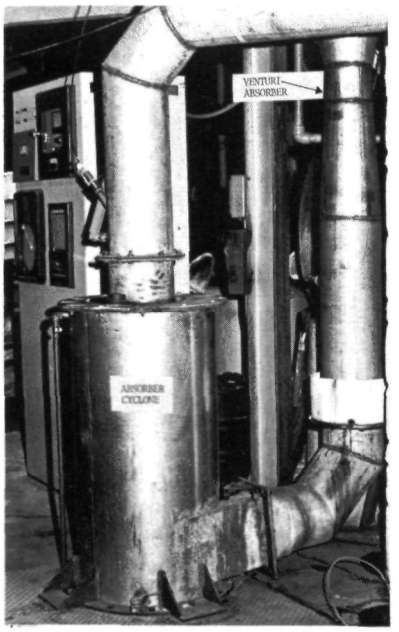

FIGURE 2.22 VENTURI ABSORBER SYSTEM DIMENSIONS

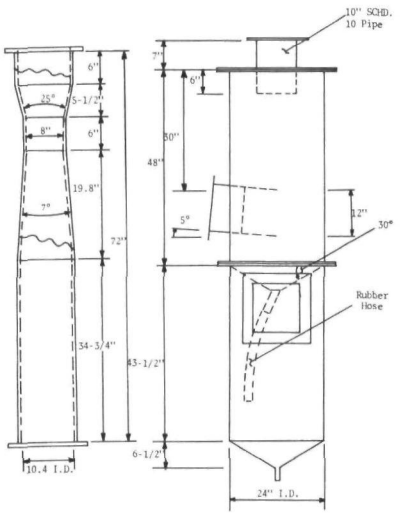

which in turn, could result in SO_2 and NO_x sampling errors due to scrubbing of the gas by the slurry in the probe.

2.6.2 Venturi Absorber System

Gas leaving the particulate scrubber first passes through an orifice meter and then can be directed in either of two ways: through the venturi absorber or through the floating bed absorber.

The venturi absorber and cyclone are shown in Figures 2.20 and 2.21. The absorbent slurry spray nozzle enters just ahead of the venturi throat. The venturi promotes gas absorption by providing a zone with a high liquid-to-gas specific surface. The gases enter the cyclone separator, where the absorbent slurry is removed from the gas stream. As in the particulate cyclone, vortex eliminators are installed on the bottom cone of the cyclone. The slurry flows by gravity to the sump located immediately under the cyclone. The system dimensions are shown in Figure 2.22.

The liquid level in the sump is controlled by a level controller, which maintains a constant level with treated makeup water. The slurry composition is maintained indirectly by adjustment of the product flow rate, which in turn controls the water makeup rate via the level controller.

Due to problems with solids settling an air-driven mixer is installed in the venturi absorber sump to help keep solids in suspension. The sump has a 12-by-12 inch Plexiglas observation window, a pressure equilizing connection with the cyclone, and a liquid level indicator.

2.6.3 Floating Bed Absorber

The floating bed absorber (hereafter referred to as the FBA) includes a sump, two contact stages, and a liquid disengagement section. The FBA is depicted in Figures 2.23 and 2.24. This countercurrent device takes in the flue gas through the sump. Ancillary components of the FBA sump include the following: a liquid level controller, sump observation window, level indicator, and air-driven mixer. The sump is fitted with piping to allow sump recirculation to promote agitation to keep the solids in suspension. Sump recirculation, however, was abandoned in favor of the air-driven mixer.

Above the sump the FBA consists of two stages. Each tray has an effective flow area of 2 square feet and consists of a 1/8-inch-thick stainless steel plate perforated with 3/8-inch-diameter holes on staggered 1/2-inch centers. Each stage is packed with 6 to 8 inches of "wiffle balls." An inspection of the plastic balls after all tests showed that the balls on the lower tray were deformed, but those on the top tray retained their original shape; see Figure 2.25. The

FIGURE 2.23 . FLOATING BED ABSORBER

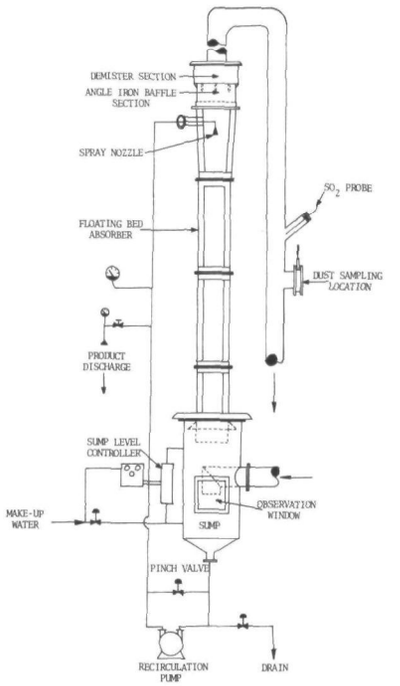

FIGURE 2.24 FLOATING BED ABSORBER

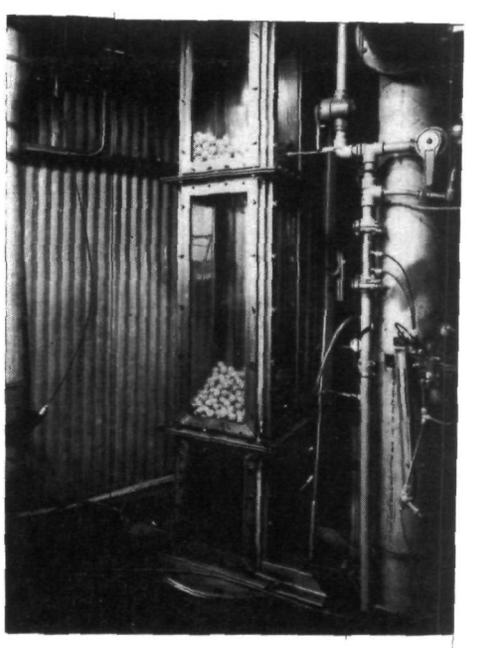

FIGURE 2.25 PLASTIC "WIFFLE" BALLS DEFORMED

FIGURE 2.26 FLOATING BED ABSORBER DIMENSIONS

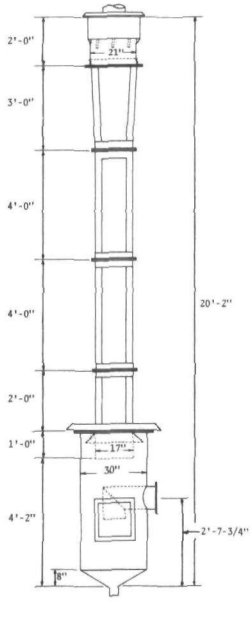

deformed balls were flattened on the two sides parallel to the seam where the two halves are fused together. Evidently the slight increase in wall thickness along the seam was enough to prevent deformation along this plane. The first time that this deformation was noticed was after series M extended tests, in which the FBA was used for both SO_2 scrubbing and particulate collection. Since hot gas directly from the furnace was entering the FBA, possibly hot spots developed on the lower tray, causing the balls to deform. The overall dimensions of the FBA are shown in Figure 2.26.

The spray nozzle located above the top tray directs the spray of absorbing slurry onto the top tray. Since the gas rises countercurrent through the slurry, it comes into intimate contact with the absorbing slurry. Gas leaving the top tray flows through an angle iron baffle section which serves to trap large water drops, then through a York Demister to ensure that all remaining droplets are removed. The Demister is located at the very top of the FBA and consists of about 6 inches of Teflon mesh fibers; see Figures 2.27 and 2.28.

Flow to the spray nozzle is controlled by the aforementioned pinch valve arrangement, and the slurry

composition in the sump is controlled by the product nozzle flow and MgO makeup rates.

2.7 FLUE GAS EXHAUST SECTION

The cleansed flue gas leaving the scrubber and absorbers passes downward through a vertical length containing an orifice meter, a gas sampling probe, and a particulate sampling port with slide valve. The vertical duct ends in a blank flange; approximately 3 feet up from the flange is the takeoff for the induced draft fan. The purpose of this length of pipe is to trap any large liquid or solid particles before the gas enters the I.D. fan. A pneumatically operated damper was located at the fan inlet. After leaving the fan, the gas is released to the atmosphere.

2.8 PILOT PLANT MONITORING SYSTEM

Several thermometers and thermocouples are located throughout the system at important points; see Figure 2.29. Also at various locations are manometers measuring static pressures as well as pressure differentials. Two water meters measure the amount of makeup water used in the particulate cyclone and to the absorption systems.

2.9 MgO MAKEUP AND PRODUCT DISPOSAL

The magnesium hydroxide makeup slurry is prepared in the MgO slaking tank. This

FIGURE 2.27 TOP OF FLOATING BED ABSORBER

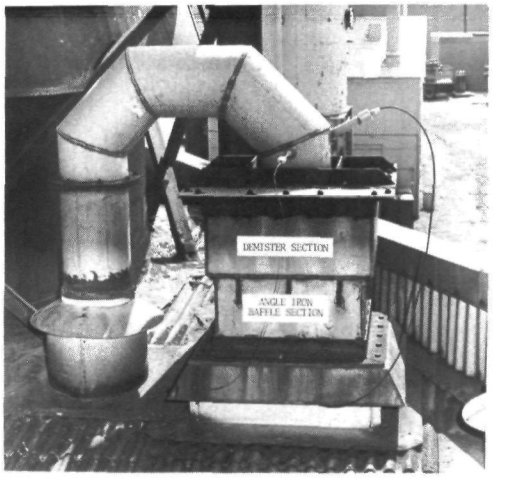

FIGURE 2.28 MOISTURE DISENGAGEMENT REGION - SECTIONAL VIEW

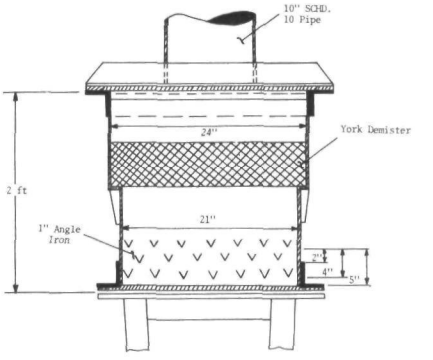

FIGURE 2.29 MEASUREMENT LOCATIONS

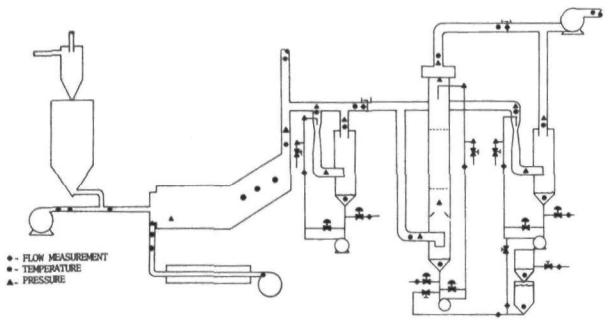

FIGURE 2.30 MAKEUP SYSTEM

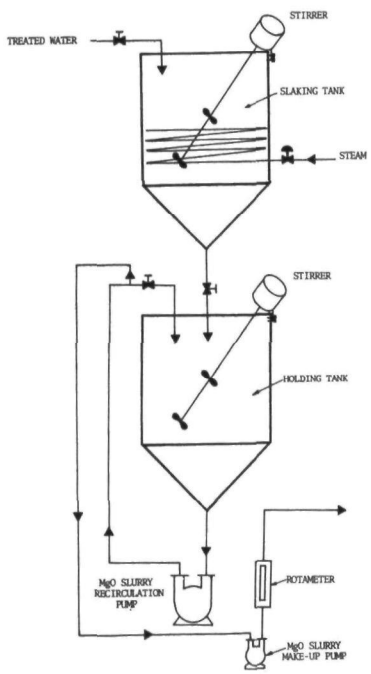

tank is equipped with steam coils and a large stirrer. The steam coils are used only if the slurry is slaked; otherwise the slurry is mixed and dumped into the $Mg(OH)_2$ holding tank below; see Figure 2.30. The holding tank has a large stirrer and a recirculation pump, which helps to keep the solids in suspension. The makeup slurry is drawn from this recirculation line. A small flexible impeller chemical feed pump feeds the slurry through a rotameter to the proper point. This pump required a variable speed drive. Note that no valves are used in this line. See Figure 2.30.

In the early stages of the test, MgO slurry was added at the suction side of the venturi spray pump (recirculation pump). However, when changes were made in spray rates, the pressure changes also affected the MgO slurry flow rate. Therefore the MgO makeup line was changed to direct flow into either the venturi absorber cyclone sump or the FBA sump, depending on which system was operating.

During the tests with the venturi absorber, problems were encountered with deposits forming in the sump. Therefore, on the last test using the venturi absorber, J Series, it was decided to add the magnesium hydroxide makeup at the venturi throat in order that the makeup stream would be more completely mixed with recirculated slurry.

The magnesium hydroxide makeup slurry was added to the FBA sump until the beginning of L series extended tests. During the L, M, and N series tests, the makeup was added to the top tray of the FBA for better mixing.

The product from the particulate scrubbing and the SO_2 scrubbing systems was collected in four leach beds. See Figure 2.31. Each leach bed consisted of a cylindrical steel tank, 4 feet in diameter by 5 feet high. Each bed was filled with sand to a depth of about 1 foot. The particulate product entered one tank while the sulfite slurry flowed simultaneously into the other three tanks.

FIGURE 2.31 PRODUCT DISPOSAL LEACH BEDS

2.10 CHEMICAL ANALYSIS LAB

The laboratory where all chemical analyses were performed is shown in Figure 2.32. The lab was located just behind the furnace and was equipped with a stainless steel sink, ample table space, and storage space for samples.

FIGURE 2.32 PILOT PLANT ANALYSIS LAB

2.11 OVERALL PILOT PLANT SCHEMATIC

Figure 2.33 shows in schematic form the overall arrangement and the approximate nominal flow rates of the various streams.

FIGURE 2.33 SCHEMATIC ARRANGEMENT OF TEST FACILITIES

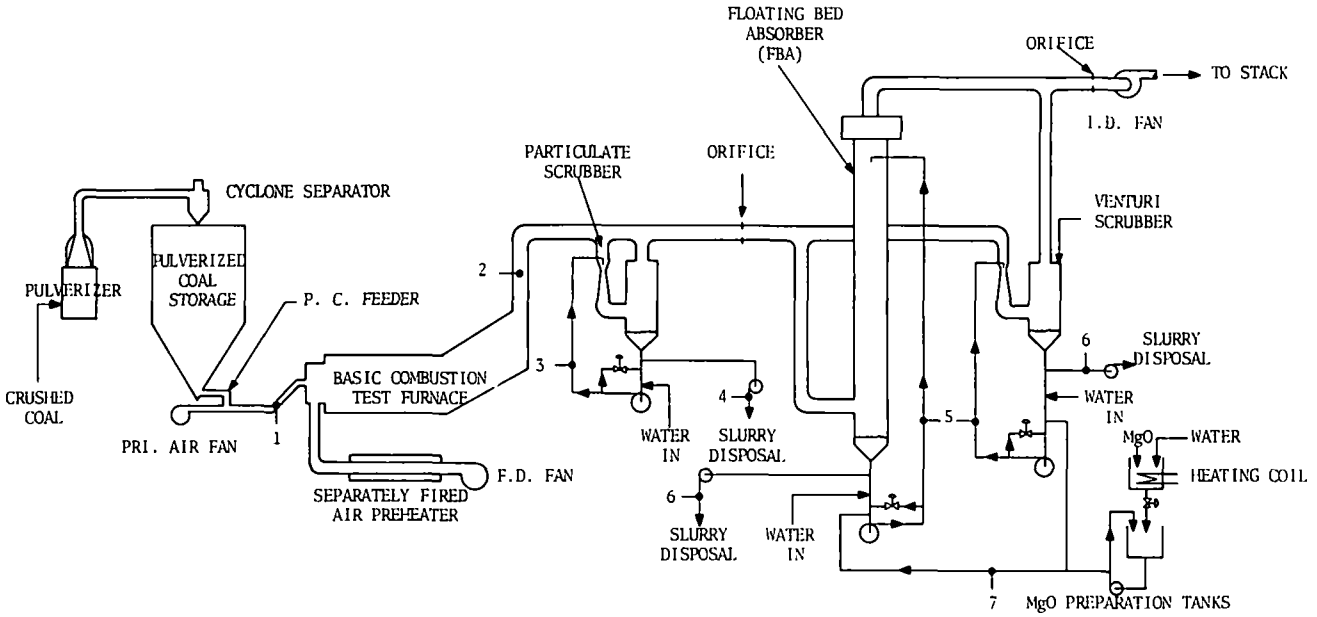

LOCATION	APPROXIMATE FLOW RATES	
1	COAL FIRED	500 LB/HR
2	FLUE GAS	5,400 LB/HR (1100 SCFM)
3	PARTICULATE SPRAY	10,000 LB/HR
4	PARTICULATE PRODUCT	2,500 LB/HR
5	ABSORBER SPRAY	30,000 LB/HR
6	ABSORBER PRODUCT	900 LB/HR
7	MAGNESIA MAKEUP (10% SLURRY)	400 LB/HR

3.0 TEST APPARATUS AND PROCEDURES

3.1 TEST PROCEDURE FOR 1-DAY OPERATION

A typical testing day in which four tests were usually completed is described below.

A test day began with the start-up of the furnace. First, this necessitated firing of the air heaters and allowing them to reach temperature (~750 F). This usually took about an hour. The coal feed was then ignited. The furnace gases at this time were vented directly to the atmosphere via the stack relief. A waiting period of approximately 1 to 2 hours followed until the furnace ignition was stable.

While waiting for the desired furnace conditions, the particulate scrubbing system and the appropriate gas absorber were being readied for operation. During this time the MgO makeup slurry was prepared to the proper concentration. If slaking of the makeup was required, preparation was made the night before, and the MgO was allowed to slake overnight. When the furnace was ready, the relief valve was closed, thereby directing the flue gas to the scrubbing systems.

After the transfer of gas was made, it usually took about an hour or so after the MgO makeup was started before the chemical composition of the absorber system reached steady state and the first test could begin. Steady state was assumed when two or three Palmrose analyses taken at 10 minute intervals showed that the system had reached the desired operating conditions and also when the SO_2 concentration at the pilot plant exit was constant. A typical test lasted for about an hour, during which a complete set of data was taken. Test data was usually taken midway in the 1 hour test period.

During a test several samples were taken and put into storage in the event that they were needed at a later date. If certain test data were found to be unusual, an analysis of the stored samples could provide a means for determining what occurred. Samples collected and stored in 8-ounce bottles consisted of the following: MgO makeup slurry, particulate cyclone slurry, SO_2 scrubber slurry, and a makeup water sample.

After a test was completed, the operating conditions were changed for the next test. Depending upon the operating parameter changed, there was usually a waiting period of about 1/2 to 1 hour before steady state was again reached and the next test could begin. Following this procedure, about four 1 hour tests were completed per day.

3.2 TEST PROCEDURE FOR EXTENDED OPERATION

The start-up for extended operation did not differ from that of a normal test day. Test conditions were specified to be constant for each 24-hour period. Excess air was the only variable scheduled for change at 24-hour intervals.

Each extended run was designated by a letter and separated into a number of tests designated by a number preceded by the letter of the extended run. Each individual test lasted for 1-1/2 hours, during which complete data were taken consisting of chemical analyses and temperature and pressure measurements. The 1-1/2-hour tests were attempted consecutively. However, due to some problems with deposits and the like, continuous operation was interrupted. Selected tests such as SO_3, NO_x, and Thorston dust sampling were done at about 5-hour intervals.

Prior to starting an extended run, the pulverized coal bunker was filled completely, to 30-ton capacity, which provided enough coal for a typical 4-day extended test. Magnesium oxide makeup slurry was prepared about every 7 hours in the slaking tank and then dumped into the holding tank.

3.3 SPECIAL TESTS

3.3.1 High Sulfate Concentration Tests

Two series of tests, K and N, were run with an artificially induced high-sulfate concentration. These tests were run to determine the effect of high-sulfate concentration on the absorption of SO_2. The high-sulfate level was attained by adding Epsom salt, $MgSO_4 \cdot 7H_2O$, to the magnesium oxide slurry in the holding tank; enough Epsom salt was added to obtain a saturated solution in the makeup. Addition of this makeup to the SO_2 absorber system resulted in a sulfate concentration of about 15% of saturation in the absorbent slurry. These tests were run as normal 1-hour tests.

3.3.2 NO_x Absorption Tests

The NO_x absorption tests involved injecting nitrogen dioxide into the gas stream and relying on the following reaction to occur:

$$NO + NO_2(\text{injected}) \rightarrow N_2O_3$$

FIGURE 3.1 NO_2 INJECTION APPARATUS

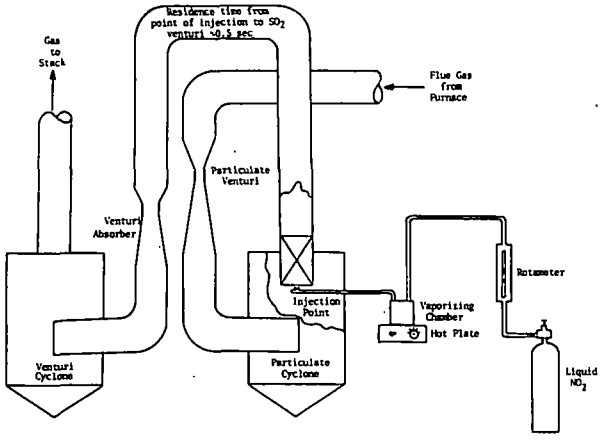

FIGURE 3.2 SO_2 SAMPLING SYSTEM

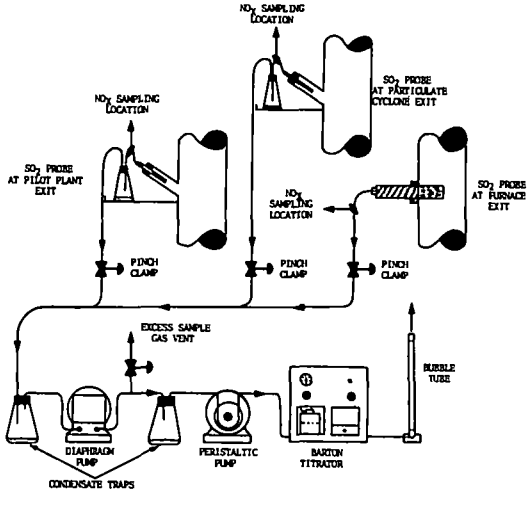

This compound nitrogen trioxide, would then be absorbed by the absorbent slurry by the reaction:

$$N_2O_3 + Mg(OH)_2 \rightarrow Mg(NO_2)_2 + H_2O$$

An attempt was made to add a stoichiometric quantity of NO_2 required to react with the NO from the furnace. It was intended to meter liquid NO_2 from a bottle of liquid NO_2 through a rotameter and vaporize it in a cylindrical container over a hot plate. However the elutriation tube in the bottled NO_2 which was to supply the liquid NO_2 was absent. Therefore a suitable rotameter was obtained, and gaseous NO_2 was metered, passed through the vaporizer, and injected into the system. The apparatus is shown in Figure 3.1.

The gaseous NO_2 was injected at the particulate cyclone exit, just a few inches upstream of the straightening vanes. It was thought that the vortex action of the gas leaving the cyclone would promote complete mixing of the injected NO_2.

3.4 SULFUR DIOXIDE SAMPLING AND ANALYSIS

3.4.1 Barton Titrator

One of the most important analyses was the measurement of the sulfur dioxide concentration in the

flue gas. SO_2 sampling probes were located at the furnace exit duct, the particulate cyclone exit, and the pilot plant exit; see Figure 3.2. This analysis was performed for the most part by a Barton Model 286 Recording Electrolytic Titrator; see Figure 3.3. The Barton Titrator works on the principle of coulometry titration. This method employs electrolysis to generate a reagent which reacts stoichiometrically with the substance to be determined. The quantity of substance reacted is computed via Faraday's Law from the current. This is analogous to the volume of standard solution used in chemical titrations. The details of the sampling procedure are described in Section A.1.

FIGURE 3.3 BARTON TITRATORS

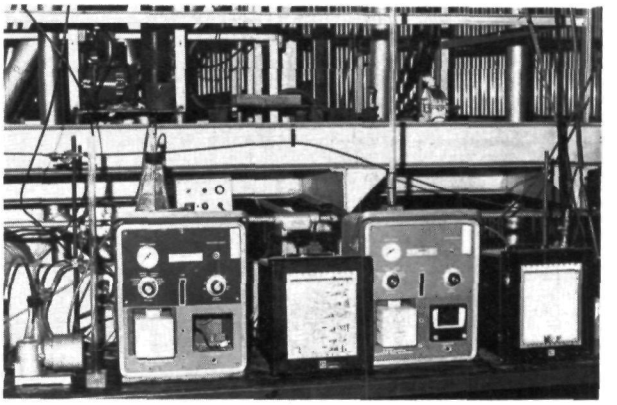

The instrument consists of three basic modules: a titration cell, a solid-state electronic control circuit, and a strip chart recorder.

The heart of the unit is the titration cell, which consists of a combination electrode enclosed in a chamber containing hydrobromic acid and free bromine. The gas being analyzed is bubbled through the solution, where the sulfur dioxide is allowed to react with the bromine by the following reaction:

$$SO_2 + Br_2 + 2H_2O \rightarrow H_2SO_4 + 2HBr \qquad (3.1)$$

The instrument attempts to maintain a constant bromine concentration by electrolytically reducing some of the hydrobromic acid to bromine and free hydrogen. The amount of current required to maintain a steady-state concentration of free bromine in solution is a measure of the amount of bromine reacted and is therefore a measure of the amount of SO_2 reacted. A schematic diagram of the electrodes and reaction chamber appears in Figure 3.4.

The Barton instrument is extremely sensitive. The accuracy of coulometric titration has been noted by Lingane [1]. "The precision and accuracy of coulometric titration are both excellent, and the method is conveniently applicable

FIGURE 3.4 BARTON ELECTRICAL CIRCUIT

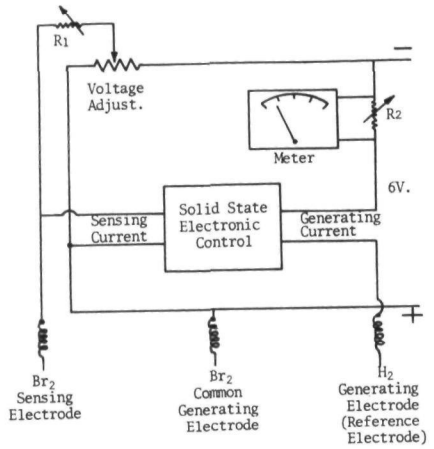

FIGURE 3.5 REICH BOARD

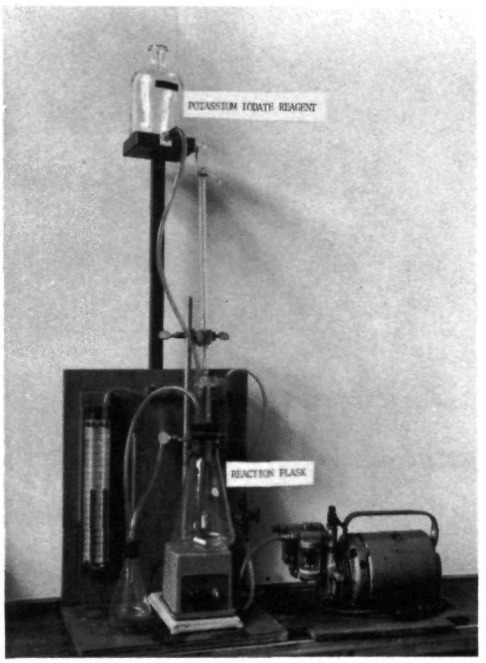

to amounts ranging from about 100 milligrams down to as little as a few hundredths of a microgram in volumes of the order of 10 to 50 cc. Even in the microgram range titrations with errors of only a few tenths of a percent are possible."

The accuracy of the Barton instrument is also increased because coulometric titrimetry involves a fundamental quantity, current. This measurement is relatively "absolute" and free from the uncertainties associated with a normal chemical titration.

In a study carried out by the U. S. Department of Health, Education, and Welfare, Performance Characteristics of Instrumental Methods for Monitoring Sulfur Dioxide,[2] lag and response time for the Barton instrument were shown to be superior to those for most of the other commercial SO_2 analyzers tested. Sensitivity was also good, being 0.03 ppm SO_2 with the base level at 1.00 ppm SO_2. Sensitivity was defined as the smallest change in SO_2 input concentration that produces a readable change in recorder output.

3.4.2 Reich Method for SO_2 Analysis

The Reich method for SO_2 analysis was used as a spot check on the Barton SO_2 analyzer. This method is useful for the determination of SO_2 in a gas stream when H_2S is absent. This test consists

of aspirating the gas through standard iodine solution until it is decolorized. Since the amount of iodine used is known and the volume of the aspirated gas is measured, the percentage of SO_2 can readily be calculated. A photograph of the Reich apparatus is shown in Figure 3.5.

3.5 SULFUR TRIOXIDE SAMPLING

The determination of sulfur trioxide concentration was accomplished by condensation of the sulfur trioxide vapor followed by titration of the condensate. This method was adopted from H. Goksoyr and K. Ross.[3] The titration procedure was developed in-plant. The sampling apparatus and method are presented in Section A.2.

A sampling probe consisting of a quartz tube wrapped with a heating element was placed in the furnace exit duct. The flue gas was drawn through the quartz tube and into the sulfur trioxide collector, which consisted of a helical coil enclosed in a water jacket. The purpose of the water jacket was to keep the helical coil below the dew point of SO_3 and above the dew point of water vapor.

From the collector the gas then passed through a sulfur dioxide absorber, drying column, gas meter, and finally to the vacuum pump; see Figures 3.6 and 3.7.

FIGURE 3.6 SO_3 COLLECTION APPARATUS

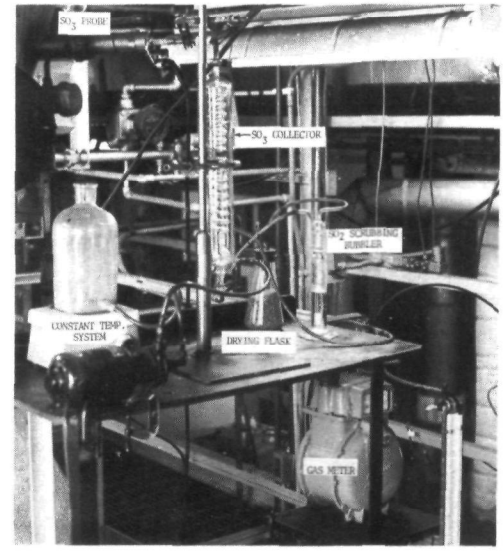

FIGURE 3.7 SO_3 COLLECTION APPARATUS

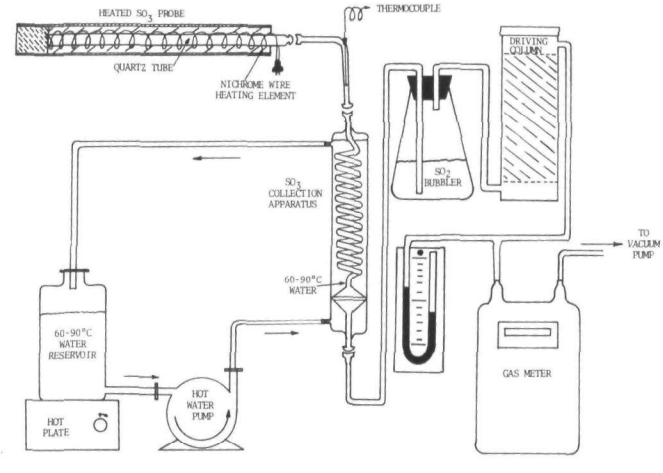

A total of about 2-1/2 cubic feet of gas was sampled, after which the collector was washed out with 80% isopropyl alcohol. The washings from the collector were then titrated with barium chloride solution to determine the amount of sulfur trioxide gas in solution as sulfate.

Sulfur trioxide measurements were attempted at the particulate cyclone outlet duct. However, they were unsuccessful. When sampling, the sulfur trioxide collector trapped fly ash, liquid carryover, and other solid particles which escaped collection by the particulate scrubber. Fly ash itself does contain sulfates, which would cause errors in analysis. Using a glass wool filter to filter out solid particles was precluded because it would also filter out the sulfur trioxide, which would have been in the form of a mist at the temperatures encountered.

3.6 NO_x SAMPLING AND ANALYSIS

NO_x analyses were taken in duplicate and at times in triplicate at three points: the furnace exit, particulate cyclone exit, and pilot plant exit. Sulfur dioxide sampling lines running from these points were fitted with a glass tee near the probe from which the NO_x samples were taken. The Phenol-Disulfonic Acid Method was used for analysis.

A typical NO_x sampling and analysis consists of the following. To a 1000 ml flask is added an absorbing solution consisting of hydrogen peroxide and dilute sulfuric acid. The flask is then evacuated; a gas sample is now ready to be taken. The line to the Barton SO_2 Analyzer is pinched off, and one arm of the three-way stopcock is connected to the tee. The stopcock is opened, and the gas sample is drawn into the flask.

The nitrogen oxides are converted to nitric acid by the absorbent solution and are then reacted with phenoldisulfonic acid to produce a yellow compound, which is measured colorimetrically. The color is measured with a photometer and compared with calibration curves made with a solution containing a known amount of nitrite.

A more complete and descriptive explanation of the phenoldisulfonic acid method used in these tests is given in the American Society for Testing and Materials, Standard Method of Test for OXIDES OF NITROGEN IN GASEOUS COMBUSTION PRODUCTS (PHENOL-DISULFONIC ACID PROCEDURE), ASTM Designation: D1608-60.

With the exception of the following modifications, the ASTM Method was followed as written:

Modifications to ASTM Method:

1. Absorbent Solution - 2 ml of H_2O_2 (3%) was added to 50 ml of 0.1N H_2SO_4. This is about 4 times the peroxide concentration called for in the ASME Standard.
2. In place of 1N sodium hydroxide solution, 1N potassium hydroxide solution was used.

The modified Saltzman method for the determination of NO_x concentrations in flue gas was initially selected as the preferred method because it is more rapid and easier to use than the phenol-disulfonic acid method. However, before accepting the Saltzman method, bench-scale tests were made to determine the effects of sulfur dioxide on the results. These tests showed that sulfur dioxide, at the expected concentrations, would bleach the Saltzman reagent color. Rapid bleaching started within 15 minutes. Therefore it was decided to use the more accurate, but more tedious, PDS method for NO_x analysis.

3.7 DUST LOADING

Dust sampling is carried out at three points in the pilot plant: the furnace exit, the particulate cyclone exit, and the pilot plant exit. A dust probe especially designed to

FIGURE 3.8 PARTICULATE SAMPLING NOZZLE

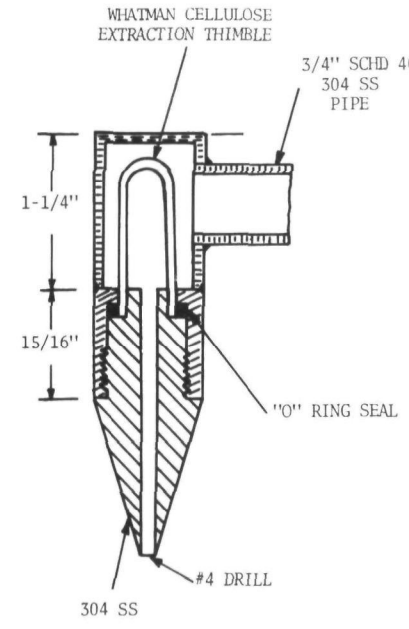

FIGURE 3.9 PARTICULATE SAMPLING APPARATUS

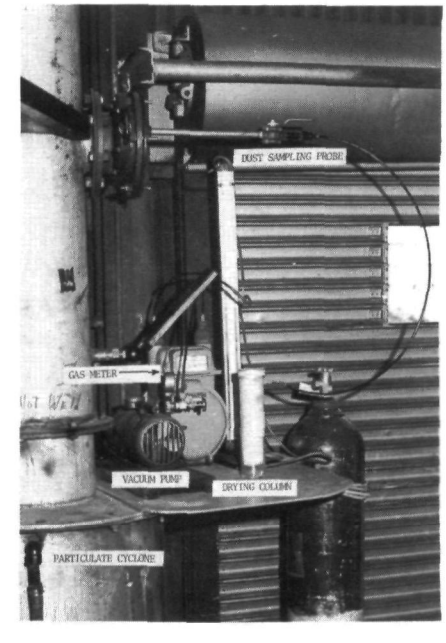

FIGURE 3.10 PARTICULATE SAMPLING APPARATUS

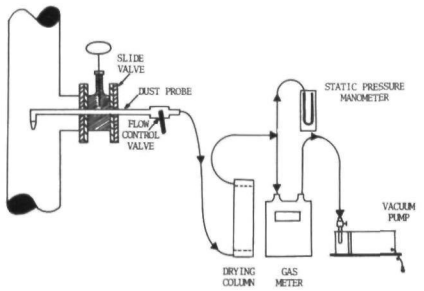

FIGURE 3.11 THORSTON DUST SAMPLER

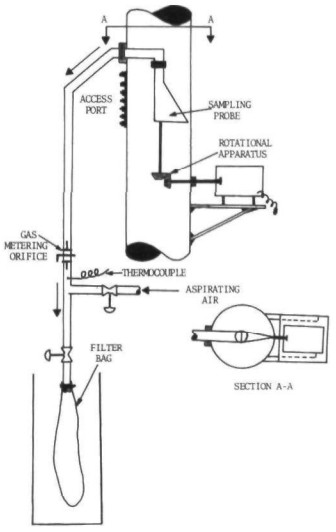

accommodate a filtering thimble placed immediately behind the sample nozzle (see Figure 3.8) is used to sample gas at the particulate scrubber and pilot plant exits. The thimbles are Whatman cellulose extraction thimbles used for this purpose in the past. The probe is designed to avoid the usual shortcomings of conventional sampling normally employing a large filter at the end of the probe. Deposition of dust in these probes ahead of the filters is a recurring problem. The remainder of the dust sampling system includes a drying column, a gas meter, and a vacuum pump, Figures 3.9 and 3.10. The sampling apparatus is described more fully in Section A.3.

Isokinetic sampling is performed by regulating the flow rate to correspond with the calculated velocity at the sampling point. This method is used instead of the null balance method since the gas flow rate through the pilot plant is relatively constant.

Representative dust sampling at the exit of the particulate cyclone separator was potentially difficult because of the spinning action of the gas leaving the cyclone. However, this problem was circumvented by placing a flow straightener at the cyclone discharge, which stopped the spin and thereby redispersed the dust.

Use of the dust sampling probe was attempted at the furnace exit. For this

attempt we tried using the Whatman cellulose extraction thimble. However, as might be expected, the furnace exit gas temperature was high enough to char the thimble.

A Thorston dust sampler installed in the furnace exit duct was used. This device samples much larger gas volumes than the mini sampling probe. It consists of a wedged-shape nozzle driven at a constant rotational speed so that it progressively traverses all areas of the stack at about 4 rpm; see Figure 3.11. The sample nozzle area covers one % of the duct area. Gas sampling rates were measured by an orifice. The gas was filtered through a nylon bag. This sampler was normally run for an hour, during which several grams of material were collected.

FIGURE 3.12 CASCADE IMPACTOR

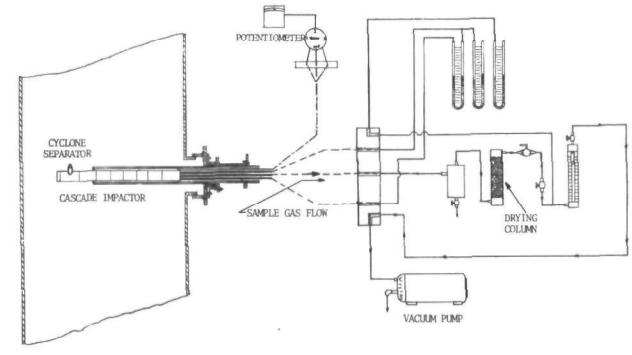

FIGURE 3.13 IMPACTOR STAGE

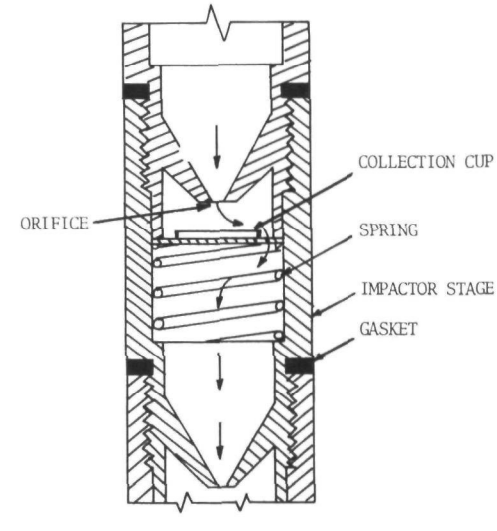

3.8 CASCADE IMPACTOR

A cascade impactor, shown in Figure 3.12, developed in-plant was used on one occasion to determine particle size distribution at the furnace outlet. The cascade impactor consists of a cyclone and five impactor stages.

The principle of the impactor is as follows. The cyclone is sized to collect 2.5-micron particles with an efficiency of 50%. The remaining particulate matter passes through the impactor stages. A typical stage is

shown in Figure 3.13. The particle laden gas passes through an orifice, which increases its velocity. The gas stream is deflected by the collection cup, and the heavier particles fail to make the abrupt change in direction and impact upon the collection cup. Placing the orifice closer to the collection cup traps smaller particles on the cup. The five stages are designed to collect different particle sizes, and the collection cups are weighed after sampling to determine the relative distribution of particle sizes.

3.9 ORSAT ANALYZER

A Fisher Orsat apparatus was used from time to time to analyze the flue gas for oxygen and carbon dioxide. The Bailey analyzer was used more or less as a check on the Bailey oxygen analyzer Model A57 and also to detect air leaks into the system. The Orsat apparatus used in this test is shown in Figure 3.14.

3.10 MAGNESIUM SULFITE-BISULFITE ANALYSIS

A modified Palmrose analysis was used in these tests to determine the chemical composition of the absorbing slurry. The recirculated slurry used to absorb SO_2 in the scrubbers is an aqueous mixture of magnesium sulfite, magnesium bisulfite, and magnesia. The magnesium sulfite is only partially soluble at the temperatures and concentrations encountered in this application. Thus, the actual major constituents are $MgSO_3 \cdot 6H_2O_{(s)}$, Mg^{++}, $SO_3^{=}$, HSO_3^-, OH^-, MgO, and $Mg(OH)_2$. This procedure is presented in Section A.4.

During each test two different Palmrose analyses were made from an unfiltered sample and a filtered sample.

FIGURE 3.14 ORSAT APPARATUS

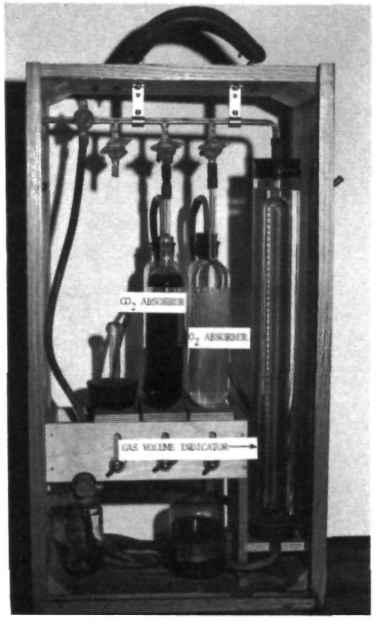

The analysis on the unfiltered sample was representative of the total sample, containing both dissolved and undissolved species. The filtered sample represented only those constituents which were dissolved. By taking both a filtered sample and an unfiltered sample, one can obtain a better idea of the actual makeup of the absorbing slurry. A photograph of the syringe filter holder is shown in Figure 3.15.

FIGURE 3.15 SYRINGE FILTER HOLDER

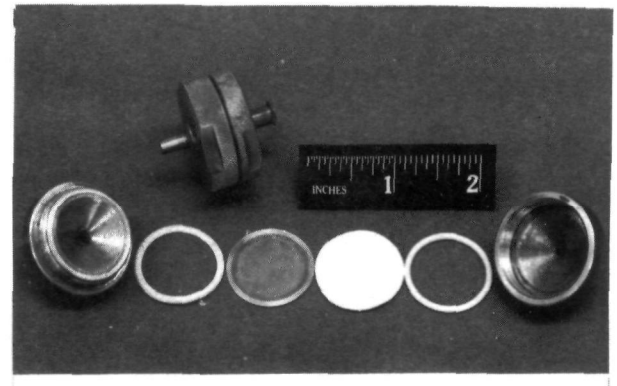

The 2 ml sample is withdrawn by a syringe from the SO_2 scrubbing system recirculation slurry line; see Figure 3.16. This line is fitted with a septum for insertion of the needle into the line. Figure 3.17 shown the Palmrose titration apparatus.

FIGURE 3.16 SYRINGE IN SEPTUM

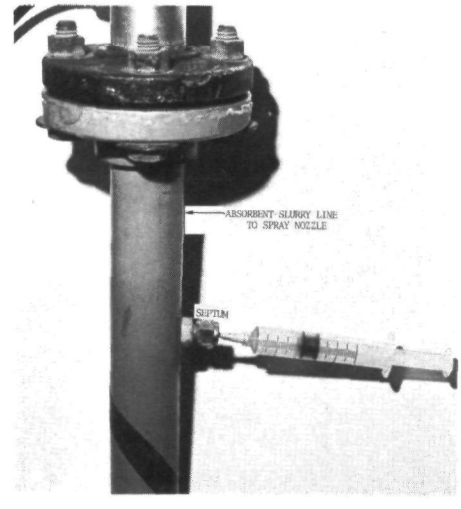

3.11 SULFATE ANALYSIS

3.11.1 Titration Method

The analysis of the absorbing slurry for sulfate concentration was another important determination required in these tests. During every test performed, at least one 10 ml sample was taken for sulfate analysis. Samples were taken with a 10 ml syringe and withdrawn through a septum from the SO_2 scrubbing slurry recirculation line; see Figure 3.16.

FIGURE 3.17 PALMROSE TITRATION APPARATUS

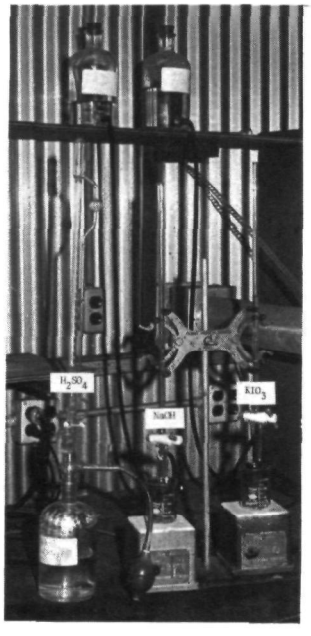

FIGURE 3.18 SULFATE SAMPLE PREPARATION APPARATUS

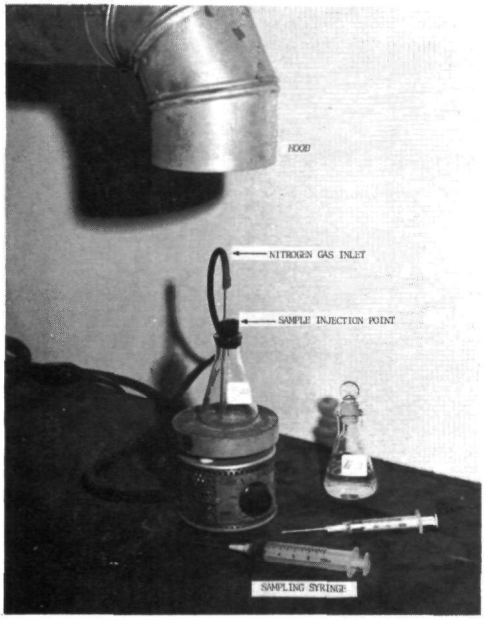

Sulfate analysis was carried out by a method developed in plant. Sampling was done so that oxidation was avoided. Sulfites and bisulfites were expelled from the sample by boiling in acid under nitrogen atmosphere, Figure 3.18. Interfering cations were removed by a cation (H^+) exchange column, Figure 3.19. The resulting sample was titrated under controlled conditions with barium chloride. See Section A.5 for a detailed description of the method.

3.11.2 Sulfate Sample for Chemistry Lab Analysis

A sample of the absorbent slurry from the SO_2 absorber was taken at various times, and the sulfate concentration was determined by our Chemistry Department using a standard gravimetric analysis. This was to provide a check on the sulfate analysis method developed in plant. The sample was taken from the product nozzle into an 8-ounce bottle containing 75 ml of isopropyl alcohol to prevent further oxidation of the sample.

3.12 PARTICULATE SOLIDS SAMPLING

A method was devised to determine the relative amount of solids, principally fly ash, contained in the particulate scrubbing slurry. This measurement was taken for a general documentation of data and also for the

future possibility of relating it to the "wear rate" of equipment such as pumps.

The actual test was very simple and consisted of filtering a known volume of sample and weighing the collected solids, thus determining the percent solids in the slurry. See Section A.6 for a more detailed description.

3.13 MAGNESIUM SULFITE SOLIDS SAMPLING

The method for the determination of percent solids in the SO_2 scrubber is exactly the same as that used in the particulate scrubber slurry analysis. The amount of sulfite solids is determined so that a material balance around the SO_2 scrubbing system can be made. See Section A.6, Particulate Solids Apparatus and Procedure, for a detailed discussion. The only deviation from this procedure was that only about 40 ml of sample was filtered because of the greater solids content.

3.14 MgO MAKEUP SLURRY TITRATION

In order to determine the amount of magnesium hydroxide solids in the makeup slurry, a simple acid titration of a known volume of sample was done. Previous to this a set of MgO slurry standards was prepared, and a curve of percent MgO solids versus ml of acid was drawn. See Figure 3.20

FIGURE 3.19 SULFATE TITRATION APPARATUS

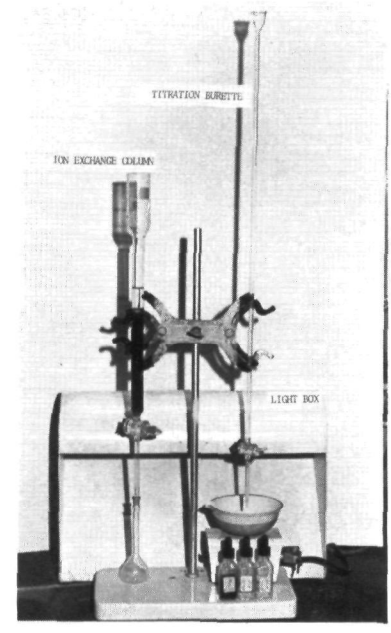

FIGURE 3.20 MgO MAKEUP TITRATION CURVE

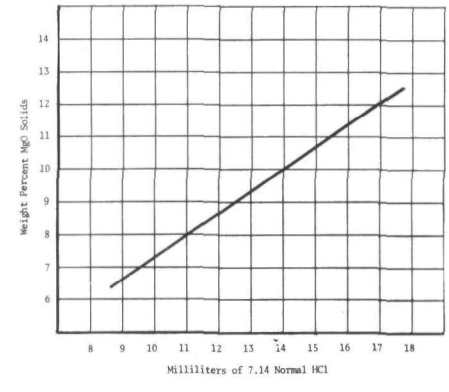

The curve was based on using a 20 ml sample and titrating with 7N HCl. See Section A.7 for the procedure.

3.15 OTHER MEASUREMENTS

The density of the various slurries was determined by a hydrometer. Measurements of pH of the slurries were made with a Leeds-Northrop pH indicator (Cat. #7664).

4.0 RESULTS

The results of both the parametric and extended tests are consolidated into one set of results. The only tests treated separately are the NO_x injection tests. Because of the great volume of data gathered, the computer printout for all tests will be included in an addendum to this report. A consolidating table of summary results will also be included in that addendum.

4.1 SO_2 ABSORPTION - PARTICULATE SCRUBBER

No SO_2 absorption in the particulate scrubber was discernible under any conditions tested. The pH of the water fly ash slurry ran between 2.0 and 3.5. No chemical additives were used in this scrubber.

4.2 SO_2 ABSORPTION - FLOATING BED ABSORBER

4.2.1 Parameter Study

The SO_2 absorption capability of the floating bed absorber (FBA) showed varying dependence upon the several parameters studied. Qualitatively, this dependence was as follows:

1. Liquid-to-gas-ratio: Absorption increased significantly with increasing L/G.
2. Stoichiometric ratio of MgO to SO_2: Absorption increased with increasing MgO flow up to a molar ratio of $MgO/SO_2 = 1.0$. Above this value absorption did not increase significantly.
3. pH of scrubbing slurry: Absorption increased with increasing pH up to a pH $\cong$ 7. Above this value absorption remained nearly constant.
4. Pressure drop: Absorption increased with increasing pressure drop across the bed.
5. Fly ash: The effect of the presence of high levels of fly ash (during extended operations when the particulate scrubber was bypassed) was uncertain.
6. Magnesium sulfate: The presence of high concentrations of dissolved magnesium sulfate reduced SO_2 absorption in the low pH range. At higher pH values, SO_2 absorption was not adversely affected.
7. Slaking: Conversion of magnesium oxide to the hydroxide before injection into the absorber did not improve SO_2 absorption.
8. Residence time: Increasing the total residence time of liquid within the FBA (including the sump) did not improve absorption. This should

not be confused with the residence time of liquid in intimate contact with the gas, which most surely could affect absorption.

4.2.2 Floating Bed Absorber - Absorption Correlation

In the presence of less than 0.10 gm fly ash/100 ml solution and 0.5 gm $MgSO_4$/100 ml solution, the SO_2 absorption data correlated well in terms of two operating parameters, L/G and spray slurry composition. The slurry composition, which is dependent upon the ratio of MgO/SO_2 and the solubility of $MgSO_3$, can be expressed indirectly in terms of the bisulfite concentration, $Mg(HSO_3)_2$ or slurry pH. Figure 4.1 illustrates the absorption as a function of L/G and bisulfite concentration. This data includes absorption across the sump, the two stages, and the mist disengagement section. Figure 4.2 is a similar plot in which the chemical composition is expressed in terms of pH.

The results illustrated in Figure 1 have been correlated by the following semiempirical expression using nonlinear regression analysis:

$$\ln \left| \frac{y_i' - 24.97\ B_o^2}{y_o' - 24.97\ B_o^2} \right| = 0.633\ L/G + 2.26 \qquad (4\text{-}1)$$

FIGURE 4.1 SO_2 ABSORPTION - FBA

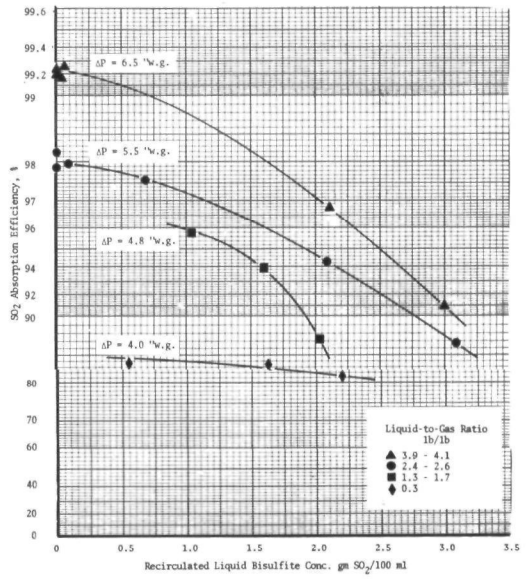

FIGURE 4.2 SO_2 ABSORPTION - FBA

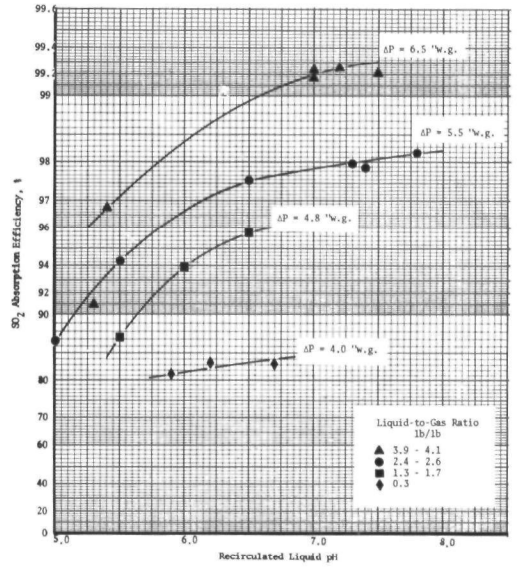

FIGURE 4.3 CORRELATION FOR EQUATION 4-1, SO_2 ABSORPTION - FBA

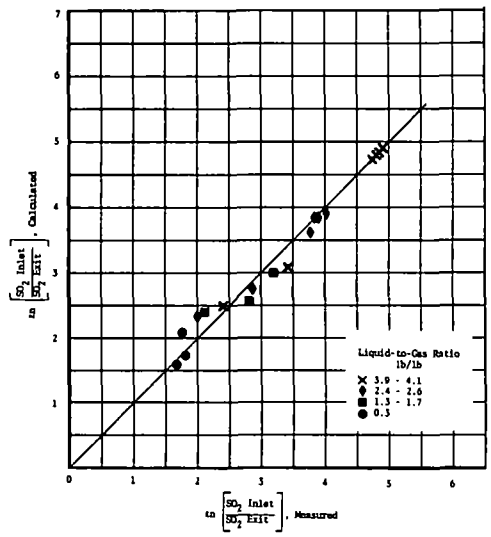

FIGURE 4.4 PRESSURE DROP - FBA

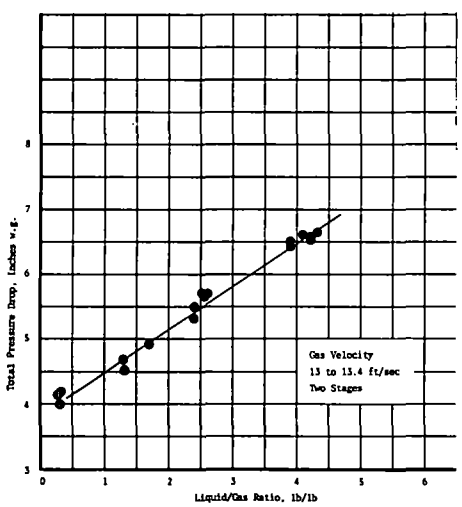

where y_i' = inlet SO_2 concentration, ppm

y_o' = exit SO_2 concentration, ppm

B_o = exit bisulfite concentration, gm/100 ml as SO_2

L/G = liquid-to-gas ratio

The correlation coefficient (R^2)* is 97.45. The second term in the argument of the log term represents the vapor pressure effect. The correlated data is illustrated in Figure 4.3. The derivation of the expression is described in Section 5.3.2.

Although absorption did seem to relate to pressure drop, this factor could not be isolated from the L/G effect as expressed above. This follows because a one-to-one correspondence existed between L/G and pressure drop (the gas velocity was constant). This relationship is expressed in Figure 4.4.

An uncertainty about the effect of fly ash upon SO_2 absorption exists because of the high level of absorption data scatter associated with the final extended test. Figure 4.5 illustrates this scatter. This figure is a plot of measured k_gA values versus calculated values based upon a rearrangement of Equation (4-1). The standard deviation is 69.0 compared to 17.0 for the correlated data in Figure 4.3.

*The statistical meaning behind the correlation coefficient is explained in Appendix B.

Only five data points were obtained on elevated sulfates. The sulfate concentration in the scrubbing slurry was between ∿18% and 60% of saturation. However these points showed a significant effect upon absorption. This data is illustrated in Figure 4.6 against the correlated curve for the normal sulfate situation.

The effect of slaking upon SO_2 absorption was minimal partly because the MgO was sufficiently reactive to convert a substantial portion to $Mg(OH)_2$ in cold water. Table 4.1 lists the fractional conversion of MgO with various conditions under which this conversion took place.

TABLE 4.1 MgO CONVERSION TO $Mg(OH)_2$

Test	Slaking Period, Hours	Slaking Temp., F	Conversion, %
D-030	5-7	45°	54.4
D-043	5-7	60°	83.3
D-036	2-3	180°	94.9

4.3 SO_2 ABSORPTION - VENTURI ABSORBER

4.3.1 Parameter Study

Except for pressure drop, the venturi absorber SO_2 performance showed a minimal dependence upon the parameters examined. The qualitative response is described below:

1. Liquid-to-gas ratio:
   Absorption was largely unaffected by changing L/G except when L/G fell below 2.2 lb/lb.

FIGURE 4.5 SO_2 ABSORPTION - FBA WITHOUT PRESCRUBBER

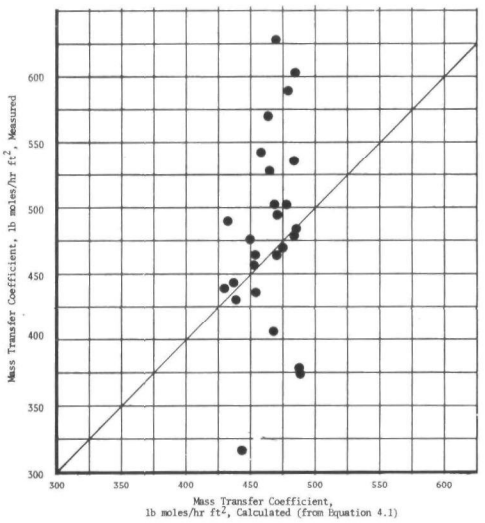

FIGURE 4.6 COMPARISON OF EFFECT OF HIGH SULFATES UPON SO_2 ABSORPTION - FBA

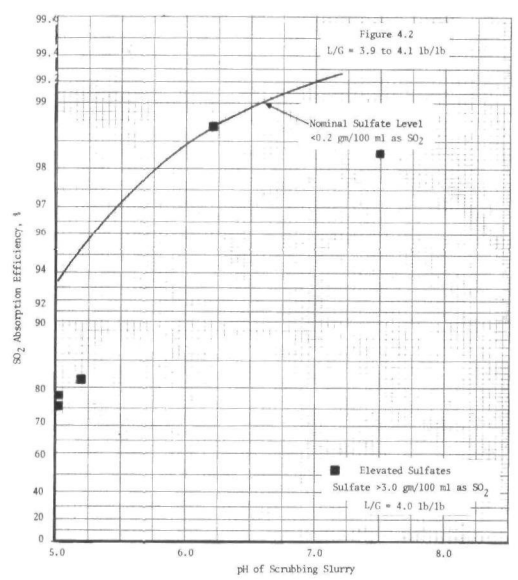

2. Stoichiometric ratio, MgO/SO_2: Sulfur dioxide absorption increased slightly with increasing MgO feed rate.
3. pH of scrubbing slurry: Sulfur dioxide absorption increased moderately with increasing pH.
4. Pressure drop: Sulfur dioxide absorption increased significantly with increasing pressure drop.
5. Fly ash: The presence of fly ash had no measurable effect upon SO_2 absorption performance.
6. Magnesium sulfate: The presence of moderate concentrations of magnesium sulfate had a retarding effect upon SO_2 absorption. This effect was determined only for low pH.
7. Slaking: Conversion of magnesium oxide to the hydroxide before injection into the venturi did not improve SO_2 absorption.
8. Residence time of liquid: Increasing liquid holdup (including the sump) did not improve SO_2 absorption.

FIGURE 4.7 SO_2 ABSORPTION - VENTURI ABSORBER

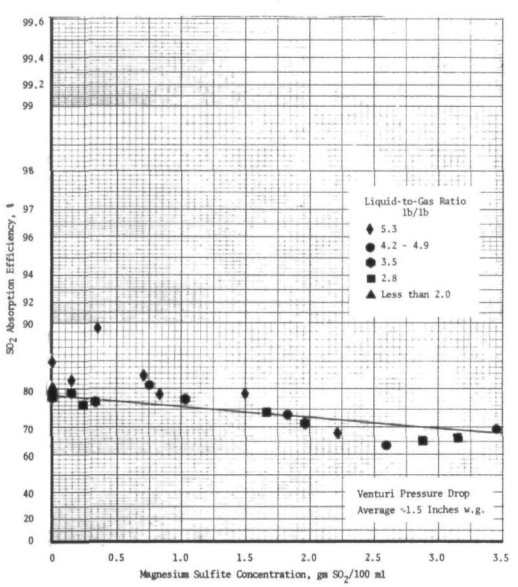

4.3.2 Venturi Absorber Absorption Correlations

Since the bulk of the SO_2 absorption data ranged only from 65 to 85%, no strong correlations between absorption and operating parameters (with the possible exception of pressure drop) were determined. The effect of composition upon absorption for a wide range of L/G's is shown in Figures 4.7 and 4.8. Mathematically this data is correlated as follows:

$$\ln(1-E) = -0.694[1-e^{-1.633(pH - 5.0)}] - 0.8779 \qquad (4\text{-}2)$$

where E = absorption efficiency, fractional

pH = acid strength

The correlation coefficient of 35% was low primarily because the variance in the percentage absorption was narrow. This curve fit applied only for pressure drops between 1.0 and 2.0 inches w.g.

Although there are only three data points at elevated pressure drop, arising by an accidental test complication, the effect is sufficient to warrant presentation here. The correlation between efficiency and pressure drop is shown in Figure 4.9. A dotted straight line is used because there is insufficient data to justify a linear relationship. Mathematically this data is correlated as follows:

$$\ln(1-E) = -1.039 - 0.3137\ (\Delta P) \qquad (4.3)$$

Correlation coefficient = 67%

$$\ln(1-E) = -0.3298\ \Delta P\ [1-e^{-0.9547(pH-5.0)}] - 1.122 \qquad (4.4)$$

Correlation coefficient = 65%

where E = absorption efficiency, fractional

ΔP = venturi absorber pressure drop, "w.g.

pH = acid strength of recirculating slurry

Equation 4.3 is a simple straight line least squares fit, and the second correlation is a nonlinear regression analysis curve fit which includes the

FIGURE 4.8 SO_2 ABSORPTION - VENTURI ABSORBER

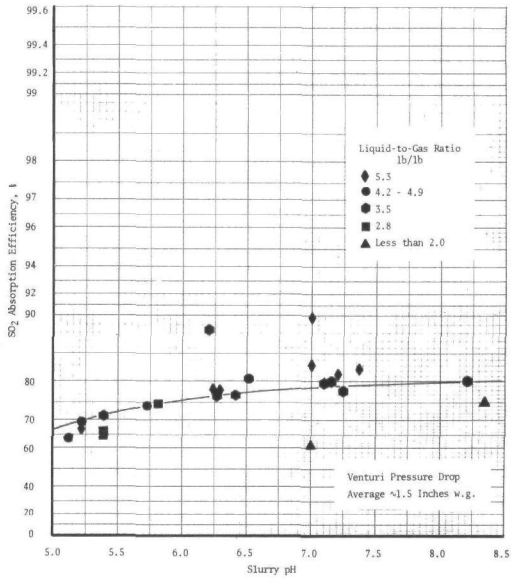

FIGURE 4.9 PRESSURE DROP EFFECT UPON SO_2 ABSORPTION - VENTURI ABSORBER

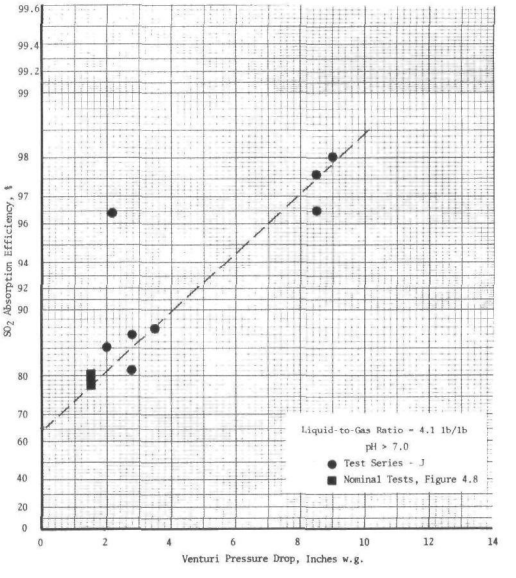

FIGURE 4.10 SO_2 ABSORPTION CORRELATION FOR VENTURI ABSORBER

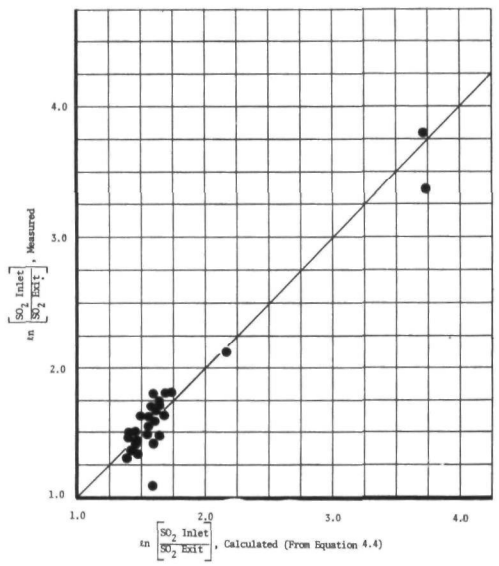

FIGURE 4.11 COMPARISON OF EFFECT OF HIGH SULFATES UPON SO_2 ABSORPTION - VENTURI ABSORBER

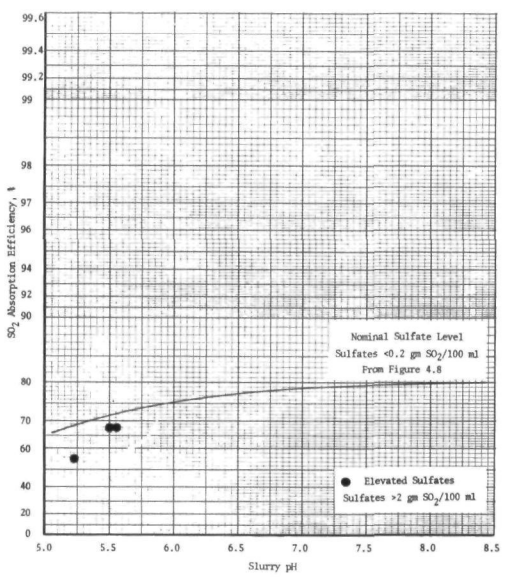

slurry pH effect. This latter correlation must be used with caution since the pH and pressure drop effects were determined separately. The interaction between low pH and high pressure drop was not determined experimentally. Nevertheless Figure 4.10 shows how Equation 4.4 correlates all venturi absorption data except that from the elevated sulfate tests. All of the venturi absorber SO_2 absorption data is tabulated in Table 4.2 of the addendum.

Although only three data points were obtained on the effect of elevated sulfate concentration (approximately 10% of saturation) and all were below a pH of 5.7, the data was consistent and showed a definite retarding effect. This data is shown in Figure 4.11 plotted against the datum condition as correlated by Equation 4-2. Whether this effect would vanish at higher pH, as was indicated in the analogous FBA tests, was not explored.

4.4 CRYSTALLINE DEPOSITION

Deposition of hard crystalline deposits in piping, pumps, sumps, and spray nozzles varied from not at all to extremely rapid. The degree and rate of deposition were not quantified except in terms of how rapidly the scrubbing system was adversely affected.

The deposits resulted primarily from precipitation of magnesium sulfite. The form of the deposit was identified by X-ray diffraction and is reported in Table 4.2.

TABLE 4.2 X-RAY DIFFRACTION ANALYSIS OF CRYSTALLINE DEPOSITS

Location	Identification
Venturi Absorber Sump Outlet Flange	$MgSO_3 \cdot 6H_2O$ (Major)
Recirculation Pump Suction in Plastic Pipe Section	$MgSO_3 \cdot 6H_2O$ (Major) $MgSO_4 \cdot H_2O$ (Possible Trace)
Venturi Absorber Slurry Spray Nozzle	$MgSO_3 \cdot 6H_2O$ (Major) $MgSO_4 \cdot H_2O$ (Possible Trace)

4.4.1 Parameters Affecting Deposition

The parameters affecting the formation are described below:

1. Fly ash in spray slurry: Fly ash in concentrations of 1 to 3% by weight completely eliminated the formation of crystalline deposits within the scrubbing system. This is illustrated in Figure 4.12, which depicts the effect of fly ash upon deposits found in a 2-inch S.S. pipe leading to the spray nozzle.
2. Chemical composition of scrubbing slurry: The rate of deposition was correlated to the acidity of the scrubbing slurry. On the strongly acid side, $Mg(HSO_3)_2$ >∿1.0 gm/100 ml as SO_2, deposition

FIGURE 4.12 THE EFFECT OF FLY ASH UPON DEPOSITS FORMATION

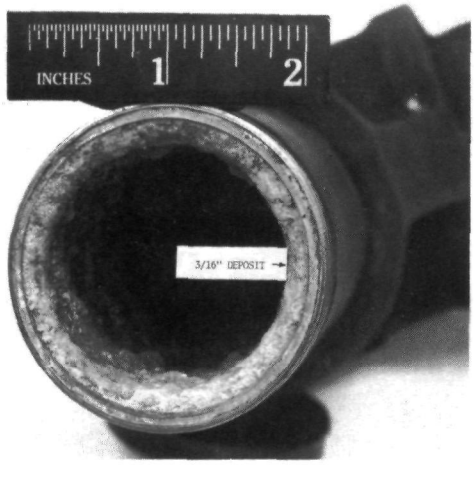

Without Fly Ash

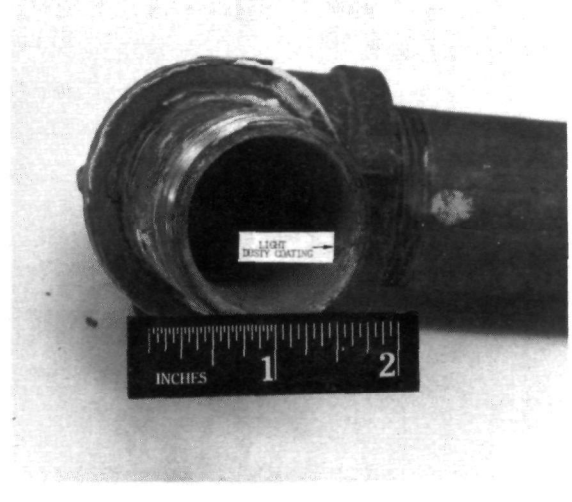

With Fly Ash

formed to a sufficient degree to adversely affect scrubber operation within 2 to 3 hours. If the slurry was maintained slightly alkaline, the system operated for about 24 hours without excessive deposition.

Summarizing:

Bisulfite Conc., gm/100 ml as SO_2	pH	Operating Period, Hours
>∿1.0	>6	2-3
∿0	<7	∿24

3. MgO makeup modifications: By relocating the makeup MgO feed location from the sump to the active mass transfer section (the top plate of the FBA and the throat of the venturi absorber), by slaking the MgO to the hydroxide, and by providing supplemental agitation in the sumps, the deposition rate was reduced substantially. Prior to these modifications, 24 hours was about the maximum operating life. These modifications permitted runs up to 90 hours (the maximum possible because of a limited coal supply) without operating problems due to deposition. Examination did show however that deposits had formed under these operating conditions.
4. Materials: Deposition varied as a function of materials and the location of these materials within the scrubber and auxiliary components. Deposits at no time formed within the vertical PVDC line from the recirculation pump to the spray nozzle. Deposition was however a recurring problem at the spray nozzle and product nozzle (both of stainless steel). Deposition was severe at times within the recirculation pump and the sump. The plastic pipe (PVDC) from the sump to the recirculation pump accumulated deposits differing in appearance from those formed in the stainless steel pipe. The deposits that formed within the plastic pipe were not bonded to the surface as they were to the stainless steel surfaces. No crystalline deposits formed at any time within the scrubbing sections exposed to flue gas. Deposition seemed to be most

pronounced at points of extreme turbulence such as the sump suction and discharge and even along the threaded sections of plastic pipe. Deposition occurrence is summarized in Table 4.3.

TABLE 4.3 DEGREE OF DEPOSITION AT VARIOUS LOCATIONS DURING PERIODS OF RAPID FORMATION

Location	Degree of Deposit Formation
Venturi and cyclone: gas-liquid contact zone	nil
Floating bed absorber: gas-liquid contact zone	nil
PVDC recirculation line	nil
Spray nozzles	severe
Recirculation pump (casing and impeller)	severe
PVDC line from sump to pump	moderate
Sumps below liquid level	severe
Sumps above liquid level	nil
Iron angle baffle (see Figure 2.28)	moderate

4.5 DEPOSITION AT WET-DRY LINES

Deposition of solids where the flue gases first contact the spray slurry was a problem which occurred in various degrees as follows:

1. Hot flue gases* at particulate scrubber inlet: No deposits formed at any time. The particulate venturi in Figure 4.13 after several hundred hours of operation is shown to be free of deposits.

FIGURE 4.13 PARTICULATE SCRUBBER - INSIDE VIEW

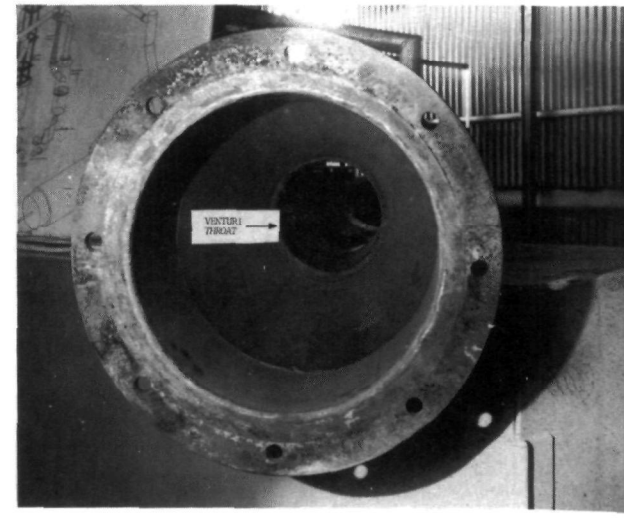

*Flue gases from furnace exit at 400 to 650 F.

FIGURE 4.14 SULFATE FORMATION - FBA WITH PRESCRUBBER

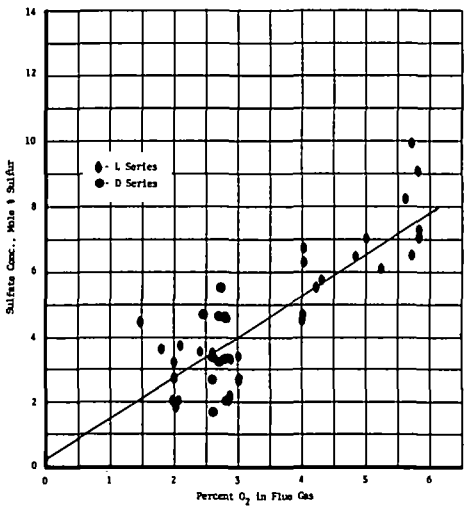

FIGURE 4.15 SULFATE FORMATION - FBA WITHOUT PRESCRUBBER

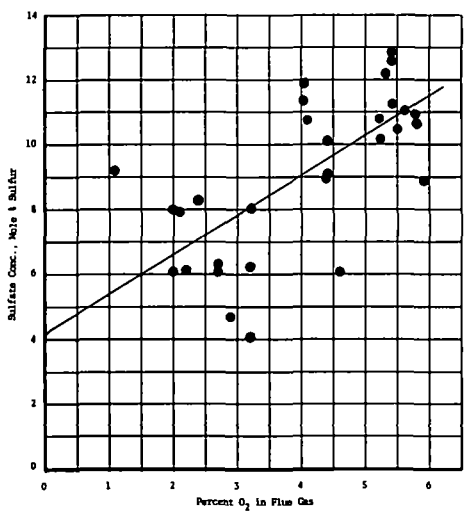

*Flue gases from particulate scrubber cooled to ∿130F.

2. Attemperated flue gases* at FBA and venturi absorber: No deposits were formed at any time.
3. Hot flue gases at venturi absorber: Deposits formed rapidly. The analysis by X-ray diffraction of these deposits identified this material to be an aggregate of fly ash and $MgSO_3 \cdot 3H_2O$. These deposits formed near the top of the throat.
4. Hot flue gases at FBA inlet: Deposits formed around the rim of the inlet duct and within the horizontal section leading to the inlet. See Section 2.6.3 for details of the inlet design.

4.6 SULFATE FORMATION

4.6.1 Floating Bed Absorber

Sulfate formation within the FBA was examined as a function of slurry pH, bisulfite concentration, SO_2 mass transfer coefficient, oxygen concentration in the gas phase, and operation with and without the prescrubber. The following results were apparent:

1. With the prescrubber in service the sulfate formation was a function of oxygen concentration only. This data correlated as follows and is plotted in Figure 4.14.

   Mole % sulfate = 0.287 + 1.2647 Yo_2

   Standard deviation = 1.163

   Correlation coefficient = 69.3%

2. With the prescrubber not in service, i.e., with the furnace exit gases proceeding directly to the FBA, the sulfate level was again a function of oxygen concentration only. However the level averaged 4.9 mole % higher than that found in the tests with the prescrubber in operation. This data is correlated as follows:

   Mole % sulfate = 5.186 + 1.213 Yo_2

   Standard deviation = 1.94

   Correlation coefficient = 44.5%

   This data is plotted in Figure 4.15. The averages of the individual tests are listed in Table 4.4.

TABLE 4.4 AVERAGE SULFATE FORMATION IN FBA FOR INDIVIDUAL TEST SERIES

Test Series	Sulfate Conc. Molarity	Sulfate Conc. Std. Dev.	Sulfate Conv. Mole %	Sulfate Conv. Std. Dev.	Oxygen Conc.
D	0.0247	0.0075	3.62	1.277	2.4
L	0.0230	0.0073	2.85	0.80	2.0
L	0.0254	0.0093	2.94	0.739	3.0
L	0.0347	0.0056	5.62	0.87	4.0
L	0.0386	0.0092	5.93	1.30	5.0
L	0.0414	0.0049	8.01	1.31	5.7
M	0.0360	0.0108	7.20	1.98	3.2
M	0.0527	0.0143	10.91	2.13	4.3
M	0.0542	0.0089	12.1	1.25	5.5

4.6.2 Venturi Absorber

The rate of sulfate formation in the venturi absorber was quite erratic. The tendency to form sulfates was examined as a function of slurry pH, bisulfite concentration, SO_2 mass transfer coefficient, oxygen concentration in the gas phase, and operation with and without the prescrubber.

The following results were apparent:

1. With the particulate scrubber functioning, the rate of sulfate formation in the venturi absorber appeared to be independent of the above parameters. The average formation rate was as follows:

   Average sulfate = 3.8 mole % of total sulfur gases absorbed. This data is plotted in Figure 4.16. In terms of individual test series, the sulfate formation rate is categorized as in Table 4.5.

FIGURE 4.16 SULFATE FORMATION - VENTURI ABSORBER WITH PRESCRUBBER

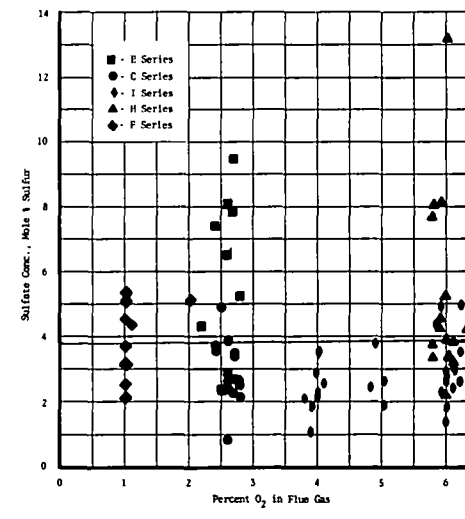

TABLE 4.5 AVERAGE SULFATE FORMATION IN VENTURI ABSORBER FOR INDIVIDUAL TEST SERIES

Test Series	Sulfate Conc. Molarity	Sulfate Conc. Std. Dev.	Mole % Total Sulfur Mole %**	Mole % Total Sulfur Std. Dev.	Oxygen Conc.
C	0.0179	0.0059	2.87	0.97	2.6
E	0.0506	0.0196	6.00	2.45	2.6
F	0.0443	0.0144	3.76	1.13	1.0
H	0.0439	0.0185	5.64	2.85	6.0
I	0.0182	0.0054	2.28	0.736	4.0
I	0.0226	0.0108	2.68	0.75	5.0
I	0.0237	0.0081	3.097	0.991	6.0

**Mole % of total sulfur gases present as sulfates.

FIGURE 4.17 SULFATE FORMATION - VENTURI ABSORBER WITHOUT PRESCRUBBER

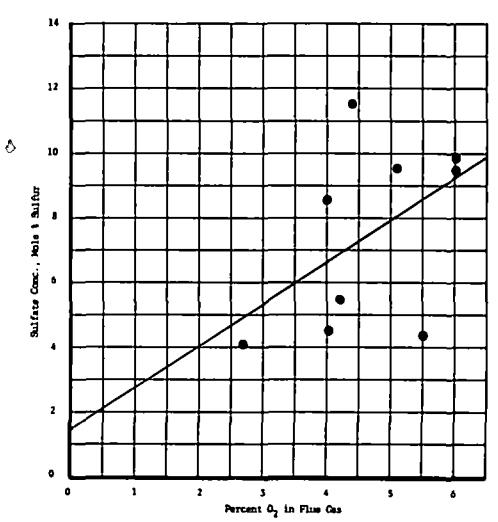

2. With the particulate scrubber removed from the circuit, i.e., with the furnace exit gases taken direct to the venturi absorber, the sulfate formation levels showed two significant effects:
   a. The sulfate formation level was significantly elevated.
   b. The sulfate formation rate showed a possible dependence upon oxygen concentration.

A least squares linear fit of this data yielded:

Mole % sulfate = 1.485 + 1.2867 Y_{O_2}

Standard deviation = 2.6 mole %

Correlation coefficient (R^2) = 25%

This data and curve fit are plotted in Figure 4.17. No other dependence such as venturi pressure drop or SO_2 mass transfer coefficient had any apparent influence upon sulfate formation.

4.7 PARTICULATE COLLECTION

4.7.1 Particulate Venturi Scrubber

This scrubber operated under a limited range of conditions listed as follows:

Pressure drop, 5.0 to 8.2" w.g.

Liquid-to-gas ratio, 1.6 to 2.1 lb/lb

Ash slurry concentration, 0.4 to 1.1% by wt.

Gas velocity at throat, 145 to 165 ft/sec

With the exception of six points believed to be in error because the filter was contaminated with slurry droplets carried over from the cyclone, the results ranged from 0.010 to 0.045 grain/DSCF. These results were not correlatable to any of the above parameters. The results plotted as a function of pressure drop are shown in

Figures 4.18 and 4.19. The average particulate scrubber dust loading was 0.0248 grain/DSCF with a standard deviation of 0.0091 grain/DSCF. The equivalent average efficiency was 99.24% for an average pressure drop of 6.2" w.g. This data is listed in Table 4.6.

For those tests in which inlet loadings to the particulate scrubber were obtained simultaneously with exit loadings, the average efficiency amounted to 99.19% at an average pressure drop of 6.4" w.g.

The pressure drop relationship for this venturi for a constant gas velocity of 136 ft/sec is shown in Figure 4.20.

FIGURE 4.18 DUST COLLECTION PERFORMANCE PARTICULATE SCRUBBER

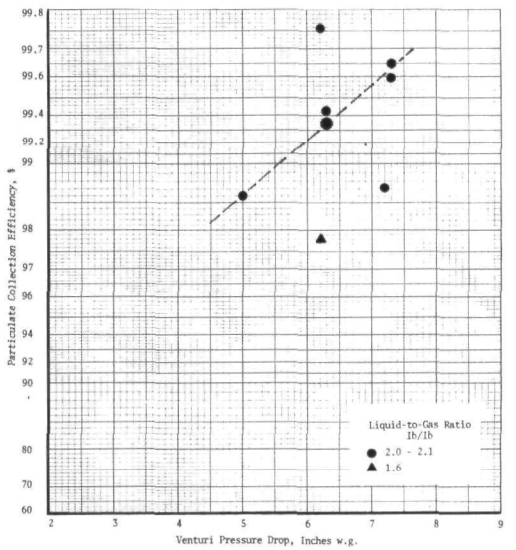

FIGURE 4.19 DUST COLLECTION PERFORMANCE PARTICULATE SCRUBBER

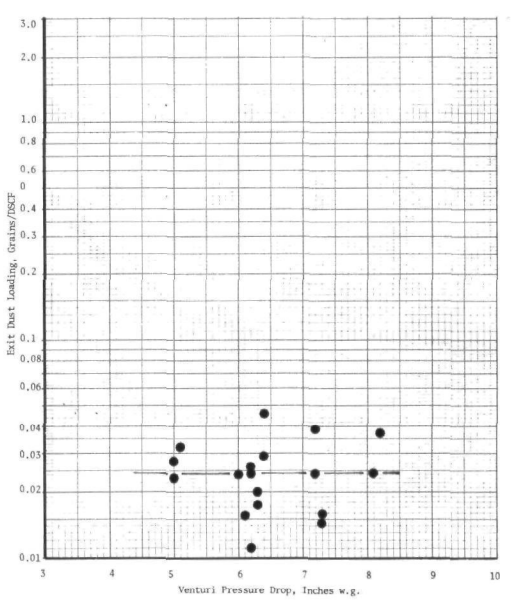

4.7.2 Floating Bed Absorber With Prescrubber

The particulate collection capability of the FBA upon the fine ash passing through the particulate scrubber was too low to measure with confidence. The average exit dust loading was 0.0256 grain/DSCF compared to an average inlet loading of 0.245 grain/DSCF. There appears to be a tendency for the FBA particulate collection to decrease slightly with increasing L/G and pressure drop. This is illustrated in Figure 4.21. The results are listed in Table 4.7.

4.7.3 Floating Bed Absorber Without Prescrubber

The floating bed absorber operating upon the hot furnace gases performed

TABLE 4.6 PARTICULATE COLLECTION PERFORMANCE OF PARTICULATE SCRUBBER

Test No.	Dust Loadings Grains/DSCF Inlet	Exit	% Eff.	ΔP "w.g.	L/G #/#	Comments
B007	---	0.0288	---	6.4	1.6	
B008	1.1330	0.0254	97.76	6.2	1.6	
B009	---	0.0237	---	6.0	1.6	
B010	1.1881	---	---	5.8	1.6	
C013	1.8448	0.0626	96.60	6.1	1.6	Contaminated Filter
C014	---	0.1009	---	5.9	1.6	"
C015	---	0.0579	---	6.1	1.6	"
C016	3.0647	0.0198	99.35	6.3	2.0	
C017	---	0.0277	---	6.3	2.0	"
C018	2.6291	0.0328	98.75	6.3	2.0	"
C019	---	0.0332	---	6.3	2.0	"
C020	1.5974	0.0227	98.58	5.0	2.1	
C021	---	0.0272	---	5.0	2.1	
C022	3.5799	---	---	5.5	2.3	
C023	17.5586	---	---	5.4	2.1	
C025	4.1494	---	---	5.7	2.0	
D034	5.4823	---	---	7.6	2.0	

FIGURE 4.20 PRESSURE DROP - PARTICULATE SCRUBBER

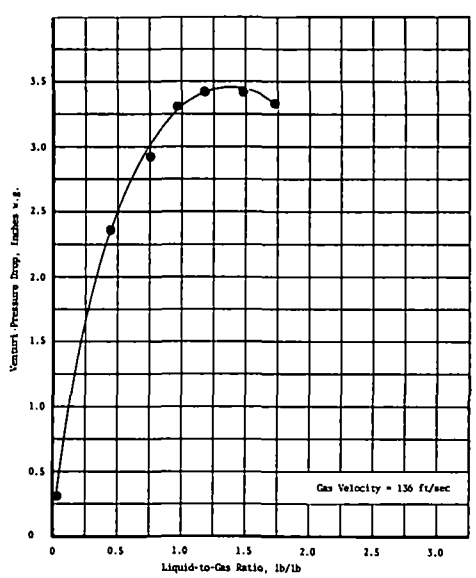

moderately well. An average exit dust loading of 0.0609 corresponded to an average collection efficiency of 98.2% at a pressure drop of 6.0 "w.g. The operating parameters are listed as follows:

Pressure drop, 5.0 to 6.8 "w.g.

Liquid-to-gas ratio, 3.7 to 4.3 lb/lb

Gas velocity, 13 to 14 ft/sec

The primary results are listed in Table 4.8 and plotted in Figure 4.21.

4.7.4 Venturi Absorber With Prescrubber

The particulate collection capability of the venturi absorber acting on the fine ash passing through the particulate collector was too low to measure with confidence. The average measured dust concentration leaving the venturi absorber was 0.0238 grain/DSCF. Compared to the average 0.0248 grain/DSCF leaving the particulate scrubber, this corresponds to less than 5% collection, which represents a finer resolution than that data justifies. The particulate collection results for the venturi absorber are plotted in Figure 4.22. The parameter ranges and results are summarized as follows:

Pressure drop, 1.4 to 1.7" w.g.

Liquid-to-gas ratio, 2.8 to 4.9 lb/lb

Average exit dust loading, 0.0238 grain/DSCF

Average inlet dust loading, 0.0248 grain/DSCF

All of the results are listed in Table 4.9.

4.7.5 Venturi Absorber Without Prescrubber

Although only two data points were obtained, these were consistent with usual venturi scrubber experience. These results are summarized in Table 4.10. These results show a substantial improvement in particulate collection as a function of pressure drop. Note that the venturi absorber operating at 8.4" w.g. is about as effective as the particulate venturi operating at ∿6.5" w.g. but is significantly less effective at 2.7" w.g. This data is also plotted in Figure 4.22 to illustrate the composition effect of the exit dust loading with and without the particulate scrubber in operation.

4.8 NO_x ABSORPTION

The degree of absorption of nitrogen oxides across the particulate scrubber and gas absorber was negligible. The average NO_x concentrations measured are listed in Table 4.11. Although this

FIGURE 4.21 DUST COLLECTION PERFORMANCE - FBA

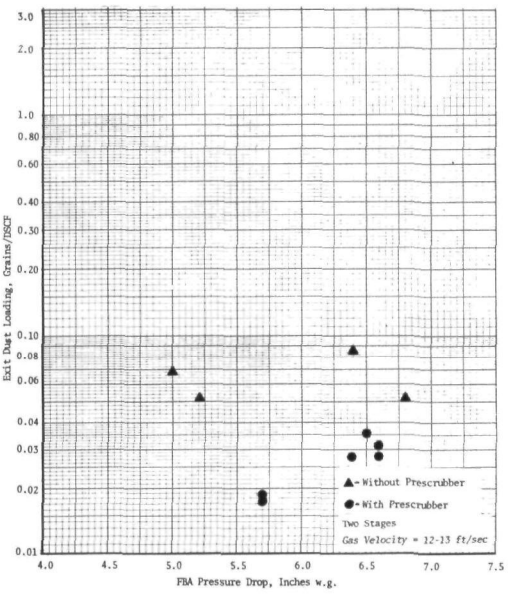

TABLE 4.7 PARTICULATE COLLECTION ACROSS FBA WITH PRE-SCRUBBER

Test #	Dust Loadings Grains/DSCF Inlet	Exit	ΔP "w.g.	L/G #/#
D038	0.0240	0.0354	6.5	3.9
D042	0.0365	0.0302	6.6	4.2
D043	0.0241	0.0167	5.7	2.6
D044	0.0145	0.0266	6.6	4.3
D047	0.0159	0.0179	5.7	2.6
L149	0.0317	0.0269	6.4	5.0

TABLE 4.8 PARTICULATE COLLECTION ACROSS FBA WITHOUT PRE-SCRUBBER

Test #	Dust Loadings Grains/DSCF Inlet	Exit	% Eff.	ΔP "w.g.	L/G #/#
M175	3.9848	0.0502	98.74	6.8	4.3
M186	1.9907	0.0816	95.90	6.4	6.0
M195	---	0.0482	---	5.2	4.0
M197	2.4981	0.0638	97.45	5.0	4.1
M202	4.9815	---	---	6.4	3.7

TABLE 4.9 PARTICULATE COLLECTION ACROSS VENTURI ABSORBER WITH PRESCRUBBER

Test #	Dust Loadings Grains/DSCF Inlet	Exit	ΔP 'w.g.	L/G #/#
E049	0.0104	0.0171	1.7	4.9
E053	0.0172	0.0216	1.5	3.0
E054	0.0155	0.0214	1.4	2.8
F062	0.0247	0.0286	1.6	4.4
F074	0.0460	0.0303	1.4	4.6

FIGURE 4.22 DUST COLLECTION PERFORMANCE - VENTURI ABSORBER

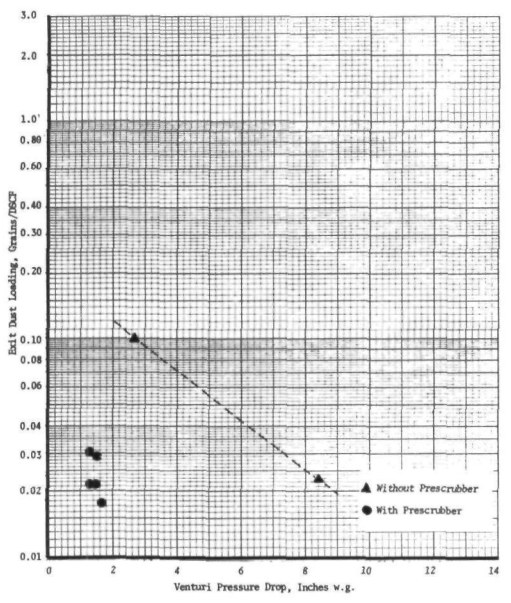

TABLE 4.10 PARTICULATE COLLECTION IN VENTURI ABSORBER (WITHOUT PRESCRUBBER)

Test No.	Dust Loading, Grains/DSCF Inlet	Exit	Pressure Drop, 'w.g.	Liquid/Gas, #/#
J130	3.0191	--	9.0	4.8
J131	--	0.0240	8.4	5.2
J132	4.3868	0.1003	2.7	5.4

data indicates a reduction in NO_x across each scrubber, this is not a valid conclusion since the standard deviation in the NO_x measurements is larger than the indicated NO_x absorption. All of the NO_x results are listed in Table 4.12.

4.9 NO_x INJECTION TEST

The feasibility of promoting NO_x absorption by injecting nitrogen dioxide (NO_2) into the flue gas ahead of the venturi absorber was tested. The principal results of this test are as follows:

1. The total NO_x absorption was not improved. In fact, the total NO_x increased from 635 ppm at the furnace exit to 984 ppm at the pilot plant exit.
2. The magnesium sulfate concentration increased substantially. The nominal sulfate concentration without NO_2 injection ran approximately 3.8 mole % total sulfurous gases absorbed. This value increased to between 15 and 23 mole % of the total absorbed sulfurous gases when NO_2 was injected.

The primary results of this test are listed in Table 4.13.

See Section 3.3.2 for a detailed description of this test.

4.10 SO_3 FORMATION

The sulfur trioxide concentration at the furnace exit varied between 1.10 and 144 ppm and averaged 18.7 ppm. These

results are tabulated in Table 4.14. The variance was examined as a function of excess air and adiabatic flame temperature but could not be resolved.

4.11 THE FLOATING BED ABSORBER TRAY HYDRAULICS

The effect of packing height upon the dry pressure drop across the FBA was evaluated. The results are listed in Table 4.15.

The attrition or weight loss of the balls after 270 hours of operation was examined. The results are shown in Table 4.16.

TABLE 4.11 AVERAGE NO_x CONCENTRATIONS THROUGHOUT PILOT PLANT

	Average NO_x, ppm	Standard Deviation, ppm
Furnace Exit	847	140
Particulate Scrubber Exit	807	125
Pilot Plant Exit	792	125

TABLE 4.13 NO_2 INJECTION TEST RESULTS

Test No.	NO_x Concentration, ppm Furn. Exit	Part. Scrub. Exit	Pilot Plant Exit	Sulfate Conc. GM Moles/Liter
K-138	657	1609*	1036	0.203
K-139	740	1692*	999	0.157

TABLE 4.12 SUMMARY OF NO_x RESULTS

Test #	Furnace Outlet	ppm NO_x Concentrations Particulate Outlet	Pilot Plant Outlet
B007	875		--
B008	991		953
B009		890	
B010		849	
B011			899
C012			782
C013		771	
C014		857	
C016	999		1124
C017	1209		1055
C018	1123	1077	
C019		1129	926
C024	903 908 832		
C025	--	926 844 885	
C026	--		882 690 924
E048	--	761 763	753 769
E050	--	773 774	698 864
E051	--	575 738	696 617
E052	--	752 680	777 807
E055	713 833		
F065	769 721		760 558
F076			701 618
H084			
H099			
K138			
K139			
M176			
M184	752 635		777 763
M186	769 727		
M195	746 752		689
M202	848 805		
L169			663 706
L157		648 758	754 693
L148		694 723	824 764
D037		698	794 876
D039		982 965	663
D040		866 852	688 864
D041		739 759	706 755

*This NO_x concentration is based upon an estimated NO_2 injection rate as measured on an uncalibrated rotameter. The estimated NO_2 injection via the rotameter was equivalent to 952 ppm. Based upon the sulfate formation increase however, the estimated NO_2 concentration would be approximately equivalent to 590 ppm NO_2.

TABLE 4.14 SULFUR TRIOXIDE CONCENTRATION AT FURNACE EXIT

	Test #	SO_3 Conc.	O_2 Conc.	Comments
	C-020	15.30		Chem. Lab. Method, not N_2 purged
		3.85		Chem. Lab. Method, purged
	C-022	3.43		Chem. Lab. Method, not purged
		0.94		Chem. Lab. Method, purged
	C-023	1.17		Chem. Lab. Method, purged
		1.41		Chem. Lab. Method, purged
	C-027	2.83		Chem. Lab. Method, not N_2 purged
		1.23		Chem. Lab. Method, purged
	D-031	6.42		Chem. Lab. Method, purged, acidified with HCl
		6.26		Chem. Lab. Method, purged, acidified with HCl
		4.50		Chem. Lab. Method, purged
		3.86		Chem. Lab. Method, purged
	D-032	2.88		Chem. Lab. Method, purged
		3.19		Chem. Lab. Method, purged
2/24/70	SO_3-1	29.6	2.8	Goksoyr and Ross Method
	SO_3-2	9.6	2.9	"
	SO_3-3	45.2	2.5	"
	SO_3-4	86.5	5.0	"
	SO_3-5	--	5.0	"
	SO_3-6	--	5.0	"
	SO_3-7	17.1	2.5	"
	SO_3-8	52.2	2.5	"
	SO_3-9	6.4	2.2	"
	SO_3-10	62.0	2.3	"
	SO_3-11	144.0	2.4	"
	SO_3-12	96.3	2.2	"

	Test #	SO_3 Conc.	O_2 Conc.	Comments
	F-158	2.89		Goksoyr and Ross Method
	F-160	5.00		"
	F-168	9.30		"
	F-177	22.0		"
3/5/70	#1			"
	#2	2.31		"
	#3	5.88		"
	#4	6.79		"
	#5	6.40		"
	#6	5.04		"
	F078	21.0	2.0	"
	H088	26.6	6.2	"
	H100	32.0	6.0	"
	L141	22.2	5.2	"
	L149	18.5	4.0	"
	L159	6.6	2.0	"
	L161	0.0	2.8	"
	L169	8.7	2.0	"
	L172	8.4	4.0	"
	M178	10.5	4.4	"
	M184	11.4	5.2	"
	M188	6.3	5.8	"
	M194	16.5	1.1	"

TABLE 4.15 EFFECT OF BED HEIGHT ON DRY PRESSURE DROP ACROSS FBA

Height of Bottom Bed, inches	Height of Top Bed, inches	Overall FBA ΔP, "w.g.*
6.5	7.5	4.15
3.5	3.5	3.40
0	0	2.95

* Air Density = 0.074 lb/ft^3
Air Velocity = 12.5 ft/sec

TABLE 4.16 FBA PACKING ATTRITION AFTER 270 HOURS

	Average Weight, grams	Standard Deviation, grams	% Wt. Loss
Top Tray	4.24	0.16	16.5
Bottom Tray	4.60	0.12	9.1

*A description of these various methods is given in Sections A.2 and A.2.6 of Appendix A.

5.0 DISCUSSION OF RESULTS

5.1 DATA ANALYSIS

The results reported in Section 4.0 included all of the most pertinent findings from this project. For the sake of completeness, however, all of the recorded data and computed results are included in an addendum. The addendum includes the method of calculation of each item, a table of primary results, and the computer printout from each test. Examples of the computer sheets are illustrated in Figure 5.1.

FIGURE 5.1 COMPUTER RESULTS

MAGNESIUM BASE SLURRY SCRUBBING PROGRAM

RUN NUMBER I-112 DATE 4-1-70 TIME OF DAY 0340

FLUE GAS DATA	FLOW #/HR	TEMP. F	SO2 PPM	SO3 PPM	NOX PPM	FLYASH GR/DSCF	HUM. #/#	DEW POINT F	DRY FLOW #/HR	STAT PRES IN.H2O
PRIMARY AIR	499.	120.0	------	-----	-----	-------	0.006	46.5	496.	17.6
SECONDARY AIR	4878.	648.3	------	-----	-----	-------	0.004	37.4	4858.	10.9
FURNACE EXIT	5742.	700.0	2987.9	*****	*****	*******	0.041	105.3	5517.	5.4
PART.SCRB.INLET	5742.	650.0	******	*****	*****	*******	0.041	105.3	N.A.	2.7
PART.CYC.EXIT	5667.	138.0	2568.9	*****	*****	*******	0.128	140.8	5022.	-9.5
VENT ABS.INLET	5667.	138.0	******	*****	*****	*******	0.128	140.8	-----	-13.9
ABS CYC.EXIT	5953.	138.0	******	*****	*****	*******	0.114	135.4	-----	-25.7
FLOATING BED IN	*****	******	******	*****	*****	*******	******	*****	-----	*****
FLOATING BED EX	*****	******	******	*****	*****	*******	******	*****	-----	*****
P.P. EXIT ORIF.	5953.	136.0	519.8	*****	*****	*******	0.114	135.4	5344.	-25.7

SCRUBBER STREAM DATA	TEMP.F	FLOW.GPM
PARTICULATE		
MAKEUP WATER	59.0	5.69
PRODUCT LIQ.	139.5	5.09
RECIRCULATED LIQ.	139.5	23.15

	VENTURI ABSORBER TEMP.F	FLOW.#/M	FBA TEMP.F	FLOW.#/M
GAS ABSORBER				
MAKEUP WATER	59.0	9.7	*****	*****
MAKEUP MGO SL.	73.0	5.8	*****	*****
PRODUCT LIQ.	138.0	16.3	*****	*****
REC.(SPRAY NOZ)	138.0	488.0	*****	*****
REC.(FLOW NOZ.)		436.3		*****

FURNACE PERFORMANCE	
HEAT RELEASE,BTU/HR	0.685E 07
% FUEL AS COAL	96.1
COAL FLOW RATE,#/HR	382.6
NAT.GAS FLOW,#/HR	8.6
% EXCESS AIR	28.6
OXYGEN,DRY,MEAS.	6.00
CO2,DRY-CALC.	12.87
HUMIDITY,#/# - CALC.	0.041

SCRUBBER PERFORMANCE	PART.	VENT ABS.	FLOAT.BED
SO2 ABSORB.EFF	14.02	79.76	******
FLYASH COL.EFF	******	******	******
SO3 ABSORB.EFF	******	******	******
NOX ABSORB.EFF	******	******	******
GAS VELOCITY,FPS	155.6	80.0	******
LIQ/GAS,GAL/MCF	15.0	31.1	******
LIQ/GAS,#/#	2.0	4.4	******
PRES.DROP,IN.WG	6.3	1.7	******

SO2 ABSORPTION PARAMETERS

VENTURI		FLOATING BED		
KGA,#MOLE/HR-FT2.	= 103.7	KGA,#MOLE/HR-FT2	=	******
SULFITE/SO2-MOL/MOL	= 10.70	SULFITE/SO2-MOL/MOL	=	******
SUMP RESID.TIME,MIN	= 9.1	SUMP RESID.TIME,MIN	=	*****

SULFATE FORMATION PARAMETERS

CONC.,GM-MOLE/L=	0.0198
MOLE TOTAL SULF=	1.87
O2 AT FURN. EX.=	6.00
O2 AT ABSORB.IN=	*****
O2 AT ABSORB.EX=	*****

***** MEANS ITEM NOT MEASURED

MAGNESIUM BASE SLURRY SCRUBBING PROGRAM - PAGE 2

RUN NUMBER I-112 DATE 4-1-70 TIME OF DAY 0340

MATERIAL BALANCES

	SULFUR	MAGNESIUM	FLYASH	WATER	DRY GAS
FURNACE					
INPUT,#/HR	14.16	------	28.31	206.5	5511.
OUTPUT,#/HR	17.36	------	******	229.1	5517.
PART.SCRUBBER					
INPUT,#/HR	17.36	------	******	3071.	5517.
OUTPUT,#/HR	13.58	------	******	3196.	5022.
SO2 ABSORBERS					
INPUT,#/HR	13.98	13.65	******	1436.	5022.
OUTPUT,#/HR	59.99	50.23	******	1659.	5344.

SO2 ABSORBERS-PRODUCT COMP.	GM SO2/ 100ML	GM-MOLE/ LITER	GRAM/ 100ML
TOTAL,	7.45	1.1638	------
COMBINED	7.45	1.1638	------
FREE	0.0	0.0	------
MONO(TOTAL)	7.45	1.1638	------
MONO(DISSOLVED)	1.18	0.1844	1.937
MONO(SOLID)	6.27	0.9794	70.764
BISULFITE	0.09	0.0062	0.116
MGO	0.65	0.1014	0.405
SULFATE	0.13	0.0199	0.238
MAGNESIUM	8.22	1.2850	------
FLYASH	-----	------	******
SOLIDS,MG	-----	------	******

COAL COMPOSITION-MASS

CARBON	0.7150
HYDROGEN	0.0485
OXY+NIT	0.0817
SULFUR	0.0370
ASH	0.0740
WATER	0.0438

INPUT FOR EQ. - KIN.PROG.

INPUT FLOWS,#ATOMS/100#FEED	
CARBON	0.409990
HYDROGEN	0.451260
OXYGEN	1.401460
NITROGEN	5.112221
SULFUR	0.007700

FEED RATE,#/SEC= 1.60

ENTHALPY,BTU/# = 2273.

MAKEUP MGO COMPOSITION

SLURRY CONC.- GM MGO/100ML =	10.00
MGO PRESLAKED, NO = 0, YES = 1	1
% SLAKED TO MG(OH)2,MEAS. =	******

PRODUCT MG BASE PHYSICAL PROPERTIES

ACID STRENGTH, PH =	7.80
SP.GRAVITY,HYDROM. =	1.0220

PARTICULATE SCRUBBER PRODUCT

ACID STRENGTH	= *****
FLYASH CONC. GM/100ML	= *****

SOLIDS FREE BASIS, MASS/VOLUME SOLUTION

5.2 ERROR ANALYSIS

The results reported here and in the addendum are of limited value unless their accuracy is determined. To accomplish a measure of confidence in these results, several methods were used to evaluate potential errors. This error analysis is included in Appendix C. The analysis shows that none of the primary measurements except possibly the sulfate concentrations were seriously in error. The reported sulfates might be as much as 60% or so higher than the actual values. None of the other potential errors reflect significantly upon the reported results and conclusions.

5.3 SO_2 ABSORPTION

5.3.1 Comparison Between Absorbers

Although both the venturi absorber and floating bed absorber operated under similar conditions, their responses were in some respects substantially different. For example,

significant differences between these two absorbers were noted in the effect of L/G. The floating bed absorber was quite sensitive to L/G, but the venturi absorber performance was almost completely uneffected by that parameter. Theoretical rational for this effect will be presented later.

Probably the most obvious difference between scrubbers was the level of SO_2 absorption. This, however, is countered in part by the difference in operating energy level between these two mass transfer devices. The maximum operating proficiency for both absorbers is summarized as follows:

	Total Energy,* HP/MCFM	% Absorption
Floating bed absorber	1.84	99.2
Floating bed absorber	0.80	88.0
Venturi absorber	2.34	98.0
Venturi absorber	0.87	80.0

This data is based upon the following:

Electrical efficiency of both pump and fan, 80%
Liquid-to-gas ratio, 4#/#
Pump pressure, 25 psig

Another apparent difference between the venturi and FBA was the lesser sensitivity of the venturi to chemical composition of the spray slurry. This difference arises not from any basic difference between these two devices but simply because the FBA was operated at such a high level that the equilibrium SO_2 vapor pressure became a significant factor in limiting further absorption. Note in Figure 4.2 for an L/G of 0.3 #/# that composition did not strongly affect SO_2 absorption in the FBA. Thus, one would expect the venturi absorber operating at high absorption efficiencies (>90%) to have a similar dependence upon slurry composition.

5.3.2 Mathematical Models of SO_2 Absorption

A theoretical analysis of the gas absorbers would be valuable for correlating the collected data and for delineating the observed trends. However, no theoretical

*Note: As a point of reference, the electrical energy produced from pulverized coal in a 40% efficient cycle is 3140 HP/MCFM.

treatment of anything analogous to the FBA could be found in the recent literature. A theoretical treatment of a sieve tray without downcomers could have some application here, but this possibility was not explored. A theoretical treatment of the venturi absorber[4] was found and considered in this regard. However, upon examination, the paper was found to have many fundamental errors that made it useless.

Since no adequate theoretical treatments are available, and since a detailed mathematical model development is beyond the scope of this work, some very simple models of both the FBA and venturi absorber were developed. The basic material balance is as follows:

$$-d(Gy) = K_g a\ (y-y^*)dV_s \qquad (5\text{-}1)$$

where G = total gas mass flow, # mole/Hr

y = mole fraction SO_2

K_g = mass transfer coefficient, # mole/Hr ft^2

a = interfacial mass transfer surface area, ft^2 surface/ft^3 space

y^* = equilibrium concentration of SO_2 over liquid = p^*/P_t

dV_s = differential element of space

Tacitly assumed in this equation is that the system is gas film controlling. The two following assumptions greatly simplify Equation 5-1.

1. Since SO_2 is a minor constituent, G is nearly constant.
2. Since the stoichimetric ratio of liquid to absorbed gas in the scrubber is so large, the chemical composition can be assumed to be constant so that y^* is constant.

Equation 5-1 can now be simplified as follows:

$$\frac{-dy}{(y-y^*)} = \frac{K_g a}{G}\ dV_s \qquad (5\text{-}2)$$

But, $\int a\ dV_s$ = Total effective interfacial surface area.

If a' is defined as the interfacial area per unit mass of liquid on the tray, and if a' is assumed constant, then,

$$\int a dV_s = a'H \text{ where } H = \text{total mass of liquid on the tray}$$

Therefore,

$$\int \frac{-dy}{y-y^*} = K_g \frac{(a'H)}{G} \qquad (5\text{-}3)$$

$$\ln \left(\frac{y_i - y^*}{y_o - y^*} \right) = K_g a' \frac{H}{G} \qquad (5\text{-}4)$$

Equation 5-4 is the basis of Equation 4-1, which was used to correlate the FBA SO_2 absorption data. It was necessary, however, to modify Equation 5-4 so that the unknowns y^* and H could be expressed in terms of known parameters. This was done as follows:

For a constant gas flow, as was the case here, the holdup was equated to L/G as,

$$\frac{H}{G} = C_1 \ (L/G) + C_2 \qquad (5\text{-}5)$$

Since the vapor pressure of SO_2 over the liquor was unknown, it was necessary to postulate the vapor pressure relationship to composition in a manner similar to Johnstone's[5].

$$y^* = \frac{C_3 B^2}{M} \qquad (5\text{-}6)$$

where B = magnesium bisulfite concentration, as gm SO_2/100 ml

M = dissolved magnesium sulfite conc., as gm SO_2/100 ml

However, since M was nearly constant for this test condition, the vapor pressure equation was simplified:

$$y^* = C_3 B^2 \qquad (5\text{-}7)$$

Inserting these equations into Equation 5-4 and combining the constants:

$$\ln \left(\frac{y_i - C_3 B^2}{y_o - C_3 B^2} \right) = C_4 \ (L/G) + C_5 \qquad (5\text{-}8)$$

where $C_4 = kga'C_1$

$C_5 = kga'C_2$

As reported in Section 4.2.2, this equation was solved by nonlinear regression analysis with the following results:

$$C_3 = 24.97$$
$$C_4 = 0.633$$
$$C_5 = 2.26$$

and the Correlation Coefficient (R^2) = 97.45%.

An even simpler model that is employed in the computer program is based upon the total volume of the active section of the FBA and assumes that the vapor pressure is negligible.

$$\ln\left(\frac{y_i}{y_o}\right) = \frac{K_g a}{G} A \int dh = \frac{K_g a}{G} A\Delta h \qquad (5\text{-}9)$$

or

$$K_g a = -\ln(1-E)\ \frac{G}{A\Delta h} \qquad (5\text{-}10)$$

where A = flow area = 1.97 ft^2

Δh = height of active section = 4 ft/section x 2 sections = 8 ft

Although simple, this equation is of limited value since it does not really delineate any important effects and ignores vapor pressure in an operating region where vapor pressure evidently has a very significant effect.

The same simplifying assumptions applicable to Equation (5-1) for the FBA are applicable to the venturi absorber situation so that,

$$\frac{-dy}{y-y^*} = \frac{K_g a}{G} dV_s \qquad (5\text{-}3)$$

If a is constant and independent of position and if the absorption is completed within the venturi, then,

$$\ln\left(\frac{y_i-y^*}{y_o-y^*}\right) = \frac{K_g a}{G} V_s \qquad (5\text{-}11)$$

where V_s = total volume of the spray zone in the venturi, ft^3.

If the vapor pressure is ignored, then Equation 5-11 reduces to the form utilized in the computer program and reported in the printout.

$$K_g a = \frac{-G \ln (1-E)}{V_s} \qquad (5\text{-}12)$$

Since vapor pressure did not have a great effect upon SO_2 absorption in the venturi absorber at E less than 80%, this equation has somewhat more credence than Equation 5-10 for the FBA.

5.3.3 SO_2 Vapor Pressure from Literature

From the above discussion, it is apparent that reliable vapor pressure data for the MgO-SO_2-H_2O system is needed. Without this data, N_T, the number of transfer units, cannot be determined. Therefore a meaningful K_g cannot be calculated.

Some SO_2 vapor pressure data exists in the literature for the MgO-SO_2-H_2O system [6], [7], [8]. However, this data covers a range of compositions and a vapor pressure range that are not applicable here. Data presented by Markant [8] covers the lowest vapor pressure available from the literature. This range and the present operating range are summarized as follows:

	Vapor Pressure, "Hg	Monosulfite	Bisulfite gm SO_2/100ml
Markant	1.0 to 15	0.2 to 0.6	3.8 to 6.0
Pleasant work	0.01 to 0.4	0.8 to 1.2	0 to 3.5

The impetus behind the available data in the literature was technical support for the magnesium base pulping process. This differs from the present system in that absorption of SO_2 into the bisulfite acid is at a much higher concentration. Vapor pressure data is available for other sulfite-bisulfite systems, notably containing sodium, calcium, and ammonia[5], [9]. However, although the form of the correlation is generally similar to that employed in Equation 5-6, the proportionality constants differ substantially. Thus, it would appear that development of vapor pressure data in the range at hand would be in order.

5.3.4 Effect of Sulfates Upon SO_2 Absorption

The magnitude of the adverse effect created by sulfates upon SO_2 absorption in both absorbers was unexpected. However, a paper by Chertkov[10] dealing with

the effects of sulfates upon the SO_2 vapor pressure over solutions of ammonium sulfite and bisulfite seems to present a plausible explanation for this observed trend. In the ammonia base system, Chertkov found the vapor pressure to change as follows:

$$P^*_{SO_2} = P_{SO_2} \left(\frac{C+S}{C} \right) \qquad (5\text{-}13)$$

where $P^*_{SO_2}$ = actual vapor pressure
P_{SO_2} = vapor pressure over pure sulfite and bisulfite solution
C = molar concentration of sulfite and bisulfite
S = molar concentration of sulfate

Thus, if this relationship held for the magnesia base system, the effect of sulfate upon the vapor pressure would be quite substantial. Under normal conditions at a pH = 5.0, C = 2.6 gm SO_2/100 ml, and S = 0.25 gm SO_2/100 ml, then:

$$P^*_{SO_2} = P_{SO_2} \left(\frac{2.6 + 0.25}{2.6} \right) = 1.095\ P_{SO_2} \text{ or } 9.5\% \text{ increase}$$

For the elevated sulfate test series G and N,

$$P^*_{SO_2} = P_{SO_2} \left(\frac{3.50 + 4.00}{3.50} \right) = 2.14\ P_{SO_2} = 114\% \text{ increase}$$

If the sulfate concentrations were brought to near saturation (S_{sat}=22.2 gm as SO_2/100 ml), then the potential effect of sulfates upon SO_2 absorption could be very substantial indeed, which would require that the absorber operate on the alkaline side (bisulfite → 0).

Since sulfates potentially have such a strong influence upon SO_2 vapor pressure, this factor should be included in any proposed vapor pressure study.

5.3.5 Comparison of Absorber Performance with Literature

Although nothing analogous to the present magnesia system has been reported in the literature, some data on similar systems permits comparisons. A paper by Pollock[11] reporting work performed on a tray type device with spherical plastic packing showed the following similar trends:

1. A strong dependence of SO_2 absorption upon the liquid flow rate. SO_2 absorption increased with increasing liquid flow for both sodium carbonate and calcium carbonate systems.

2. Although pressure drop across the scrubber could not be compared directly with that in the FBA, analogous trends were noted.
3. Dust collection, although at a comparable level, showed a dependence upon the liquid rate. This was not observed in the FBA tests.

FIGURE 5.2 COMPARISON OF SO_2 ABSORPTION IN THE VENTURI ABSORBER WITH LITERATURE

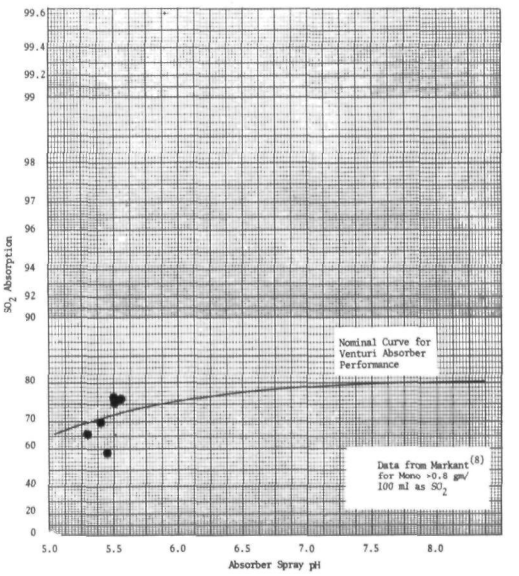

The only available data in the literature for SO_2 absorption in a venturi absorber is that by Markant [8] for a magnesium sulfite and bisulfite system. This work was performed on a small pilot venturi. The paper deals with the effect of chemical composition upon SO_2 absorption. Some overlap of the composition range in that paper and the present work shows that the SO_2 absorption compares reasonably well. This comparison is illustrated in Figure 5.2. However, the Markant work does reveal that the absorption depends upon the concentration of magnesium sulfite in solution. This is a factor which could not be explored in the present work since the system was saturated with sulfite at constant temperature and was therefore essentially constant.

5.4 CHEMISTRY OF ABSORBING SLURRY

The chemistry of the magnesia base system played an important role in the absorption of SO_2 and had a strong influence upon the tendency to form deposits. The overall reaction for this system is simply:

$$MgO + SO_2 \xrightarrow{H_2O} MgSO_3 \cdot 6H_2O \downarrow \qquad (5\text{-}14)$$

The solid phase of the product permits convenient separation from the process for subsequent removal to a regeneration facility to reconvert to MgO and SO_2.

From a mechanistic standpoint, the system can be summarized as follows:

Slaking Reactions:

$$MgO_{(s)} + H_2O \longrightarrow Mg^{++} + 2OH^- \quad (5\text{-}15)$$

$$Mg^{++} + 2OH^- \rightleftharpoons Mg(OH)_{2(s)} \quad (5\text{-}16)$$

SO_2 Absorption:

$$SO_{2(g)} \longrightarrow SO_{2(aq)} \text{ or } H_2SO_3 \quad (5\text{-}17)$$

$$SO_{2(aq)} + OH^- \longrightarrow HSO_3^- \quad (5\text{-}18)$$

$$HSO_3^- + OH^- \rightleftharpoons SO_3^= + H_2O \quad (5\text{-}19)$$

$$SO_3^= + Mg^{++} \xrightleftharpoons{H_2O} MgSO_3 \cdot 6H_2O_{(s)} \quad (5\text{-}20)$$

The composition of the absorbing slurry was controlled primarily by the rate of MgO makeup. Three classes of composition of the spray slurry were possible. These are listed as follows:

Case I - Excess bisulfite --- complete neutralization
Composition: Mg^{++}, HSO_3^-, $SO_3^=$, $MgSO_3 \cdot 6H_2O$

Case II - Excess MgO [or $Mg(OH)_2$] --- complete neutralization
Composition: Mg^{++}, $SO_3^=$, $MgSO_3 \cdot 6H_2O$, OH^-, MgO [or $Mg(OH)_2$]

Case III - Incomplete neutralization (either excess bisulfite or MgO)
Composition: Mg^{++}, $SO_3^=$, $MgSO_3 \cdot 6H_2O$, MgO [or $Mg(OH)_2$], HSO_3^-

Case III was probably most prevalent because a small fraction of the MgO is slow to react even under strongly acidic conditions. On the other hand, reactions 5-17 through 5-19 are ionic and therefore are probably instantaneous.

The fact that preslaking of the MgO did not have a measurable influence upon SO_2 absorption resulted from two factors. First, the sulfite, via reaction 5-19 tends to buffer the solution. Secondly, the MgO used, Michigan Chemical Number 5, was a fairly reactive magnesia which could hydrate quite rapidly even when preslaking was not attempted. Magnesium oxide slaking has been investigated by Smithson[12], who found the following:

> MgO reactivity is related to the crystallite size (a particle being constructed of an array of crystallites). The crystallite size in

turn is a function of the history of the MgO including the chemical form of the raw material and the calcining temperature. The optimum temperature for calcining is between 750 and 1100 F. Above calcining temperatures of about 2200 F the resulting MgO is essentially unreactive and is referred to as "dead burned". Finally, Smithson found that the reaction rate can be correlated in terms of specific surface area and that the activation energy is constant at about 14.1 ± 0.2 kcal/gm mole.

The solubility of magnesium sulfite above a pH of about 6.0 agreed fairly well with the literature. See Figure 5.3. The average solubility of magnesium sulfite was 1.1 gm/100 ml as SO_2. Since the sulfite ion concentration was nearly constant, a one-to-one correspondence existed between the magnesium bisulfite concentration and pH. This is illustrated in Figure 5.4.

In the calcium oxide and calcium carbonate absorption systems, the slurry concentration or, more explicitly, the specific surface of the limestone is a very important parameter and is possibly a controlling factor in SO_2 absorption. The magnesia base system shows no corresponding dependence on slurry concentration because of the relatively high solubility of the magnesium sulfite. The ratio of the solubility of magnesium sulfite to calcium sulfite is 485 mole/mole at 140 F.

FIGURE 5.3 SOLUBILITY OF MAGNESIUM SULFITE

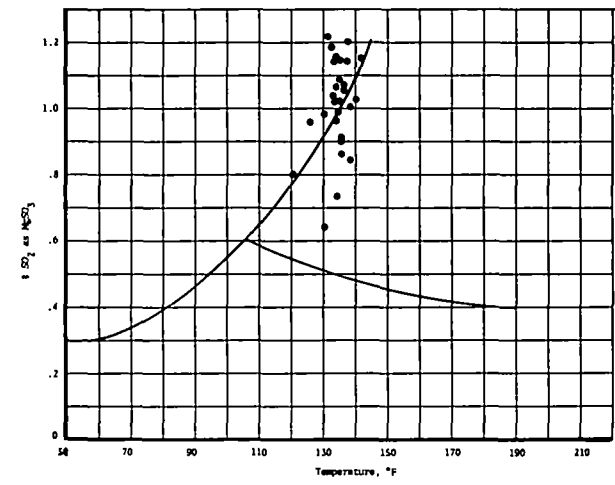

FIGURE 5.4 RELATIONSHIP BETWEEN BISULFITE CONCENTRATION AND SLURRY pH

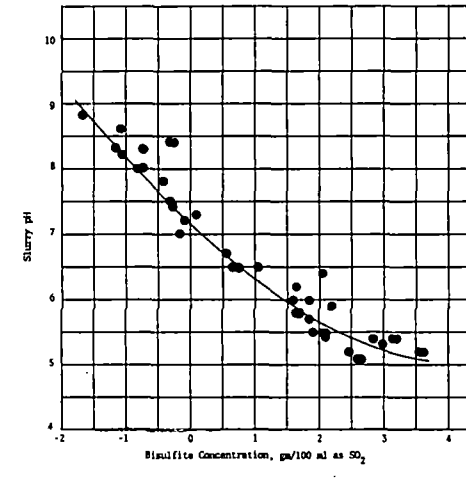

Since the sulfite ion acts as a buffer to maintain a nearly constant hydroxide ion concentration, the desolution rate of the magnesium hydroxide becomes less important. The calcium base system has no such buffering effect.

5.5 DEPOSITION

5.5.1 Deposition Mechanisms

Although the study of deposition in the two types of SO_2 absorber apparatus was not an objective of this project, the solution to this unexpected problem became a major concern. It is important, particularly for those who are familiar with deposition problems in the limestone system, to distinguish between the two different types of deposits. In limestone scrubbers the primary deposit is a calcium sulfate hydrate (gypsum), which forms a cement-like deposit in regions where it is subject to the drying influence of the flue gas. The calcium base deposit would be classed as an aggregate resulting when a portion of the slurry is permitted to separate or "hide out" within the system. Continuous wetting, slurry agitation, and design against hide out are some of the approaches used to combat the problem.

FIGURE 5.5 EXAMPLE OF COARSE DEPOSIT

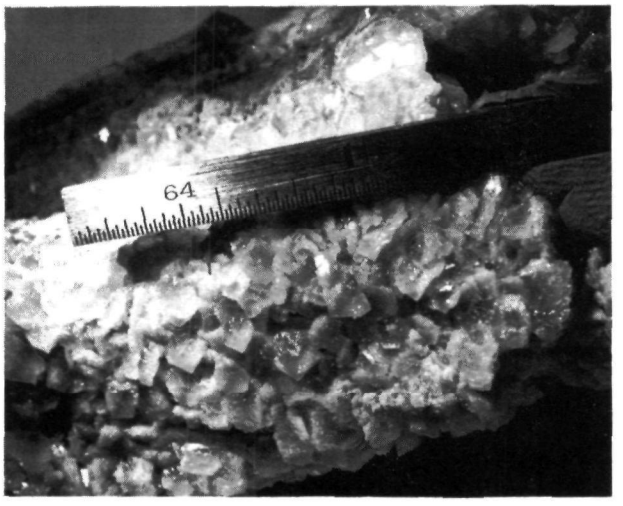

In contrast, the magnesium base deposit has been identified as a sulfite hydrate, $MgSO_3 \cdot 6H_2O$, which forms a hard, resilient platelike deposit which bonds tightly to metal surfaces. The deposit consists of a matrix of large crystals that appear under the microscope to be melted together. An example of one of the coarser deposits removed from the venturi absorber sump is shown in Figure 5.5. Unlike the deposits in the limestone system, this deposit is not an aggregate of settled solids from the slurry, but rather appears to be kind of crystal growth.

Several factors seemed to influence the tendency to form deposits. These included the systematic shifting

of the sulfite slurry concentration, the availability of precipitation surface area, the nature of the surface material, and the fluid flow environment. These factors are discussed individually below.

Systematic shifting or cycling of the solid magnesium sulfite concentration can occur by two separate mechanisms. The first involves chemical reaction, and the second occurs from temperature cycling. The chemical reaction mechanism proceeds as follows:

1. SO_2 is absorbed in the gas-liquid contacting zone according to the following successive reactions:

$$SO_2 + OH^- \rightarrow HSO_3^- \qquad (5\text{-}21)$$

$$SO_3^= + H_2O \rightarrow HSO_3^- + OH^- \qquad (5\text{-}22)$$

$$MgSO_3 \cdot 6H_2O \rightarrow Mg^{++} + SO_3^= \qquad (5\text{-}23)$$

The third reaction, which proceeds in order to maintain a constant concentration of sulfite ion, causes a net reduction in the suspended solids concentration.

2. The slurry then proceeds to the sump, where the bisulfite is partially neutralized by the incoming magnesia.

$$HSO_3^- + OH^- \rightarrow SO_3^= \qquad (5\text{-}24)$$

$$SO_3^= + Mg^{++} \xrightarrow{H_2O} MgSO_3 \cdot 6H_2O \qquad (5\text{-}25)$$

This last reaction is the mechanism by which the crystal growth can proceed. Thus, for each mole of SO_2 absorbed, two moles of sulfite can precipitate in the sump. The following facts support this mechanism hypothesis:

1. No deposition formed within the gas-liquid contacting zone. Instead the solid sulfite was actually dissolving in this region.
2. Deposition was most severe in the sump and piping when the system was operated on the acid side and when the MgO was added directly to the sump.
3. The deposition rate was substantially reduced when the makeup location for the magnesia was changed from the sump to the gas-liquid contacting zone. To ensure that the magnesia would react readily, the magnesia was preslaked. By this technique, at least in theory, the total deviation of the sulfite slurry concentration could be reduced by 50%

depending upon how readily the available hydroxide would react with the absorbed SO_2.

The second potential mechanism for deposit formation is temperature cycling. Two temperature effects can occur. The first is the temperature drop between the inside pipe wall and the bulk liquid. The second is a change in the bulk slurry temperature due to heating by the flue gas and cooling by the makeup slurry and makeup water. At 135 F the solubility of magnesium sulfite hydrate changes by 0.0234 gram/100 ml slurry for each degree change in temperature. If the "deposition potential" is defined as the maximum deviation in the concentration of $MgSO_3 \cdot 6H_2O$, then this expression can be used to describe the likelihood of deposit formation. Thus, the deposition potential for various situations are summarized as follows:

Effect	Deposition Potential
Chemical reaction	
Makeup MgO to sump	1.270 gm/100 ml
Makeup $Mg(OH)_2$ to contact zone	0.635 gm/100 ml
Temperature cycling	0.077 gm/100 ml
Pipe wall temperature drop	
Stainless steel	0.0044 gm/100 ml
PVDC	0.0007 gm/100 ml

The deposition potential is not an exact indicator of deposition formation rate, but is simply a qualitative guide. Other factors influencing deposition can predominate.

The success of fly ash in preventing deposition formation is believed to be due in part to the high surface area offered by the fly ash for receiving the precipitating sulfite. This effect is apparent by comparing the specific surface of the slurry with and without fly ash. Assume the following typical conditions:

Sulfite Slurry	Fly Ash Sulfite Slurry
Average crystal size = 200 μ	Average fly ash particle size = 12 μ
Suspended solids concentration = 5 gm/100 gm	Suspended fly ash concentration = 2.5 gm/100 gm
Specific gravity = 2.8	Specific gravity = 2.34
∴ Specific surface = 5.35 cm^2/ml	∴ Specific surface = 58.7 cm^2/ml

Since the presence of fly ash increased the suspended solids surface area by a

factor of 11, it is apparent that the deposition on suspended particles should be increased relative to the deposition on the stationary or wall surface. Typical values of deposition ratios of suspended surface to wall surface are summarized as follows:

	Deposition Ratio of Suspended Surface to Wall Surface, ft^2/ft^2	
	Without Fly Ash	With Fly Ash
Venturi absorber sump	29.8	320
2-inch pipe	6.8	66.5

The additional suspended surface created by the presence of fly ash cannot by itself explain the observed elimination of deposition. Therefore, some additional property of fly ash must have contributed to the prevention of deposition. A probable explanation is the abrasive or scouring action of fly ash upon the stationary surface. Whatever the mechanism, however, the presence of fly ash in the slurry proved very beneficial from a deposition standpoint.

Even if the stationary surface constitutes a significant fraction of the available surface area, the capability of that surface to receive deposits depends upon the affinity of that surface for the deposits. This affinity is analogous to the wetability of a surface and involves Vander Wal type forces between the wall, the liquid median, and the precipitating sulfite. Numerically, this wetability is expressed in terms of the contact angle between liquid and solid. As this angle increases between 0 and π, the wetability decreases. Thus, the contact angle of water on a newly polished automobile would be large compared to the contact angle of water on a dull finish. Applying this analogy to the present situation shows that the PVDC surface has a large contact angle, but stainless steel and brass have very small contact angles. It should be noted, however, that once a layer of deposit froms, the contact angle is no longer between liquid and wall material, but is instead between liquid and deposit.

The value of the contact angle concept is that it offers a simple method of evaluating alternate materials of construction. Thus, two materials can be compared by measuring the rise or fall of the liquid in capillary tubes made of the materials in question.

Finally, a phenomenom of deposition in this magnesium base system, which in some regards is directly contradictory to expectations, is the observation that the deposition was highly preferential at points of extreme turbulence or shearing.

These included the primary recirculation pump, the spin vanes of the spray nozzles, the sump recirculation pumps (used on two occasions), and other locations subject to high shear stresses. In contrast, deposits did not form in the recirculation flow nozzle nor in the spray orifice (immediately following the spin vanes). These are locations of relative low stress. The suggested mechanism for deposition is some type of shift in the solubility of the sulfite at localized points of intense eddy circulation, perhaps vapor flashing and condensing, which could cause temperature cycling.

5.5.2 Method of Deposit Elimination

The relatively high solubility of the magnesium sulfite deposit can be used to advantage for cleaning a fly-ash-free absorption system. The pilot plant was cleaned (descaled) on several occasions by simply stopping the magnesia makeup to the system. The remainder of the absorption system operated normally. The sulfite deposits dissolved readily according to Reactions 5-21 through 5-23. The effect was that for each mole of SO_2 absorbed, one mole of the sulfite solid was dissolved. This method could be adopted for cleaning a commercial absorption system. For the method to be effective, however, the cleaning cycle must be started before the absorption system is completely plugged. Although the SO_2 absorption drops off during the cleaning cycle, the decrease is gradual and would probably level off at about 50% absorption. The product from the absorption system could be diverted to a holding tank during the cleaning cycle and could thereafter be funneled back to the system during normal operation.

5.6 SULFATE FORMATION

Sulfate formation was one of the more important factors considered in this project. Since the sulfate concentration leaving the scrubber can vary widely, depending upon both the sulfate formation rate and the throughput rate, the sulfation tendency of the system should be expressed so that both scrubbers can be compared on common grounds. Three possibilities are as follows:

1. Mole fraction of incoming sulfur leaving product liquid as sulfate.
2. Mole fraction of absorbed sulfur leaving product liquid as sulfate.

If the liquid passes through the scrubber on a once-through basis, then the mole fraction of sulfur as sulfate in the product liquid is equivalent to (2) above.

3. Overall mass transfer coefficient for O_2 absorption.

The factors which could contribute to sulfate formation in the SO_2 absorber are as follows:

1. Absorption of O_2 followed by chemical reaction with $SO_3^=$.
2. Absorption of SO_3.
3. Sulfates in makeup water.
4. Dissolved oxygen in makeup water.
5. NO_2 absorption and chemical reaction with $SO_3^=$.
6. Carryover of sulfates from particulate scrubber.
7. Carryover of catalytic cations from particulate scrubber or from fly ash.

The maximum probable contributions from these factors can be summarized as follows:

		Mole % Absorbed Sulfur Converted to Sulfate
SO_3 absorption		0.0750%
NO_x absorption		0.0250
O_2 in makeup water		0.0825
Carryover from particulate scrubber		0.1090
Sulfate in makeup water		0.000
	TOTAL	0.2915%
Measured sulfate levels	=	∿4.300%

Therefore, from a purely stoichiometric standpoint, (1) appears to be the most likely mechanism. If this is the case, then the question which arises next is whether it is liquid phase or reaction rate controlling. If it is liquid phase controlling, then the following parameters should be important:

1. Mass transfer surface area
2. Mass transfer contact time (between gaseous O_2 and liquid)
3. Liquid and gas turbulence
4. O_2 concentration in gas

Temperature might also have a second-order effect. If chemical reaction rate were the limiting factor, then the following might be significant:

1. Sulfite ion concentration
2. Bisulfite concentration or pH
3. Light intensity
4. Catalysts such as multivalent cations

It is difficult to ascertain whether the diffusion step is limiting for O_2. However, the same factors which affect O_2 diffusion will also affect SO_2 diffusion. Since the SO_2 absorption is measureable, and since SO_2 appears to be diffusion controlling, it is likely that, if O_2 diffusion is the limiting step, the sulfate formation will be proportional to the SO_2 absorption.

In neither the venturi absorber nor the floating bed absorber does there seem to be any relationship between sulfate levels and SO_2 absorption.

From the above, it appears that the sulfate formation in this system must be predominantly (but not entirely) reaction rate controlling. The sulfite ion concentration is essentially constant, and no relationship exists between bisulfite concentrations and sulfate levels; the only remaining factors are variable and undetected catalytic effects or analytical errors. The analytical errors were checked on selected samples for sulfates, and these results are shown in Section C. 3.2. In support of this hypothesis is the large increase in sulfates which occurred when the SO_2 absorbers operated as simultaneous particulate collectors. The apparent increase in sulfates was substantially greater than that accounted for by the increase in SO_3 gas going to the scrubber.

The literature was of little value in delineating the observed effects. The literature does agree on the mechanism of diffusion of oxygen across the liquid film followed by catalytic reaction with the sulfite[13], [14], [15]. However, the detailed effects of oxygen partial pressure, slurry pH, sulfite concentration, catalyst concentration, etc. are relatively inconsistent. For example, Gunn[13] claimed a zero-order effect of oxygen concentration on reaction rate, but Linek [14] found oxygen to have a first-order effect and even a second-order effect. The effect of catalyst concentration was found by Linek to be linear, but Chertkov[15] found no effect from the catalyst concentration. Chertkov also found a sixth-order effect of bisulfite concentration.

Although the effects of slurry pH, bisulfite concentration, and temperature upon sulfate formation rate were examined, no trends could be found. Oxygen concentration and fly ash were the only parameters isolated.

To discern whether oxygen diffusion or catalytic oxidation might be controlling, the data was analyzed in the following fashion. It was rationalized that if diffusion were the controlling mechanism and other factors could be ignored, the oxygen absorption should have been proportional to the sulfur dioxide absorption (also diffusion controlling). Therefore, the sulfate formation rate should have been proportional to SO_2 absorption. As a check, the percentage

of sulfate was plotted against the SO_2 mass transfer rate for both the FBA and the venturi absorber. No trend was apparent. Therefore, it was concluded that oxygen diffusion was probably not the controlling mechanism.

Since the many possible interactions which could have an influence upon the reaction rate of sulfite to sulfate were not determined in any systematic experimental fashion, it is difficult to ascertain the magnitude or importance of these effects. As was stated previously, the presence of bulk quantities of fly ash was the only discernible parameter. If it is assumed that the catalytic quality of fly ash is derived from the iron (Fe^{++}) in the ash (an unsubstantial hypothesis), the probable concentration levels of iron in the sulfite slurry can be summarized as follows:

Maximum probable Fe^{++} concentration with prescrubber = 0.02×10^{-4} to 0.1×10^{-4} moles/liter

Maximum probable Fe^{++} concentration without prescrubber = 60×10^{-4} to 300×10^{-4} moles/liter

Although this data does show the positive effect of fly ash, it is insufficient to yield any definite correlation.

The need for an exact definition of the sulfate formation rate depends upon the consequences of that formation. If the sulfate formation constitutes an ultimate loss from the system, then it is important to be able to describe and limit this formation. However, if the sulfate is reclaimed in the regeneration process, then this parameter is less significant. In any event, the sulfate formation rate appears to be less than that reported by Stone and Webster[16] for the venturi and comparable to that reported by Stone and Webster for the FBA.

5.7 NO_x ABSORPTION

One of the most significant potential attributes for any SO_2 removal process is its capacity for simultaneous SO_2 - NO_2 reduction. Such was the purpose behind the NO_x feasibility test performed on April 9, 1970. This test entailed the injection of nitrogen dioxide (NO_2) into the flue gas stream ahead of the venturi absorber. A schematic of the apparatus appears in Figure 3.1.

As was obvious from the results, as reported in Section 4.9, the above approach was not compatible with the process at hand. Basic to the present MgO process is the low inception of sulfates within the scrubbing system. In contrast, the injection of NO_2 in the presence of SO_2 and subsequent absorption

into a sulfite solution or slurry is the principle upon which the Tyco SO_2 - H_2SO_4 absorption process depends. That process was investigated under HEW Contract PH86-68-75. The Tyco process relies upon the oxidation of the SO_2 by either of the following reactions:

Gas Phase

$$NO_2 + SO_2 \rightarrow NO + SO_3 \qquad (5\text{-}26)$$

$$SO_3 + H_2O \rightarrow H_2SO_4 \qquad (5\text{-}27)$$

Liquid Phase

$$NO_2 + SO_3^{=} \rightarrow NO + SO_4^{=} \qquad (5\text{-}28)$$

The fact that the sulfate level was significantly elevated during the current feasibility test supports the validity of these reaction mechanisms. The equilibrium constant of reaction (5-26) among others is shown in Figure 5.6 as a function of temperature. Note that the sulfate found in the product liquor accounted for a substantial portion of the NO_2 added to the gas stream.

In retrospect it appears obvious that, to accomplish significant NO_x removal by wet scrubbing with MgO via the NO_2 injection method, the process must entail a two-step operation. The SO_2 must first be reduced in a scrubber to a level substantially lower than the NO_x concentration leaving the furnace. NO_2 could then be injected into the flue gas so that it could react with NO and residual SO_2 and be absorbed in an $Mg(OH)_2$ slurry tower. Such a potential process is shown in Figure 5.7. A method similar to this approach was suggested by W. Bartok[17] for a calcium-base system. However, no process limits or requirements were specified, and no provisions for desulfating the product from the NO_x absorber were suggested by Bartok. A material balance around the absorber indicates, however, that in order

FIGURE 5.6 EQUILIBRIUM CONSTANTS FOR NO_x-SO_x-H_2O SYSTEMS

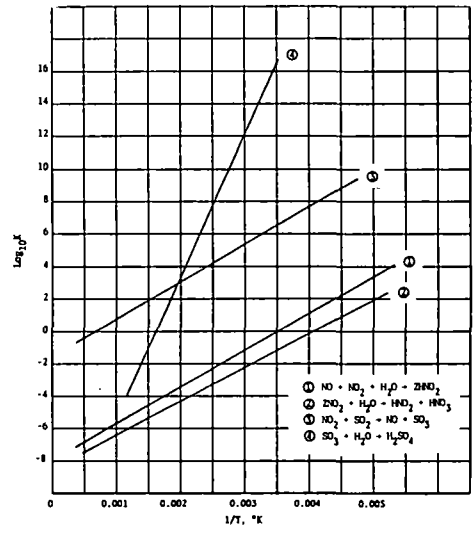

to have a self-sustaining supply of NO_2 to react with all of the NO leaving the boiler, the absorber must be at least 85% efficient, the nitration step must be essentially complete, and the NO oxidation must be at least 95% complete. Little is known of the requirements of the nitration step, but the NO oxidation should be quite simple.

FIGURE 5.7 SO_2-NO_x ABSORPTION PROCESS

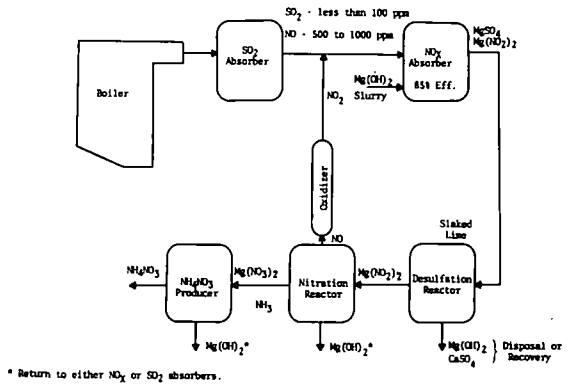

The concept of injection of NO_2 into an NO-laden gas for the subsequent absorption of both species has been proposed by several investigators[17], [18], [19]. The bulk-gas-phase reactions most often assumed are as follows:

$$NO_{(g)} + NO_{2(g)} + H_2O_{(g)} \rightleftarrows 2HNO_{2(g)} \qquad (5\text{-}29)$$

$$2NO_{2(g)} + H_2O_{(g)} \rightleftarrows HNO_{2(g)} + HNO_{3(g)} \qquad (5\text{-}30)$$

$$N_2O_{4(g)} + H_2O_{(g)} \rightleftarrows HNO_{2(g)} + HNO_{3(g)} \qquad (5\text{-}31)$$

$$2NO_2 \rightleftarrows N_2O_4 \qquad (5\text{-}32)$$

$$NO_{(g)} + NO_{2(g)} \rightleftarrows N_2O_{3(g)} \qquad (5\text{-}33)$$

The first reaction, 5-29, is the basis for the NO_2 injection concept. The kinetics of this reaction were studied by Wayne[20], who expressed the rate as follows:

$$\frac{d[HNO_2]}{dt} = k[NO][NO_2][H_2O] \qquad (5\text{-}34)$$

where $k = 7.3 \times 10^4$ $atm^{-2}sec^{-1}$ at T = 298 K

Assuming that $[NO] = [NO_2] = 10^{-3}$ and $[H_2O] = 0.15$ and that there is no change at 150 F, which is the temperature at the point of injection, then the forward reaction would yield about 90% conversion during a 1-second reaction time.

However, because of chemical equilibrium effects (see Figure 5.7), the reverse reaction would predominate and limit the bulk-gas-phase reaction to less than 10% conversion. Therefore, this bulk-gas-phase reaction would not play a significant role in the absorption of NO_x. However, at the gas-liquid interface, where the product of the forward reaction could be continuously removed from the gas film, reaction 5-29 could predominate. If this were the limiting mechanism, then as a very rough estimate a gas contact time on the order of 1 second would be required for substantial NO_x removal in a scheme such as that shown in Figure 5.6.

The effect of reactions 5-30 and 5-31 upon the total NO_x reduction is important. If these reactions were to occur more rapidly and completely than reaction 5-29, reaction 5-29 would not proceed. Thermodynamics answers the first portion of this concern by showing that the fractional conversion assuming an NO_2 concentration of 1000 ppm is less than 1% at 150 F. However, the kinetics of this reaction are unknown, and the extent to which it might occur in the gas film when the reaction products can be continuously removed is a potentially limiting factor. Peters[21] has shown that this reaction is a significant contribution to NO_2 absorption in alkali solutions. However, since it has been shown[18] that the mutual presence of both NO and NO_2 promotes the absorption of both species, it would appear that reaction 5-29 is probably faster than reactions 5-30 and 5-31.

The reactions which are believed to predominate in the liquid film of the NO_x-SO_x-MgO system are as follows:

$$2NO_{2(g)} + 2OH^- \rightleftarrows NO_2 + NO_3 + H_2O \qquad (5\text{-}35)$$

$$N_2O_{4(g)} + 2OH^- \rightleftarrows NO_2^- + NO_3^- + H_2O \qquad (5\text{-}36)$$

$$SO_2 + 2OH^- \rightleftarrows SO_3^= + H_2O \qquad (5\text{-}37)$$

$$NO_2^- + SO_3^= \rightleftarrows NO\uparrow + SO_4^= \qquad (5\text{-}38)$$

$$HNO_2 + OH^- \rightleftarrows NO_2^- + H_2O \qquad (5\text{-}39)$$

$$HNO_3 + OH^- \rightleftarrows NO_3^- + H_2O \qquad (5\text{-}40)$$

$$SO_{3(g)} + H_2O_{(g)} \rightleftarrows H_2SO_{4(aerosol)} \quad (5\text{-}41)$$

$$H_2SO_{4(aerosol)} + 2OH^- \rightleftarrows SO_4^= + H_2O \quad (5\text{-}42)$$

The relatively low pH of the magnesia slurry (∿8.0) precludes any appreciable CO_2 absorption. Reactions 5-35, 5-36, 5-39, and 5-40 are the only liquid film reactions likely to be less than instantaneous since they involve the absorption of a gaseous species into a liquid while the others are simple ionic reactions. In the case of HNO_2 + HNO_3, however, these constituents are almost completely soluble at the condition under consideration. With the possible exception of 5-35 and 5-36, the above reactions will be driven almost completely to the right.

The requirements of an NO_x-$Mg(OH)_2$ scrubber are probably as follows:

1. Reaction 5-29 must occur more rapidly than reactions 5-30, 5-31, 5-35, and 5-36.
2. The $SO_{2(g)}$ or $SO^=_{3(aq)}$ concentration must be small compared to the NO_2 concentration.
3. The gas must be in intimate contact with the liquid for a period in the order of 1 second or more.

The NO_x scrubbing aspects of this concept could be readily included in the present contract by adding a packed tower following the floating bed absorber.

6.0 CONCLUSIONS

The magnesia base wet scrubbing process can perform adequately for SO_x and particulate cleanup of pulverized coal generated flue gas. Acceptable operating conditions are in all aspects compatible with envisioned regeneration processes. In fact, since it is desirable to carry a fly ash load in the absorbing slurry, the wet scrubbing process potentially could be simplified to use a single scrubber as a simultaneous particulate and SO_2 scrubbing device. Conclusions regarding specific aspects of this scrubbing process are presented below:

6.1 SO_2 ABSORPTION

In terms of the evaluating parameter γ*, the floating bed absorber was superior to the venturi absorber. However, neither absorber has been optimized from this standpoint. See Section 5.3.1.

The performance of both absorbers was either comparable to or superior to that of similar hardware presently employed for the calcium base system.

Final selection of gas absorber hardware must not be based solely upon absorption performance but must include other factors such as capital cost, power requirements, scaleup difficulties, pluggage trends, turndown, replacement requirements of internals, etc.

6.2 SULFATE FORMATION

The rate of sulfate formation was at no time prohibitively excessive as long as the regeneration process is capable of thermal decomposition of the sulfate.

The sulfates as reported (based upon the titration method) were probably about 60% higher than the actual values (based upon gravimetric analysis).

The difference in rates of sulfate formation was not significant between the floating bed absorber (long residence time) and the venturi absorber (short residence time).

The major parameters affecting sulfate formation were fly ash concentration and oxygen concentration.

---

*Note: γ is defined as $\frac{-\ln(1-Eff)}{P_r}$ where P_r is the power consumption expressed as HP/MCFM.

6.3 DEPOSITION WITHIN ABSORBER

Deposition of $MgSO_3 \cdot 6H_2O$ was the most serious problem encountered. It can be prevented by proper operation and design. Deposition is preventable by permitting a fly ash load in the absorption slurry. If formed, the deposition can be removed by simple desolution.

6.4 OTHERS

The energy required to collect fly ash at levels comparable to those for high performing electrostatic precipitators (99^+) is commercially practical.

Potential SO_3 absorption in the gas absorbers is not a significant factor in sulfate formation.

No significant NO_x absorption could be credited since the error potential in the PDS analysis is larger than the observed changes in NO_x concentration.

7.0 RECOMMENDATIONS

7.1 PARTICULATE SCRUBBER OPERATION AND DESIGN

A venturi type scrubber should be used for this application. The design and operation should be optimized. However, until this is done, the following operating conditions are recommended for PC fly ash only:

1. Gas velocity at the throat = 150 ft/sec
2. Liquid-to-gas ratio = 15 gal/1000 cu ft.

7.2 SO_2 ABSORBER OPERATION AND DESIGN

1. The stoichiometric ratio of MgO/SO_2 should be maintained at 1.0 or slightly greater.
2. The makeup preslaked magnesia should be added directly at the active gas-liquid contacting zone.
3. Materials in contact with the absorber slurry (except at the gas-liquid contacting zone) should be selected based upon their ability to resist these deposits.
4. The design of the sumps, holding tanks, and horizontal piping provide for supplemental agitation of the rapidly settling sulfite solids.

7.3 FUTURE WORK

1. A regeneration facility should be added to the present pilot plant to demonstrate its capability to regenerate magnesia for reuse and to produce a usable sulfur product. This regeneration facility should be compatible with wet scrubbing in the following important aspects:
    a. Should be capable of thermally decomposing magnesium sulfate in addition to the sulfite.
    b. Should permit a fly ash load in the sulfite slurry.
    c. The regenerated magnesia must be reactive to be reusable. Therefore, the thermal decomposition temperature should be minimized.
    d. To prevent a disposal problem, the water cycle should be closed.

2. The feasibility of employing a single dual-purpose scrubber in the wet scrubbing process should be investigated. This would require the following:
    a. Means for separating the fly ash solids from the relatively coarse sulfite crystals.
    b. Collecting 99^+% of fly ash and 98^+% of SO_2 in a single scrubber at reasonable energy levels.
3. A laboratory study should be implemented for determining physical property data such as vapor pressure of SO_2 over the sulfite slurry, which is needed for complete analysis of absorber performance in terms of the number of transfer units; settling rate and particle size distribution of slurry solids, which is needed for proper specification of separation equipment; and viscosity and specific gravity data needed for pump sizing.
4. Materials appropriate for the spray zone, sumps, piping, etc. which are suitable for construction, are abrasive resistant and which do not exhibit a tendency to receive the sulfite deposit should be identified and specified. Extrapolation of specifications from other wet scrubbing systems is not appropriate and is not recommended.
5. The gas absorbers, both the floating bed type and the venturi type, should be optimized from an absorption-versus-power-consumption standpoint. This could potentially reduce the capital and operating costs of the wet scrubbing components substantially. It would also help clarify the suitability of the proper scrubber type.
6. The feasibility of adopting the magnesia base scrubbing system to NO_x absorption through an add-on scrubber should be investigated. Such a process would entail NO_2 injection ahead of the NO_x absorber. Magnesia slurry would be used as the contacting medium.
7. A system control study from an instrumentation standpoint is suggested. It is recommended that a control system be simulated and then installed on the pilot plant to develop and demonstrate a continuous, controllable system.

Important analysis of flow streams, such as continuous monitoring of slurry composition, should be developed. For example, there should be a capability of analyzing the bisulfite-sulfite-magnesia content (possibly by pH only) and the magnesium sulfate concentration (possibly by specific gravity).

8.0 ACKNOWLEDGEMENTS

The authors wish to recognize several persons who aided measurably in the progress and success of this project. W. L. Sage devised the preliminary design of the pilot plant, including several innovations which later proved invaluable to the steady operation of the plant. Mr. Sage also directed the modification of the test furnace, including the feed system to burn pulverized coal. E. D. Scott aided Mr. Sage in these activities in addition to helping with the actual plant installation. J. T. Eunson directed the detailed design and erection of the plant, including ordering all materials and directing the necessary engineering drawings. J. P. Rooney devised a unique means of constructing,the floating bed absorber, which saved substantially on its erected cost. J. M. Gidley helped establish the procedures used in this project for both gas and liquid analysis. C. W. Goddard developed the sulfate titration method employed here. Operating personnel included E. D. Scott, B. T. Lucaric, J. W. Vick, J. M. Gidley, and C. G. Bozeka.

jlr

Submitted by: W. Downs
W. Downs

A. J. Kubasco
A. J. Kubasco

Approved by: H. P. Markant
H. P. Markant

REFERENCES

1. J. J. Lingane, Electroanalytical Chemistry, second edition, Interscience Publishers, Inc., 1968, Chapter 20.

2. C. E. Rodes, et al, "Performance Characteristics of Instrumental Methods for Monitoring Sulfur Dioxide, Laboratory Evaluation", JAPCA, Vol. 19, No. 8, August 1969.

3. H. Goksoyr and K. Ross, "The Determination of Sulfur Trioxide in Flue Gases", Research Report M211, Thornton Research Center, 1961.

4. M. D. Kuznetsov and V. I. Oratovskii, "Rate of Chemisorption in a Venturi-type Apparatus", Inter. Chem. Eng., Vol. 2, No. 2, April 1962.

5. H. F. Johnstone, et al, "Recovery of Sulfur Dioxide from Waste Gases", Ind. & Eng. Chem., Vol. 30, No. 1, January 1938.

6. W. T. Smith and R. B. Parkhurst, "The Solubility of Sulfur Dioxide in Suspensions of Calcium and Magnesium Hydroxides", J. Am. Chem. Soc., Vol. 44, 1922, pp. 1918-1927.

7. F. H. Conrad and D. B. Brice, "Some Equilibrium Relations in the System Magnesium Oxide - Sulfur Dioxide - Water at Pressures Below Atmospheric", J. Am. Chem. Soc., Vol. 70, June 1948, pp. 2179-2182.

8. H. P. Markant, et al, Babcock & Wilcox Co., "Absorption Studies, $MgO-SO_2$ Systems", 47th Annual Meeting of Tappi, February 20, 1962.

9. F. H. Conrad and W. L. Beuschlein, "Some Equilibrium Relations in the System Calcium Oxide-Sulfur Dioxide-Water at Pressures Below Atmospheric", J. Am. Chem. Soc., Vol. 56, 1934, pp. 2554-2562.

10. B. A. Chertkov and N. S. Dobromyslova, "The Influence of Traces of Sulfate on the Partial Pressure of SO_2 over Ammonium Sulfite-Bisulfite Solutions",, Translated from Zhurnal Prekladnoi Khemii, Vol. 37, No. 8, pp. 1718-1723, August 1964.

11. W. A. Pollock, et al, "Sulfur Dioxide and Fly Ash Removal From Coal Burning Power Plant", Air Eng., September 1967.

12. G. L. Smithson and N. N. Bakhshi, "The Kinetics and Mechanism of the Hydration of Magnesium Oxide in a Batch Reactor", Am. J. Chem. Eng., Vol. 47, October 1969.

13. D. J. Gunn, "Absorption and Liquid Phase Oxidation of Sulfur Dioxide", Trans. Inst. Chem. Eng., Vol. 48, 1970.

14. V. Linek and J. Mayrhoferova, "The Kinetics of Oxidation of Aqueous Sodium Sulphite Solution", Chem. Eng. Science, Vol. 25, 1970, pp. 787-800.

15. B. A. Chertkov, "General Equation for the Oxidation Rate of Sulfite-Disulfite Solutions in the Extraction of SO_2 from Gases", Translated from Zhurnal Prekladnoi Khemii, Vol. 34, No. 4, pp. 771-776, April 1961.

REFERENCES (Cont'd).

16. E. G. Lowrance, "Sulfur Dioxide Scrubbers, Stone & Webster-Ionics Process", Final Report for Contract No. CPA 22-69-80 for NAPCA, January 1970.

17. W. Bartok, et al, "Systems Study of Nitrogen Oxide Control Methods for Stationary Sources", Esso Research and Engineering Co., Interim Report on Contract PH 22-68-55, May 1, 1969.

18. S. N. Gang. "Increased Removal of Nitrogen Oxides from Exit Gases by Alkaline Absorption", Izv. Vysshikh Uchebn. Zavedonii Khim i Khim Tekhnol. 4, 998-1002 (1961).

19. N. M. Zhovorankov, et al, "The Study of Absorption of Nitrogen Oxides by Alkaline Solution in Columns with Filler Bodies", Khim Prom. 754.

20. L. G. Wayne and D. M. Yost, J. Chem. Phys. 18, 767-768, 1950.

21. M. S. Peters and J. L. Holman, "Vapor and Liquid Phase Reactions between Nitrogen Dioxide and Water", Ind. & Eng. Chem., Vol. 47, No. 1, December 1955.

22. J. H. Perry, "Chemical Engineer's Handbook", Fourth Edition, McGraw-Hill Book Company, Inc., 1963, pp. 3-61.

23. S. Badzioch, "Correction for Anisokenetic Sampling of Gas-borne Dust Particles", J. Inst. Fuels, March 1960.

APPENDIX A

DETAILS OF ANALYSIS TECHNIQUES

A.1 SULFUR DIOXIDE SAMPLING

Sampling of flue gases for sulfur dioxide determination was accomplished by passing the sample gas through a Barton Electrolytic Titrator, the output of which is continuously recorded on a strip chart recorder. Operation of the equipment is simple and requires little of an operator's time, yet it has been found to be very accurate.

A.1.1 Apparatus

The complete sampling train is shown in Figure 3.2 and consists of the apparatus described in the section below.

(a) Sampling Probe in Furnace Exit Duct

The sampling probe used at the furnace exit consists of a 1-3/4" stainless steel pipe 9 inches long, one end of which is capped and fitted with a 1/4" connector. A plug of glass wool is placed in the end of the sampling probe to filter fly ash.

(b) Sampling Tube in Particulate Cyclone Exit and Pilot Plant Exit

The sampling tube consists of a one-fourth-inch O.D. glass tube inserted in a two-inch diameter by eight-inch long stainless steel pipe nipple. This sampling tube is designed to avoid liquid carryover from being sucked into the small sampling line by providing a relatively quiescent zone ahead of the sampling tube. The large volume-to-area ratio in the nipple reduces the possibility of the gas sample being scrubbed by the slurry.

(c) Dry Trap

A 500 ml Erlenmeyer flask is placed after the sampling tube to trap any moisture which may condense in the sampling tube.

(d) Gas Pump

A single-acting diaphragm pump draws the gas sample through about 10 feet of "Polyflow" tubing.

(e) Excess Gas Vent

A tee located in the sample line is fitted with a 1/4-inch needle valve and a gas trap. Excess gas, pumped by the diaphragm pump, which does not flow through the Barton Titrator is vented.

(f) Titrator Gas Pump

A Cole-Parmer peristaltic pump with variable speed control is used to pump the gas sample through the Barton Titrator. A dry trap located just ahead of this pump removes any water from the line before entering the Barton Titrator.

(g) Model 286 Barton Recording Electrolytic Titrator

The Barton Electrolytic Titrator is a coulometric gas analyzer. The sample gas is passed through an electrolytic solution in which a triple electrode is immersed. The sulfur dioxide reacts with part of the reactant in the electrolyte. Simultaneously the electrode attempts to maintain the concentration of the reactant constant by passing a current through the electrolyte. The amount of current used is proportional to the amount of SO_2 reacted and hence to the concentration of SO_2 in the gas stream.

(h) Bubble Tube

A plastic bubble tube is used to measure the gas flow rate. This consists of a 5/8" inside diameter, clear plastic tube with a support base. The flow rate is determined by the time taken for a bubble to rise between two marks which defines a volume.

A.1.2 Procedure

(a) Sampling

(1) Connect the sampling train as shown in Figure 3.2 making sure that all joints are gas-tight. Make sure that the appropriate sampling line is open and the NO_x lines pinched off.

(2) Switch on the diaphragm pump. Next, turn on the variable speed peristaltic pump to a flow of 250 ml/min sample gas.

(3) Turn the Barton on and run through the necessary blanking and preliminary start-up procedures. (See Barton Bulletin G1-20)

(4) By adjusting both the needle valve on the excess gas vent and the speed on the variable speed pump, maintain a gas flow rate of about 250 ml/min through the Barton. If the Barton is set for its highest range and if the recording pen goes off scale, then the gas flow rate must be reduced. This is permissible because this analyzer measures the mass flow rate of SO_2 to the instrument. However, it is not advisable to increase the

sampling rate substantially above 250 cc/min since the reaction efficiency in the cell can deteriorate.

A.1.3 Determination of Sulfur Dioxide

The Barton instruction manual contains the necessary charts, equations, and conversion factors to convert the cahrt reading into an SO_2 concentration expressed as ppm with the following exception: The manual does not indicate clearly that the correction factor for decreasing the sampling rate is linear. However, this was checked and found to be true.

A.1.4 Spinning Syringe Calibration

The spinning Syringe apparatus used for calibrating the Barton Electrolytic Titrators is shown in Figure A.1. A description of the apparatus and procedures is given below.

FIGURE A.1. SPINNING SYRINGE APPARATUS

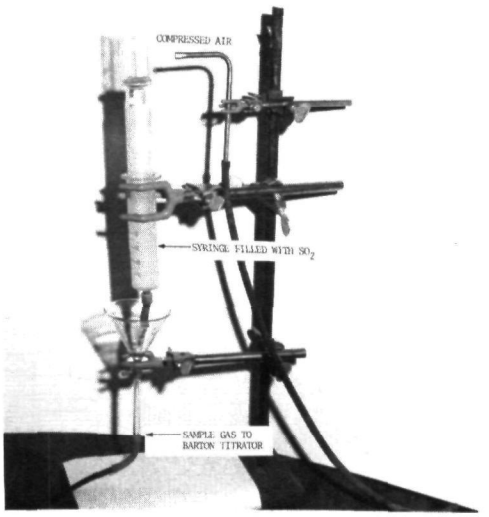

(a) Apparatus

1. Glass Hypodermic Syringe. A 50 ml Hamilton syringe with a polished ground glass plunger and barrel assembly capable of spinning freely with minimum gas leakage was prepared and used.
2. Spinning Vanes. A plastic vane structure was constructed of 1/16" thick plexiglas and epoxy glued to the plunger top.
3. Flow Orifice. A piece of 3 MM glass capillary tubing was heated and drawn to a fine orifice tip for delivery of the sample gas.
4. Spinning Force. A small nozzle made of 1/4" stainless steel tubing was connected to compressed air which has passed through a glass wool moisture trap.
5. Ring Stand and Clamps. Standard laboratory clamps and stands were used to set up the equipment as shown earlier.
6. Sample Pump. A Cole Palmer peristaltic pump with variable speed control was used to supply the sample gas to the Barton Titrator being calibrated.

(b) Calibration Procedure.

1. Check of Syringe Delivery Rate. With the syringe mounted as shown and with the plunger spinning, time the delivery of 20 ml using a stop watch. By breaking off small portions of the glass flow orifice, time of delivery is adjusted until ∿30 minutes delivery time for 50 ml is attained. After removing the orifice tip and plugging the syringe, determine the time for the plunger to descent 5 ml while spinning, this being the plunger-barrel leak rate. The corrected delivery time as ml/min is then calculated.

2. Formulation of Calibration Mixture. Using a Hamilton gas tight syringe of the appropriate size, a sample of pure SO_2 is withdrawn from a Matheson gas cylinder whose contents had been previously analyzed by the manufacturer. This SO_2 is then injected into the 50 ml glass syringe as the glass plunger is withdrawn to the 50 ml mark, thus creating a slight negative pressure which insures no sample loss and also aids in the mixing of the gases as they are diluted within the glass syringe. The orifice tip is then placed on the syringe making it ready for use.

3. Calibration. The Barton Titrator is prepared for sampling with a gas inlet flow of ∿250 ml/min in a location where ambient air is free of sulfur compounds. After blank adjustments of the Barton titration cell have been completed, the syringe is mounted so that delivery of the calibration gas is made at the inlet to the pump. The calibration gas sample is run until a stable reading is obtained and the net reading is then recorded along with range setting and actual gas flow through the Barton Titrator. Duplicate runs are made to check repeatability of the sample analysis.

4. Calculations.

Data:

Volume of pure SO_2, ml	= Vs	Barometric pressure, mm Hg	= P
Temperature, °K	= T	Flow rate through cell, ml/min	= R
Syringe delivery time, Min	= t		

(a) $V_{STP} = V_S \times \frac{P}{760 \text{ mm}} \times \frac{273^{\circ}K}{T}$

(b) $\text{PPM } SO_2 = \frac{V_{STP} \times 10^{-3}}{t \times R \times 10^{-3}}$

Example:

V = .1 ml
T = 297°K (24°C)
t = 30 min
P = 740 mm
R = 250 ml/min

$$V_{STP} = .1 \times \frac{740}{760} \times \frac{273}{297} = .09 \text{ ml}$$

$$V_{STP} = .09 \text{ ml}$$

$$\text{PPM } SO_2 = \frac{.09 \times 10^{-3}}{30 \times 250 \times 10^{-3}} = \frac{9. \times 10^{-5}}{7.5} = 1.2 \times 10^{-5} = 12.0 \text{ ppm}$$

A.2 SO_3 SAMPLING APPARATUS & PROCEDURE

The collection of SO_3 is based on a method by H. Goksoyr and K. Ross. The titration method for determining the amount of SO_3 collected was developed in-plant.

The design of the collector, Figure A.2, is based on the idea of condensing the sulfur trioxide from the flue gas as sulfuric acid "at a temperature sufficiently below the acid dewpoint to leave a negligible quantity of acid in the vapor state but high enough to prevent condensation of water vapor".[3]

FIGURE A.2. SO_3 COLLECTOR

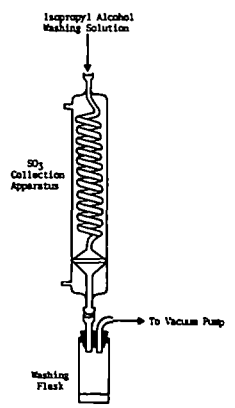

The method is described by Goksoyr and Ross as follows: "The flue gases are drawn through a glass coil and a Grade 4 sintered glass disc, both enclosed in a water-filled jacket. The water is maintained at a temperature (60-90°C) well below the acid dewpoint but slightly above the water dewpoint. Practically all the sulfuric acid condenses on the walls of the coil. Any acid mist particles left in the gas stream are retained by the sintered glass filter. The acid is then washed out and determined by titration with standard barium chloride solution."[3] They also incorporate into their sampling train a method for SO_2 determination. This method was not used as we employed a Barton Electrolytic Titrator for SO_2 analysis.

As the SO_3 vapor enters the cool region of the coil, it will condense to a fine mist. Due to centrifugal action of the gas going through the coil, these droplets will be thrown to the glass walls. According to Goksoyr and Ross, "The size of the droplet centrifuged from the gas stream is dependent upon the distance between the droplet and the collecting wall at the inlet to

the coil. When this distance is maximum, i.e., equal to the tube diameter, it has been estimated that all droplets larger than 0.63 micron in radius formed at the inlet to the coil will move to the wall. When this distance is less than the tube diameter, droplets smaller in radius than 0.63 micron will also be forced to the wall of the coil. In addition, some of these smaller particles will probably agglomerate and be thrown out of the gas stream."[3] They have shown that a very large proportion of the acid is collected on the walls of the coil. Other workers have shown that Grade 4 sintered glass filter is an effective medium for retaining small particles of acid. Therefore, Goksoyr and Ross conclude that a collector of their design will collect all the sulfur trioxide present in a gas sample.

A.2.1 Sampling Apparatus

(a) Sampling Probe

The sampling probe consists of a quartz tube 1/2" inside diameter by 18 inches long wrapped with a nichrome wire heating element. This assembly is covered by refractory and sheathed in a stainless steel pipe, see Figure 3.7. The sheath is fitted with a pipe cap which enables the probe to be screwed onto a pipe nipple on the side of the furnace exit duct.

(b) Solids Filter

A plug of glass wool in the sampling probe acts as a fly ash filter.

(c) Gas Thermocouple

A spherical glass elbow joint connected to the sampling probe is tapped with a thermocouple junction. This permits measurement of gas temperature entering the collector.

(d) Sulfur Trioxide Collector

The collector used in these tests is shown in Figure A.2.

(e) Sulfur Dioxide Absorber

A 1000 ml Erlenmeyer flask filled with about 500 ml of 3% hydrogen peroxide is used to absorb the SO_2 in the gas. This absorption is to prevent corrosion in the gas meter, a quantitative determination of the gas absorbed is not made.

(f) Drying Column

The gas is dried before entering the meter and pump by passing it through a cylinder filled with indicating silica gel.

(g) Gas Meter

A Sprague gas meter, maximum capacity 175 scfh, was used in these tests.

(h) Vacuum Pump

Fisher vacuum pump with a free air displacement of 4 cubic feet per minute at 15 psig.

A.2.2 Analytical Apparatus

(a) Burette

10 ml microburette Grade A

(b) Beakers

Assorted

(c) Evaporating Dish

White porcelain

(d) Light

Daylight fluorescent

(e) Magnetic Stirrer and Teflon-Coated Bar

(f) Pipette

10 ml

(g) Washings Flask

A.2.3 Reagents

(a) Washing solution consisting of 80% isopropyl alcohol, the remainder being deionized water.

(b) Barium chloride standard solution - dissolve 1.221 grams of $BaCl_2 \cdot 2H_2O$ in one liter of deionized water that has been adjusted to pH 3.8 to 4.0 with dilute HCl. Standardize against standard sulfate solution. (1 ml = 0.500 mg $SO_4^{=}$)

(c) Ammonium hydroxide (1:1) - Mix one volume of ammonium hydroxide (NH_4OH, sp. gr. 0.90) with one volume of deionized water.

(d) Hydrochloric acid (1:99) - Mix one volume of HCl (sp. gr. 1.19) with 99 volumes of deionized water.

(e) Thorin - "SulfaVer" (Hach Chemical Co.) or dissolve 0.2 gram of 2 (2-hydroxy-3, 6-disulfo-1-naphthylano) benzene arsonic acid in 100 ml of deionized water.

(f) Sulfate, standard solution (1 ml = 0.100 mg $SO_4^{=}$) - Dissolve 0.1479 grams of anhydrous sodium sulfate (Na_2SO_4) in deionized water and

dilute to one liter. Standardize by gravimetric determination of sulfate as $BaSO_4$.

(g) Alcohol - isopropyl (2-propanol).

A.2.4 Procedure

(a) Sampling

(1) Make sure that the helical coil and sintered glass filter of the collector are clean. To clean these parts, draw acetone then air through the collector. If the filter becomes contaminated with fly ash, it may be cleaned with chromic acid. All traces of acid must then be washed out.

(2) Connect the sampling train as shown in Figure 3.7. Apply stopcock grease to all joints to preclude the possibility of leaks.

(3) Turn the water bath pump on and adjust hot plate for a water temperature of 60-90 C.

(4) Adjust the rheostat on the sampling probe heating element to give a gas temperature of about 350 F at the collector inlet.

(5) Turn on the vacuum pump and adjust the sampling rate up to 1/2 cubic foot per minute. When the appropriate volume has been sampled, turn off the pump.

(6) The following data was taken during a test:

a. Initial and final gas meter readings

b. Meter pressure

c. Barometric pressure

d. Ambient temperature

e. Gas temperature entering collector

f. Sulfur dioxide concentration at furnace exit

(b) Determination of Sulfur Trioxide

(1) Disconnect the collector from the sampling train and connect it to the washings flash.

(2) Using a wash bottle, squirt about 50 ml of washing solution into the collector and draw it through slowly using the vacuum pump.

(3) Wash out the glass elbow which lies between the collector and the probe.

(4) Record the volume of the washings and pipette about 10 ml into the evaporating dish.

(5) To perform the titration accurately a total of 40 ml of solution must be in the evaporating dish. Therefore if 10 ml of washing solution is pipetted into the evaporating dish then 30 ml of 100% isopropyl alcohol are added, if 5 ml of washing solution are used then 35 ml of 100% isopropyl alcohol is added, and so on.

(6) Add two drops of "SulfaVer" (sulfur indicator). The pH of the solution in the evaporating dish is then adjusted by first adding 1:1 ammonium hydroxide dropwise until the solution turns a deep pink. The 1:99 hydrochloric acid is added until the solution turns a pale yellow. The solution is now ready for titration.

(7) The magnetic stirrer is turned on and the solution titrated with barium chloride solution from a microburette. As the end point is approached, the solution will begin to turn pink. When the solution stablilzes to a pink color, the end point has been reached.

A.2.5 Calculation

Calculate the SO_3 concentration by the following equation:

$$\text{ppm } SO_3 \text{ by volume of dry gas} = \frac{V_S \times V_R \times C_R \times (0.689)}{V_T \times V_S \times \rho_S}$$

where V_S = total volume of washings, ml

V_R = amount of $BaCl_2$ used in the titration, ml

C_R = $SO_4^{=}$ equivalence of $BaCl_2$, mg $SO_4^{=}$/ml $BaCl_2$

V_T = volume of washings titrated, ml

V_S = volume of gas sampled, cf of dry flue gas corrected to 0°C and 760 mm Hg

ρ_S = density of flue gas, #/cf

$$0.689 = \frac{\dfrac{(10^{-3}\ \text{gm/mg}) \times 10^{6}\ \text{ppm/mole fraction}}{(96\ \text{gm/gm mole})\ (454\ \text{gm mole/\# mole})}}{\dfrac{1\#\ \text{mole dry gas}}{30\#\ \text{dry gas}}}$$

A.2.6 Other SO_3 Methods Used

Before the Goksoyr-Ross Method was adopted, an in-plant method and alternates thereto were used. This method referred to in Table 4.14 as the Chemistry Laboratory Method (No. 206) involves bubbling the sample through an 80% isopropyl

alcohol - 20% water solution followed by a colormetric determination of the solution using barium chloranilate. A detailed description of the method is available upon request. The three forms of this method referred to in Table 4.14 are as follows:

1. Chem Lab Method, not N_2 purged - No modifications
2. Chem Lab Method, purged - After the sample was collected in the isopropanol solution, nitrogen was purged through the sample to strip any potentially absorbed SO_2 before it would have time to oxidize to the sulfate. The purging involved passage of 100 cc/min of bottled nitrogen for 30-45 minutes
3. Chem Lab Method, purged, acidified with Hcl - This method is similar to 2 above except that the absorbing solution is modified to include a 2 ml concentrated HCl to 100 ml of sample. The hope here was to further reduce the possibility of SO_2 absorption and oxidation.

A.3 DUST LOADING APPARATUS AND PROCEDURE

A special probe was designed with the filter placed immediately after the sampling nozzle. This feature eliminates the problem with some dust probes which use externally placed filters in which dust settles out along the probe length before it reaches the filter. Dust laden gas is drawn through the probe and the volume recorded by a gas meter. The weight of the dust collected is determined and from this a dust loading value can be obtained.

A.3.1 Apparatus

The assembled dust sampling train is shown in Figure 3.10 and consists of the apparatus described below.

(a) Sampling Probe

The sampling probe is shown in Figure 3.8. The nozzle is approximately 2 inches long and is screwed into the probe body. The Whatman cellulose extraction thimble fits over the back end of the nozzle. The thimble is held in place by an O-ring. When the nozzle is screwed into the probe, the O-ring is compressed and makes a gas-tight seal around the thimble. The dust therefore travels only a couple of inches into the probe before it is filtered.

(b) On-Off Valve

A ball valve provides for on and off control to the vacuum pump.

(c) Drying Column

The gas is dried before entering the gas meter by passing it through a column of indicating silica gel. This also acts to remove corrosive SO_2.

(d) Manometer

A mercury manometer is used to indicate the gas pressure at the meter.

(e) Gas Meter

A Sprague 175 scfh gas meter is used to measure the total volume of gas sampled.

(f) Vacuum Pump

A Fisher vacuum pump capable of delivering 3.2 cubic feet of air per minute at 15 psig was used to draw the gas sample through the probe.

(g) Slide Valve Air Lock

Located at the particulate scrubber and pilot plant exit duct is a 5-inch flanged slide valve on to which the probe is bolted. The probe is bolted in place with the slide valve closed; then the slide valve is opened and the probe inserted into the duct. This arrangement is an air lock which eliminates pressure upsets in the duct.

A.3.2 Procedure

(a) Sampling

(1) Connect the sampling train as shown in Figure 3.10 making sure that all joints are gas tight.

(2) With the ball valve in the closed position, open the slide valve and insert the probe into the duct.

(3) With the bleed valve on the vacuum pump wide open, turn on the pump. Immediately open the ball valve and adjust the bleed valve on the vacuum pump for a flow rate of approximately 0.5 cfm.

(4) The volume of gas sampled should be about 5 cubic feet. This will provide a measurable amount of collected dust.

(b) Analysis

(1) Before the extraction thimble is used, it is numbered for identification and then weighed to four decimal places. It

is then placed in a desiccator for 24 hours and reweighed. If the reweighing agrees to within 0.0002 grams, the filter is considered acceptable. Otherwise, it is held in lieu of reweighing. All filters are kept in individual desiccators until used. Drying by heating in an oven was found to be completely unsatisfactory since apparently some of the paper oxidized.

(2) After the extraction thimble was used, it would be subjected to the same weighing procedure as above. Care in this procedure is vital since the mass collected was often less than 1% of the filter weight. However, experience has shown this procedure to yield highly reproducible results.

A.4 MODIFIED PALMROSE ANALYSIS

The modified Palmrose analysis was used to determine the composition of of magnesia-base scrubbing slurry except the sulfate and flyash constituents. Two samples were analyzed; one of the total slurry, and the other of a filtered sample. A syringe filter was used. See Figure 3.15. The filtered sample provided a means of determining the composition of the dissolved species which are of importance from an SO_2 absorption and vapor pressure standpoint while the filtered sample provided a means of determining the suspended solids concentration and was needed to complete the sulfur and magnesium material balances.

The total concentration of SO_2 including both $SO_3^{=}$ and $HSO_3^{=}$ in the solution is determined by oxidizing the sample with potassium iodate in which the following reactions control:

$$KIO_3 + 5KI + 6H^+ \rightarrow 6K^+ + 3H_2O + 3I_2 \qquad \text{(A-1)}$$

$$\begin{matrix} 3SO_3^{=} \\ 3HSO_3^{-} \end{matrix} + 3I_2 + 3H_2O \rightarrow 6H^+ + 6I^- + \begin{matrix} 3SO_4^{=} \\ 3HSO_4^{-} \end{matrix} \qquad \text{(A-2)}$$

Before the titration is performed, an excess of potassium iodide is added to the sample. The sample is then acidified with sulfuric acid to a methyl red end point. This insures that there is an excess of H^+ so that reaction (A-1) will proceed rapidly during the titration. The sulfuric acid must be added carefully because the solubility of SO_2 is reduced as the pH drops thereby increasing the chance of stripping SO_2 from the sample before it can be oxidized to the sulfate.

During titration, reaction (A-2) occurs instantaneously while reaction (A-1) is somewhat slower. This titration is performed to a starch end point. Thus the amount of KIO_3 consumed is a measure of the total SO_2 in solution. The convention adopted for this analysis by the pulp and paper industry is to report all concentrations as equivalent grams of SO_2 per 100 gm sample. More realistically, the specific gravity correction is usually ignored and the data is actually reported as gms SO_2 per 100 ml sample. Thus the total SO_2 concentration is calculated as follows:

$$\frac{\text{gm Total } SO_2}{\text{100 ml sample}} = \frac{\text{ml } KIO_3 \text{ x Normality } KIO_3}{\text{Volume of Sample}} \text{ x } \frac{\text{32 gm } SO_2}{\text{Eq } SO_2} \text{ x } \frac{1}{10} \qquad \text{(A-3)}$$

The 1/10 enters the equation because Normality is expressed in terms of 1000 ml whereas the Total is expressed in terms of 100 ml; this is also the case with the calculation for FREE SO_2.

As shown previously, the actual oxidizable sulfur constituents of the absorbing slurry are $Mg(HSO_3)_2$ and $MgSO_3$. These can be expanded and written in yet another way as $MgSO_3 \cdot H_2SO_3$ and $MgSO_3$. This acid portion of the magnesium bisulfite namely H_2SO_3 is referred to as the Free SO_2 concentration and is <u>by convention</u> considered to be 1/2 of the molar concentration of HSO_3^- expressed as SO_2.

The Free is a measure of the acidity of the solution, the acidity being the result of the HSO_3^- ion concentration. It can be easily determined by titration with NaOH. Recalling that the first titration converted HSO_3^- to HSO_4^-, the following simple reaction controls this second titration:

$$HSO_4^- + OH^- \rightarrow SO_4^= + H_2O \qquad \text{(A-4)}$$

When the titration corrected for the amount of acid added to the sample before the first titration, the Free is calculated as follows:

$$\frac{\text{gm Free } SO_2}{\text{100 ml sample}} = \frac{1}{2}\left[\frac{\text{ml } NaOH_{net} \text{ x N. of NaOH}}{\text{ml of sample}} \text{ x } \frac{\text{81 gm } HSO_3^-}{\text{1 eg } HSO_3^-} \text{ x } \frac{\text{64 g } SO_2}{\text{81 g } HSO_3^-} \text{ x } \frac{1}{10}\right] \text{(A-5)}$$

The concentration of magnesium in the absorbing solution is easily calculated from the above results since the molar concentration of Mg^{++} is equal to the molar concentration of $SO_3^=$ plus one half the HSO_3^- concentration. The magnesium concentration is therefore calculated as follows:

$$\frac{Mg^{++}\ gm}{100\ ml\ sample} = \left(\frac{Total\ gm\ SO_2}{100\ ml} - \frac{Free\ gm\ SO_2}{100\ ml}\right)\left(\frac{24\ gm\ Mg}{64\ gm\ SO_2}\right) \qquad (A\text{-}6)$$

The first term on the right has been adopted as an indirect measure of the magnesium concentration and is referred to as the Combined SO_2.

$$Combined\ SO_2\ \frac{gm}{100\ ml} = \left(\frac{Total\ gm\ SO_2}{100\ ml} - \frac{Free\ gm\ SO_2}{100\ ml}\right) \qquad (A\text{-}7)$$

A.4.1 Apparatus

(a) 2-1/2 ml Leverlok disposable syringe with 18 gauge needle

(b) 250 ml beaker

(c) 25 ml burettes, 4 used

(d) magnetic stirrers, 3 used

A.4.2 Reagents

(a) Potassium Iodate (KIO_3): N/8

(b) Sodium Hydroxide (NaOH): N/8

(c) Sodium Thiosulfate ($Na_2S_2O_3$): 3%

(d) Sulfuric acid: N/8

(e) KI - Starch solution (100 gm KI + 200 gm Thiodene + 800 gm water)

(f) Methyl red indicator

(g) Deionized water

A.4.3 Procedure

(a) Obtaining and preparing sample

(1) Unfiltered sample - Using the 2-1/2 ml syringe, exactly 2 ml of sample are drawn. Care is taken here for if excess sample is taken and if the excess is discarded by drawing the plunger back to 2 ml, the solids may partially settle and what remains is no longer representative.

(2) Filtered sample - The sample is drawn into the syringe slowly to prevent tearing of the filter paper. Excess sample may be drawn here and the excess discarded.

(3) The sample is then injected into a beaker containing 60 to 75 ml of demineralized water. The diluted sample is redrawn into the syringe several times to completely wash or purge the sample.

(4) A few drops (3 to 5) of methyl red indicator are added to the sample. This will turn the solution yellow.

(b) Total SO_2 Titration

(1) 5 ml of starch - KI solution are added to the sample.

(2) Pipette 1/8 normal sulfuric acid into the sample until it turns slightly red. Do not exceed the end point since this may contribute to stripping of SO_2 from the sample. Note the amount of H_2SO_4 added.

(3) Titrate with 1/8 normal potassium iodate (KIO_3). Do not stir the sample until a blue color starts to appear. Titrate until one drop produces an intense blue color. Premature stirring would aggrevate the SO_2 stripping problem. Note the volume of KIO_3 used.

(c) Free SO_2 Titration

(1) To bring the sample back from the deep blue to a red color, add a couple drops of sodium thiosulfate. If more than a few drops are required to effect the color change, the KIO_3 end point was exceeded and the entire process should be started over.

(2) Titrate the sample to a bright yellow end point with 1/8 normal NaOH. Note the volume of hydroxide titrated.

A.4.4 Calculations

If this procedure is followed exactly, the composition is calculated as follows:

Total SO_2 = ml KIO_3 x 0.2 = gm SO_2/100 ml

Free SO_2 = (ml NaOH - ml H_2SO_4) x 0.2 = gm SO_2/100 ml

Combined = Total - Free = gm SO_2/100 ml

A.5 DETERMINATION OF SULFATE ION IN Mg-SO_2-H_2O SYSTEM*

A.5.1 Scope and Principle

This method covers a rapid volumetric determination of sulfate ion in Mg-SO_2-H_2O slurry systems over the range of 20 to 1000 ppm.

Sampling is performed in the absence of oxidizing media. Sulfites and bisulfites are decomposed by treatment with acid under inert gas atmosphere. Interfering cations are removed by ion exchange and the sulfate ion is titrated in an alcoholic solution under controlled acid conditions with a standard barium chloride solution using thorin (SulfaVer) as the indicator.

---

*Modified version of ASTM:D516-63T, Nonreferee Method B

A.5.2 Interferences

Cations and anions may cause coprecipitation errors with the barium sulfate precipitate. Potassium, iron, aluminum, fluoride, and nitrate interfere. Phosphate does not interfere appreciably below 300 ppm. Most metallic ions form colored complexes with thorin. Cation interference is eliminated by ion exchange. Cr and Zr may form anion complexes with the sulfate ion. Fluorides and nitrates cause no serious interference up to 2 and 50 ppm, respectively. Sulfite must be eliminated or determined and subtracted if its presence is suspected. Chlorides obscure the end point when the sulfate is low. End point detection is better the higher the sulfate concentration. Sulfides, if present, must be removed. Chromium present as chromates and dichromates must be reduced and removed by ion exchange.

A.5.3 Apparatus

(a) Beakers - assorted

(b) Burette - 1-50 ml (Na_2SO_4 solution)
1-5 ml micro, 0.01 ml graduations ($BaCl_2$ solution)

(c) Erlenmeyer flask - 50 cc capacity and rubber stopper fitted with gas inlet glass tubing reaching the flask bottom. Vertical gas outlet tubing venting flask.

(d) Evaporating dish, white porcelain

(e) Jones reductor column - 50 cm long x 2.06 cm in diameter. Insert a plug of glass wool in the bottom of the column and fill approximately 12 cm high with "HachVer" No. 252 resin (IR-120, 20 to 25 mesh can be used). Regenerate the resin after each sample by passing (1:4) HCl through and washing thoroughly with deionized water.

(f) Light - daylight fluorescent

(g) Magnetic stirrer and teflon coated bar

(h) Pipette - 1 ml volumetric type
2 ml " "
3 ml " "
5 ml " "
10 ml " "

(i) Volumetric flask - 2-1000 ml ($BaCl_2$ and Na_2SO_4 solutions)
1-50 ml (Sample)

A.5.4 Reagents

(a) Alcohol - isopropyl (2-propanol). Ethyl alcohol (95%), methyl alcohol or "HachVer Nonaqueous Solvent" (Hach Chemical Co.) may be used.

(b) Ammonium hydroxide - reagent grade.

(c) Barium chloride ($BaCl_2 \cdot 2H_2O$) - reagent grade.

(d) Hydrochloric acid (HCl) - 37-38%, sp gr 1.188-1.192, reagent grade.

(e) Ion exchange resin - "HachVer", No. 252 or IR-120 cation exchange resin, 20-25 mesh.

(f) Nitrogen gas

(g) Sodium sulfate - reagent grade

(h) Thorin - "SulfaVer" (Hach Chemical Co.) or 2 (2-hydroxy-3, 6-disulfo-1-naphthylazo) - benzene arsonic acid.

A.5.5 Solutions

(a) Ammonium hydroxide (1:1) - Mix one volume of ammonium hydroxide (NH_4OH, sp gr 0.90) with one volume of deionized water.

(b) Barium chloride standard solution - dissolve 1.221 grams of $BaCl_2 \cdot 2H_2O$ in one liter of deionized water that has been adjusted to pH 3.8 to 4.0 with dilute HCl. Standardize against standard sulfate solution. (1 ml = 0.500 mg $SO_4^{=}$).

(c) Hydrochloric acid (1:4) - Mix one volume of concentrated hydrochloric acid (HCl, sp gr 1.19) with four volumes of deionized water.

(d) Hydrochloric acid (1:99) - Mix one volume of HCl (sp gr 1.19) with 99 volumes of deionized water.

(e) Sulfate, standard solution (1 ml = 0.100 mg $SO_4^{=}$) - dissolve 0.1479 grams of anhydrous sodium sulfate (Na_2SO_4) in deionized water and dilute to one liter. Standardize by gravimetric determination of sulfate as $BaSO_4$.

(f) Thorin - "SulfaVer" (Hach Chemical Co.) or dissolve 0.2 gram of 2 (2-hydroxy-3, 6-disulfo-1-naphthylazo) benzene arsonic acid in 100 ml of deionized water.

A.5.6 Procedure

(a) Place 2 ml of concentrated HCl in the 50 ml Erlenmeyer flask. Place stopper fitted with inlet and outlet glass tubing in flask. Attach tubing supplying nitrogen gas. Purge flask with continuous nitrogen flow.

(b) Add 10 ml sample by hypodermic syringe through the outlet tube vent, see Figure 3.18.

(c) Place flask on hot plate (with N_2 flowing) and heat solution to slow boil until all trace of SO_2 is absent. (About ten minutes.)

(d) Remove flask from hot plate, wash inlet glass tube with a small amount of deionized water. Cool.

(e) Add NH_4OH (conc.) dropwise until a precipitate appears and HCl (conc.) dropwise until the precipitate just dissolves. Cool sample.

(f) Pour sample into ion exchange column. Wash flask with minimum amount of water. Pass sample through column slowly and collect in 50 ml volumetric flask. Wash column with water until flask is filled to mark. Do not allow liquid level to fall below top of resin in the column.

(g) Shake sample and, using appropriate aliquot, pipette sample into white porcelain evaporating dish. Place dish on magnetic stirrer. Stir gently.

(h) Add 40 ml of nonaqueous solvent and 2 drops of thorin indicator.

(i) Adjust the pH to 3.8 to 4.0 by carefully adding NH_4OH (1:1) dropwise until the solution just turns pink. Then add HCl (1:99) until the pink disappears and the solution changes to yellow. If NH_4OH is added too fast, it is possible to overrun the color change from yellow to pink and the sample stays yellow. It is then impossible to develop by NH_4OH addition.

(j) Titrate the solution with standard $BaCl_2$ solution (1 ml = 0.500 mg $SO_4^{=}$) to a stable pink which deepens to a reddish pink on overtitration. A blank of sulfate-free water is treated in the same manner. (Allow a time lapse of 3-5 sec between additions of the last few increments of $BaCl_2$.) The color change can best be seen using constant stirring and a daylight fluorescent light.

A.5.7 Determination of Sulfate Ion ($SO_4^{=}$) Concentration

$$SO_4^{=}, \frac{\text{gm}}{\text{ml sample}} = \frac{C_R\ V_R}{V_T}\left(\frac{V_D}{V_S}\right)$$

where: C_R = Conversion factor for titrating reagent, gm $SO_4^{=}$/ml $BaCl_2$

V_R = Volume of Reagent titrated, ml $BaCl_2$

V_T = Volume of sample titrated, ml

V_D = Volume of diluted sample, ml

V_S = Volume of original sample, ml

A.6 PARTICULATE SOLIDS APPARATUS AND PROCEDURE

The determination of percent solids in the particulate scrubber slurry is accomplished by simple filtration of a known volume of slurry and subsequent weighing of the solids. The following sections will describe the actual apparatus and procedure.

A.6.1 Apparatus

(a) 100 ml graduated cylinder

(b) Millipore filters (solvent resistant), Solvinert, UL, 1.5 μ

(c) Millipore filter holder and filtering flask

(d) Vacuum pump

(e) Desiccator

A.6.2 Procedure

(a) From the product nozzle of the particulate scrubber, take less than 100 ml of slurry in a graduated cylinder; note the volume of sample. Be sure to use the entire sample drawn.

(b) Filter the sample through a millipore filter while applying a vacuum to help filtration.

(c) Towards the end of the filtration wash the solids with a few milliliters of methanol or acetone. This helps to remove most of the remaining surface water.

(d) Remove the filter paper containing the solids from the filter holder and place it in a desiccator.

(e) Allow the sample to dry over night and then weigh.

A.7 MgO MAKEUP SLURRY TITRATION PROCEDURE

The percent MgO solids in the makeup slurry was determined as described in the following sections.

A.7.1 Apparatus

(a) Pipette with 1/8-inch O.D. tip calibrated to hold 20 ml

(b) 150 ml beaker, 500 ml beaker

(c) Magnetic stirrer with teflon-coated bar

(d) Burette with 25 ml capacity

A.7.2 Reagents

(a) 7N hydrochloric acid

(b) Methyl red indicator

A.7.3 Procedure

(a) Using a 500 ml beaker take a sample of the slurry from the holding tank.

(b) While stirring the slurry to keep a uniform suspension of solids, draw exactly 20 ml into the pipette. Do not overdraw and drain excess.

(c) Pipette the sample into a 150 ml beaker.

(d) Add a few drops of methyl red indicator, the solution turns yellow.

(e) Titrate with 7N HCl until the solution remains a clear red color.

A.7.4 Determination of Percent Solids

Noting the number of milliliters of acid used, go to the standard curve, see Figure 3.20, and read the percent solids.

A.8 MAGNESIA HYDRATION ANALYSIS

This analysis was used to determine the extent to which magnesia was converted to the hydroxide. The apparatus and procedure are outlined as follows:

A.8.1 Apparatus

(a) Butner Funnel - 500 cc capacity

(b) Funnel Flash

(c) Filter Paper

(d) Drying Oven

(e) Muffle Furnace

(f) Crucibles

A.8.2 Procedure

Approximately 300 to 500 ml of magnesia slurry are sampled. The slaking time and temperature are noted. The sample is immediately filtered and rinsed with acetone. This removes most but not all of the surface water. It is probable (but not experimentally substantiated) that no further slaking would take place. The sample is then set aside for later analysis. The actual analysis consists of drying the sample (about 30 grams) at 105°C for 2 hours. The sample is then cooled in a desiccator and weighed. The weight is noted. The sample is then calcined at 400°C for at least 15 hours, cooled, and weighed. The mole % conversion to the hydroxide is calculated as follows:

$$\% \text{ slaked} = 100\left(\frac{X}{\frac{18}{40}(1-X)}\right)$$

where X = fractional weight loss

$$= \frac{m_o - m_F}{m_o}$$

and m_o = initial sample weight

m_F = Final sample weight

APPENDIX B

CORRELATION COEFFICIENTS

The quality of a mathematical expression to a fit of experimental data is usually expressed in terms of a correlation coefficient and a standard deviation. As an example, the performance of a particulate scrubber might correlate as follows:

$$\log(OD) = 1.0295 - 0.09136(\Delta P) + 0.000720(\Delta P)^2$$

Correlation coefficient = 97.0%

Standard deviation = 0.012

where OD = outlet dust loading, grains/DSCF

ΔP = venturi pressure drop, inches H_2O

The data is actually treated in the following manner. Set $\log(OD_i) = y_i$ and $\Delta P = x_i$. This gives an array of $\underline{N}$ data (y_i, x_i). A function which the engineer feels will fit the data is then proposed. In this case $y = f(x) = k_1 + k_2x + k_3x^2$. The constants are then determined by any number of mathematical techniques such as a least squares fit. The correlation coefficient, sometimes referred to as R^2, is then determined by the following expression:

$$R^2 = 1 - \frac{\sum_{i=1}^{N} (y_o - y_c)^2}{\sum_{i=1}^{N} (y_o - \bar{y})^2} \times \frac{N-1}{N-K}$$

where y_o = the observed value of y @ x_i

y_c = the calculated values of y @ x_i as found by $y_c = f(x)$

$\bar{y}$ = the arithmetic mean average of all values of y_o

N = total number of data points

K = total number of constants in f(x)

As such, the above expression is a measure of how much better the correlation $y_c = f(x)$ fits the observed data y_o than does the correlation $y = \bar{y}$. Showing this graphically,

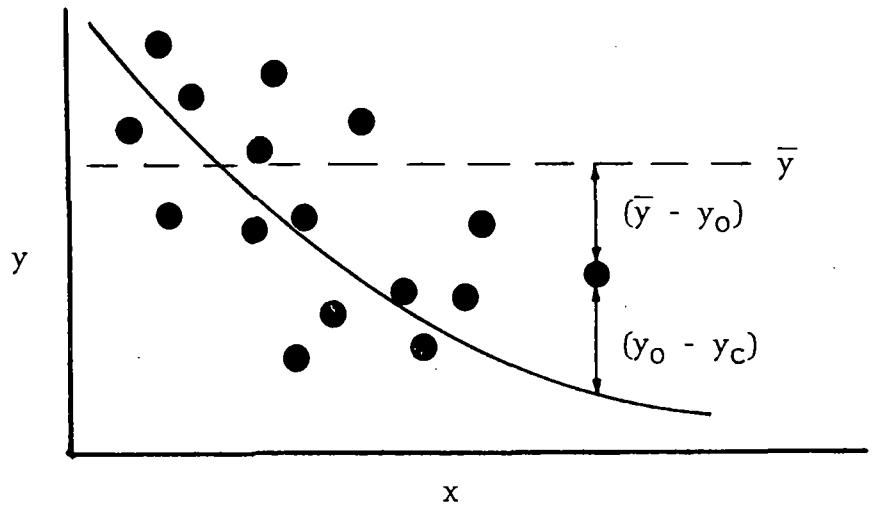

Both terms are squared to eliminate the negatives.

The second correlation factor which can be used to determine confidence bands around the data is based upon the following expression:

$$\sigma^2 = \frac{\sum_{i=1}^{N} (y_o - y_c)^2}{N - k}$$

where σ = standard deviation

N = number of data points

k = number of coefficients in the function $y_c = f(x)$

Although the meaning of this expression may not be obvious, σ is a measure of the variance or scatter in the data not rationalized by the correlation $y = f(x)$. It should be noted that if $k \geq N$, this term becomes meaningless. In other words, to obtain "true" correlations one should always obtain several more data than the number of coefficients to be used in $f(x)$.

APPENDIX C

ERROR ANALYSIS

C.1 GENERAL TECHNIQUE

Any experimental program, this one included, is subject to numerous opportunities for error. The magnitude of the errors can, of course, cloud the validity of the results being sought. Many kinds of errors are possible including instrument malfunction, human interpretation, and gross errors in technique or procedure. It is the experimentalist's task to minimize these errors by calibration and recalibration of instruments, selection of proper procedures, diligence in execution, and cross checking of measurements wherever possible. Nevertheless, errors will occur and as such it is advantageous to determine the magnitude of these potential errors so that the validity of the results can be better ascertained. In addition, this analysis helps interpret what role errors play in the observed variance of the measurement in question. The following is a discussion of the "error potential" of several of the more important measurements of this program.

The general mathematical approach used to evaluate errors is to adapt the definition of the exact differential as follows:

$$dy = \left(\frac{\delta y}{\delta x_1}\right) dx_1 + \left(\frac{\delta y}{\delta x_2}\right) dx_2 + \left(\frac{\delta y}{\delta x_3}\right) dx_3 + \ldots + \left(\frac{\delta y}{\delta x_n}\right) dx_n \qquad \text{(C-1)}$$

where: $y = f(x_1, x_2, x_3, \ldots x_n)$

and x_n are the measurements making up the calculated value of y

dx_n are the measurement errors.

The total possible error is then:

$$\Delta y \cong \left|\left(\frac{\delta y}{\delta x_1}\right) \Delta x_1\right| + \left|\left(\frac{\delta y}{\delta x_2}\right) \Delta x_2\right| + \left|\left(\frac{\delta y}{\delta x_3}\right) \Delta x_3\right| + \ldots + \left|\left(\frac{\delta y}{\delta x_n}\right) \Delta x_n\right| \qquad \text{(C-2)}$$

The maximum <u>probable</u> error is:

$$\Delta y' = \left[\left(\frac{\delta y}{\delta x_1}\right)^2 \Delta x_1^{\,2} + \left(\frac{\delta y}{\delta x_2}\right)^2 \Delta x_2^{\,2} + \left(\frac{\delta y}{\delta x_3}\right)^2 \Delta x_3^{\,2} + \ldots + \left(\frac{\delta y}{\delta x_n}\right)^2 \Delta x_n^{\,2}\right]^{1/2} \qquad \text{(C-3)}$$

Adopting either equation, C-2 or C-3, provides a convenient means for computing the magnitude of error which might arise from individual measurement error. This technique is used below along with cross check experimental procedures to assess the role of error upon the results of this test program.

C.2 GAS SAMPLING ERRORS

C.2.1 SO_2 Measurements

Errors in the SO_2 concentration determination can arise from six separate measurements, errors in the calibration factors, loss of or dilution of SO_2 in the sample line, or malfunction of the Barton Titrator. The contribution of measurement and calibration errors can be expressed as follows:

$$\frac{\Delta(SO_2)}{SO_2} = \frac{[|\Delta(CHART)| + |\Delta(BLANK)|]}{(CHART - BLANK)}_{1} + \frac{|\Delta(CELLC)|}{CELLC}_{2} + \frac{|\Delta(CONF)|}{CONF}_{3} + \frac{|\Delta(TBART)|}{TBART}_{4} + \frac{|\Delta(TGBART)|}{TGBART + 460}_{5} + \frac{|A^*\Delta(XMWDG)| + |XMWDG^*\Delta A|}{(18 + A^*XMWDG)}_{6} + \frac{|\Delta V_{BT}|}{V_{BT}}_{7} + \frac{|\Delta(XMWDG)|}{XMWDG}_{8} + \frac{\Delta PB}{PB}_{9} \quad ** \qquad \text{(C-4)}$$

where:

- CHART = Recorder output reading
- BLANK = Residual level (current leakage from titrator)
- CELLC = Cell constant (a correction factor on the calibration)
- CONF = Calibration factor, relates current output to mass of bromine generated
- TBART = Time of travel of bubble in bubble tube, sec
- TGBART = Temperature of gas in bubble tube, °F
- A = Humidity of gas in bubble tube
- XMWDG = Molecular weight of dry gas in bubble tube
- V_{BT} = Volume of bubble tube
- PB = Barometric pressure of gas at bubble tube

Terms (2) and (3) relate to the instrument calibration. When the Barton titrators were purchased, these factors were checked by the spinning syringe technique described in Section A.1.4. All of the other terms represent measurement errors. Two errors arise from assumptions which we made. First, the temperature of the gas was assumed to be constant at 70 F and secondly, the humidity was assumed to be negligible. The errors induced by these assumptions are represented by terms (5) and (6). Assuming the following variance in the measured variable as follows:

**Note the terms on the right are numbered for identification purposes.

$\Delta(TBART) = 0.5$ sec

$\Delta(TGBART) = TGBART - 70$ °F

$\Delta A = A$ lb/lb

$\Delta(XMWDG) = 0.5$ lb/lb mol

$\Delta(V_{BUB.\ TUBE}) = 0.5$ ml

$\Delta(PB) = 0.1$ "Hg

$\Delta(CHART) = 1.0$ division

$\Delta(BLANK) = 1.0$ for range = 100

1.0 for range = 30

1.0 for range = 10

2.0 for range = 3

4.0 for range = 1

The maximum probable errors due to measurement variance are depicted in Figure C.1. The major contributions are from the recording errors due to blank level uncertainty and the error due to the potential humidity effect. As a typical example, for the following set of conditions, the individual contribution can be summarized:

FIGURE C.1. BARTON SO_2 ANALYSIS ERROR POTENTIAL

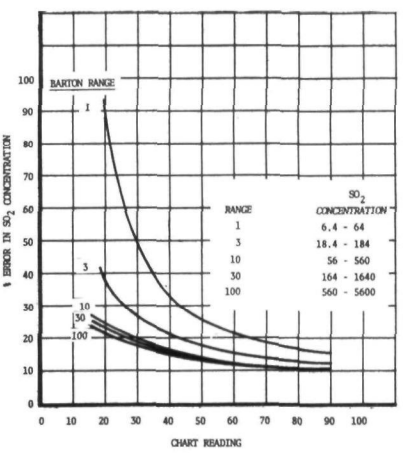

Range = 3

Blank = 4.0

TGBART = 80°F

$A = A_{SAT} = 0.023$ lb/lb

XMWDG = 30 lb/lb mol

$V_{BUB.\ TUBE} = 100$ ml

CHART = 20

PB = 30 "Hg

Error Due To:

CHART and BLANK = 18.75%

A = 3.75%

TGBART = 1.90%

TBART = 2.08%

$V_{BUB.\ TUBE} = 0.5\%$

XMWDG = 1.66%

PB = 0.33%

Max. Probable Error = $[\Sigma x_i^2]^{1/2} = 19.4\%$

The error due to calibration shift was examined experimentally by two independent means. The high concentration range (>1000 ppm) was examined by a conventional wet chemical technique described as the Reich Method in Section 3.4.2. This test was performed through the same sampling apparatus.

The results of these tests are illustrated in Figure C.2 and show the agreement to be good.

FIGURE C.2. COMPARISON BETWEEN BARTON AND REICH METHODS

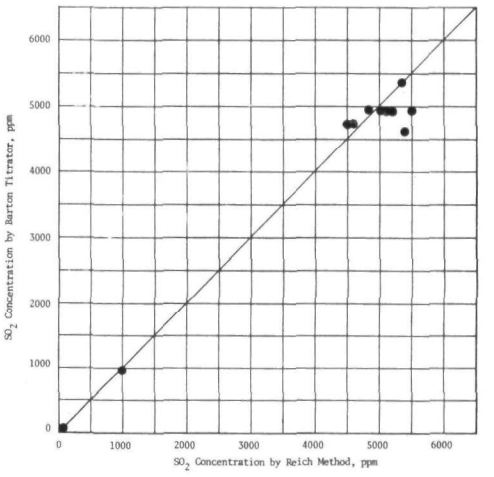

A second procedure used to check the low range of the Barton was a spinning syringe technique. This apparatus was adapted to the Barton sampling train at the pilot plant exit gas sampling location. This technique was used to assess the potential effect of the condensate traps and pumps upon the SO_2 accuracy at low concentrations.

The spinning syringe technique can be described as follows:

The syringe feeds SO_2 gas at a constant rate to the titrator. The barrel of the syringe is fitted with vanes which are spun by compressed air. The spinning of the barrel eliminates static friction between the barrel and the wall which permits uniform gas discharge. By knowing both the SO_2 gas discharge rate through a calibrated capillary tube and the air flow to the Barton Titrator, the SO_2 concentration of the gas can be accurately calculated.

The results of these tests are tabulated in Table C.1 as follows:

TABLE C.1 COMPARISON OF SO_2 CONCENTRATIONS BETWEEN BARTON AND SPINNING SYRINGE

Ma Range	ppm Calculated SO_2 (Barton)	ppm Calibrated SO_2 (Syringe)
.3	3.78	2.26
1.0	3.49	2.26
3.0	3.51	2.26
.3	0.22	0.57
1.0	0.54	0.57
3.0	0.52	0.57

These results show that the Barton response is sufficiently sensitive to detect SO_2 in the less than 10 ppm range but that excessive errors are possible in this low range. The average error at the 2.26 ppm level was +59%, and the average error at the 0.57 ppm level was -25%. It should be noted that this

is not solely a calibration error but also encompasses the measurement errors mentioned above.

Another potential interference in the SO_2 measurement is absorption of SO_2 into condensate in the sampling line between the duct and titrator. This loss can be estimated by assuming that all of the moisture in the flue gas condenses and becomes saturated with SO_2. The SO_2 absorption can be expressed as follows:

$$\frac{\Delta SO_2}{(SO_2)} = \frac{HA\left(\frac{30}{64}\right) \times 10^6}{(SO_2)} \qquad \text{(C-5)}$$

where: $H = SO_2$ solubility in liquid water, gm/gm H_2O

A = Humidity of sampled gas, gm H_2O/gm D.G.

$(SO_2) = SO_2$ concentration in flue gas, ppm

Now for a system between 70 and 90 F, the SO_2 solubility can be obtained from Perry[22]. With the appropriate units adapted and extrapolating to 10^{-6} atm, the solubility can be correlated as follows:

$$H = (9 \times 10^{-6})(SO_2)^{0.500} \qquad \text{(C-6)}$$

$$\therefore \quad \frac{\Delta(SO_2)}{(SO_2)} = (4.22)(SO_2)^{-0.5}A \qquad \text{(C-7)}$$

the humidity averaged about 0.12 lb/lb dry gas at the pilot plant exit. Therefore, condensation and absorption maximum error varied from 16.0% at 10 ppm to 1.6% at 1000 ppm.

In summary, except for gross errors such as air leakage into the sample train or depletion of hydrogen bromide in the cell, we expect that the SO_2 measurements are accurate to within 15% at the 1000 ppm range and to within 50% at the 20 ppm range. Below 20 ppm the "error potential" seems to be excessive.

C.2.2 SO_3 Error Analysis

Attempts at measuring SO_3 concentration leaving the furnace were troubled with significant variations. Whether these variations were real or the result of analytical errors is questionable. The likelihood of real variations are probable. SO_3 is believed to be formed in the furnace by both homogenous gas-phase reactions and by catalytic formation with solid constituents. In addition,

metal surface and ash deposits can have a strong affinity for SO_3. It is quite possible to have variations in the SO_3 concentration at the furnace exit even when the flow rates and temperatures seem to be relatively steady. Measured SO_3 at the furnace exit varied between 1 and 150 ppm. The degree of variance that the furnace can produce is difficult to predict. For the present, this factor is left unanswered. The potential for SO_3 variance due to analytical errors are numerous. The principal sources of error are as follow:

1. Incomplete collection of the acid mist.
2. Loss of mist in the sample probe because of low temperature.
3. Absorption of SO_3 by the probe ash filter.
4. Absorption of SO_2 and subsequent oxidation to SO_3.
5. Contamination by highly sulfated ash.
6. Catalytic oxidation within the probe.

The first three of the above effects would produce measurements lower than actual, while the final three would yield higher values. Adoption of the Goksoyr sampler eliminated (1) and (4) from the list of possibilities. The potential effects of (2) and (6) are minimized by using a heated quartz tube. While the temperature of the gas was monitored, the temperature of the probe surface was not.

Some direct measurements of SO_3 concentration leaving the particulate scrubber were attempted as described in Section 3.5. These measurements were voided because of the presence of liquid carryover from the cyclone separator into the sample tube.

The nominal concentration of SO_3 leaving the furnace ran about 18 ppm. At that level, SO_3 from the furnace would not have possessed the potential for significant effects upon the SO_2 absorber by way of the formation of undesired sulfates. Even if all of the SO_3 were to bypass the prescrubber (an unlikely occurrence) it would have amounted to less than 15% of the nominal sulfate found in the absorber liquor products. The pH of the prescrubber slurry ranging between 2.0 and 3.5 indicated that a substantial portion of the SO_3 was probably collected at that location.

Errors induced by measurement errors in the SO_3 sampling and analysis can be treated in similar fashion to the error analysis for SO_2 measurement. Combining and differentiating the equation relating SO_3 concentration to the measured variables yields the following:

$$\frac{\Delta SO_3}{SO_3} = \frac{|\Delta(MSO_3)|}{MSO_3}_1 + \frac{|\Delta T|}{T + 460}_2 + \frac{|\Delta(METCOR)|}{METCOR}_3 + \frac{|\Delta(VSO_3)|}{VSO_3}_4 + \frac{|\Delta PB| + |\Delta PS|}{(PB + PS)}_5 \qquad \text{(C-8)}$$

$$\text{But,} \quad \frac{\Delta(MSO_3)}{MSO_3}_1 = \frac{|\Delta V_R|}{V_R}_6 + \frac{|\Delta C_R|}{C_R}_7 + \frac{\Delta V_D}{V_D}_8 + \frac{\Delta V_T}{V_T}_9 + \frac{\Delta V_S}{V_S}_{10} \qquad \text{(C-9)}$$

where:
- SO_3 = Sulfur trioxide concentration, ppm
- MSO_3 = Mass of SO_3 collected, mg
- T = Gas temperature at gas meter
- $METCOR$ = Meter correction factor
- VSO_3 = Volume of gas collected during SO_3 sampling, ft^3
- V_R = Volume of reagent titrated, ml
- C_R = Conversion factor for reagent, mg $SO_4^=$/ml
- V_D = Dilution volume, ml
- V_T = Titrated volume of sample, ml
- V_S = Volume of original sample

Average values and expected maximum measurement errors for the above parameters are listed as follows:

Average Values	Maximum Expected Errors
$T = 90°F$	$\Delta T = 5°F$
$METCOR = 1.0$	$\Delta(METCOR) = 0.05$
$VSO_3 = 6.0\ ft^3$	$\Delta(VSO_3) = 0.2\ ft^3$
$PB = 29.0$ "Hg	$\Delta(PB) = 0.1$ "Hg
$PS = -18.0$ "Hg	$\Delta(PS) = 0.5$ "Hg
$V_R = 1.0$ ml	$\Delta V_R = 0.15$ ml
$C_R = 0.5$ mg $SO_4^=$/ml	$\Delta C_R = 0.01$
$V_D = 50$ ml	$\Delta V_D = 0.5$ ml
$V_T = 1$ ml	$\Delta V_T = 0.05$ ml
$V_S = 10$ ml	$\Delta V_S = 0.6$ ml

Combining these estimates gives the following:

Most probable maximum error for $\frac{\Delta MSO_3}{MSO_3} = 16.6\%$

Most probable maximum error for $\frac{\Delta SO_3}{SO_3} = 18.4\%$

This analysis reveals two factors: the first being that the dominant major measurement error arises from the deviation in the titration end point. The second conclusion is that the expected measurement errors cannot account for the large scatter in the SO_3 measurements. This means that the scatter arises either out of "real" variations or gross experimental errors such as air leakage or sample contamination.

The primary conclusions drawn from the SO_3 measurements are first that insufficient data were obtained to characterize these concentrations in terms of furnace operation (this was not a goal of the contract) and secondly, assuming that the measured nominal level was truly representative, the SO_3 could not have played a very substantial role in the formation of sulfates within the SO_2 absorbers.

C.2.3 NO_X Error Analysis

Although the Phenyldisolfonic Acid method for NO_X determination is a recognized ASTM standard, this procedure is quite tedious, time consuming, and contains a number of opportunities for experimental error. Probably, the major source for error is the chemical analysis procedure for developing the color. This involves transferring the sample from the collection flash to an evaporation dish, evaporating the sample, a filtration step, and a final dilution step. Errors made during this process are procedural and are minimized with careful technique and with experience. However, these errors are not readily subject to numerical examination.

A number of errors are possible from experimental measurements. These errors have been analyzed by the technique previously described. This analysis yields the following results:

$$\frac{\Delta NO_X}{NO_X} = 7.5\%$$

The major contributions to the 7.5% error are the uncertainty in the slope of the color absorbance curve and the uncertainty in the exact occupied volume of the collection flask.

An additional error which evidently happened on occasion was leakage of air into the evacuated collection flask either before or during the sampling

period. This probably accounts for some of the unexpectedly low NO_X values experienced on occasion.

One additional factor that should be noted is that virtually all of the potentially significant errors would tend to produce negative errors, i.e., to produce lower NO_X concentrations than the "true" value. This is important when attempting to interpret scattered NO_X data which is in fact not randomly scattered but is biased by unreal low values. It is the writer's opinion that the most nearly correct value listed in Table 4.12 for any given test is the maximum value for that test.

As a check on the PDS procedure, a prepared NO_2 gas standard was purchased and sampled. This gas contained a 900 ppm concentration of NO_2 in a nitrogen atmosphere. Three samples of this gas were analyzed with the following results:

Sample	NO_X, ppm
1	738
2	810
3	777
Avg.	775 ppm

Average error for 900 ppm = 13.9%

Average deviation from 900 ppm = 128 ppm

Two factors are worthy of note. All three samples analyzed low and secondly, the average deviation of these samples is comparable with the average deviation of the NO_X measurements reported in Table 4.11. This data confirms the trends evident in the bulk of that NO_X test.

C.2.4 Dust Loading Error Analysis

The dust loadings performed at the furnace exit and at the exit of the scrubbers were performed by different techniques. The Thorston sampling apparatus as described in Section 3.7 is a large volume high mass sampler. The potential errors with this sampler include nonrepresentative sampling because of anisokinetic effects plus a number of measurement errors. An analysis of the effect of measurement errors lead to the following net error potential:

$$\frac{\Delta(DLITH\phi)}{DLITH\phi} = 13.8\%$$

The error analysis reveals that the largest potential error arises from the deviation in the gas temperature at the flow orifice. All other measurement errors are small in comparison.

The other potential source of error here arises from possible anisokinetic sampling situations. The estimated isokinetic sampling rate error is approximately -15 to -20%. This error would tend to produce dust loadings biased slightly upwards. The magnitude of error from anisokinetic sampling can be estimated by a method described by Badzioch[23]. He relates the percentage error as follows:

$$\varepsilon = \frac{(V_S - V)}{V_S} (100)\alpha \qquad \text{(C-10)}$$

where ε = % error in dust concentration measurement

V_S = Velocity at which gas was sampled

V = The isokinetic sampling velocity

α = An inertial parameter depending upon the flow patterns around the sampling nozzle.

For normal pulverized coal flue gas, $\alpha \cong 1/2$ and therefore $\varepsilon \cong 7.5\%$ to 10%. In any event, the maximum possible value of $\alpha = 1.0$ such that the error due to anisokinetic sampling would certainly be less than 20%.

The average deviation of furnace exit dust loadings was 36%. Since the expected experimental error is probably less than 13%, the deviations are probably real. In any event, the anisokinetic error indicates that most of these dust loadings might be approximately 10% too high.

The dust loading sampling method employed at the exit of the particulate scrubber and the pilot plant exit was a mini-sampler using simple filtration in a paper thimble. This method as described in Section 3.7 differed considerably from the Thorston method. The total sample weight was around 0.01 gram, and the sampling rate at about 0.5 CFM. Primary sources of error were measurement errors with a small possibility of error from nonrepresentative sampling. Nonrepresentative sampling seems possible only if a substantial portion of the fly ash particles leaving the scrubber were larger than 4 microns. If the particle size distribution entering the particulate scrubber approximated a normal distribution for P.C. fly ash, then in order to have a substantial fraction of fly ash in the 4 micron range, the measured dust loading would have to be in error to the extent of over 1000%. This would seem very unlikely.

On the other hand, only single point, center line sampling was utilized at the particulate cyclone exit. The sampling point was located 2-1/2 pipe diameter from a flow straightener described in Section 2.6.1. One might argue that this distance is insufficient. To check this point, a pitot tube velocity profile was determined. It was reasoned that if the particle size of the ash at this point was at least nearly submicron, then the particulate concentration would not be any more maldistributed than the gas. Figure C.3 illustrates this profile which is seen to be of the normal turbulent flow shape with only a slight skewness. It was concluded from this profile and from the expected particle size distribution that nonrepresentative sampling was not a factor contributing to the error potential for the outlet dust loadings.

FIGURE C.3. VELOCITY PROFILE DOWNSTREAM OF FLOW STRAIGHTENER

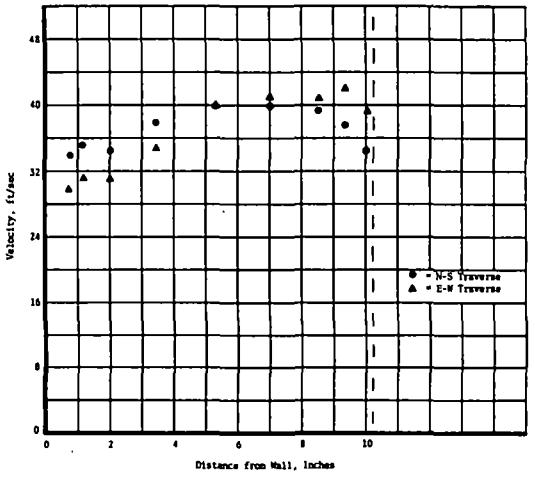

The effect of anisokinetic sampling was determined as above. For a 4-micron particle, $\alpha = 0.0224$ and the maximum deviation from isokinetic sampling rate was ∿25%. Therefore, for a 4-micron particle, the potential error would only be ∿0.56%. The value of α was determined assuming that the flow disturbance upstream of the sampling nozzle was 8 cm. This value is an extrapolation of the data presented by Badzioch. Again, the anisokinetic sampling factor is probably not significant.

Errors arising from sampling measurements were determined in the usual manner with the following results:

$$\text{Most Probable Maximum Error: } \frac{\Delta DL}{DL} = 10.6\%$$

This error is dominated almost completely by the filter weight errors.

C.3 CHEMICAL ANALYSIS ERRORS - LIQUID

C.3.1 Palmrose Analysis

The Palmrose technique for chemical analysis of the composition of the $MgO-SO_2-H_2O$ system was developed for application in the pulp and paper industry. This technique is a wet chemical method involving two titrations. Potential errors arise from sampling, titration, and premature stripping of sulfur dioxide.

Since sampling was performed with a syringe (using a #18 gauge needle), the question of whether the slurry was sampled representatively was investigated by comparing samples obtained in this manner with those obtained with a sample flask from the product spray. This test showed that the syringe did sample representatively.

Errors arising during chemical analysis involve volume error in the syringe (2-1/2 ml syringes were used) titration errors, and errors in the chemical reagents.

The maximum probable errors for each analysis are shown in Figure C.4. For the most part, these error potentials are not too significant from the standpoint of their effects upon the absorption system. Possible exceptions are the dissolved monosulfite concentration and the bisulfite concentration. Both these parameters could have significant effects upon the SO_2 absorption capability of the slurry. It was, therefore, desirable to know these concentrations with some degree of certainty.

The precision of the palmrose analysis to determine the suspended solids concentration is illustrated in Figure C.5. It is a plot of the monosulfite solids concentration determined by the Palmrose analysis against the total solids determined by filtration. This plot shows that the agreement is fairly good over the full range on a majority of the tests but that deviations are biased towards the Palmrose analysis.

C.4. MAXIMUM PROBABLE ERROR IN PALMROSE ANALYSIS

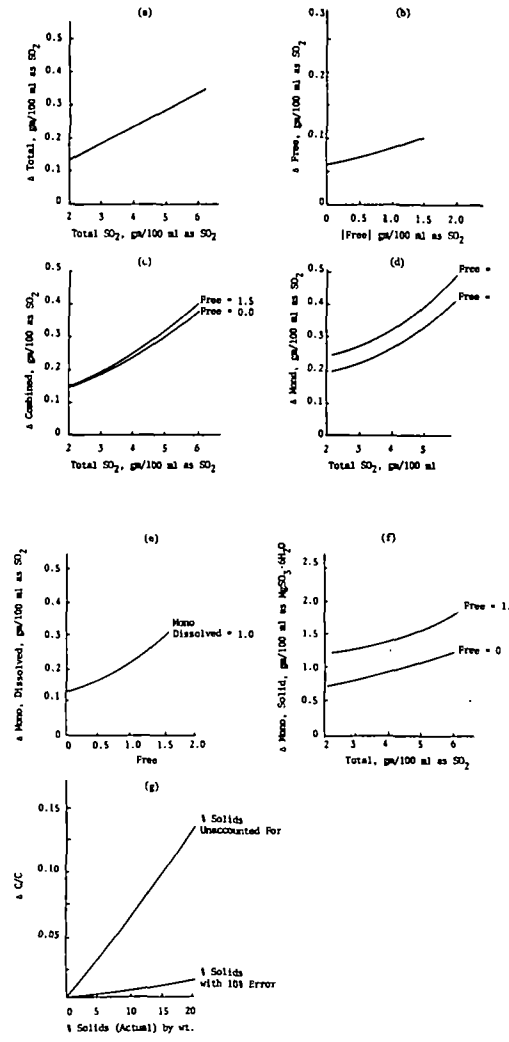

C.5. COMPARISON OF SLURRY STRENGTH BY TWO TECHNIQUES

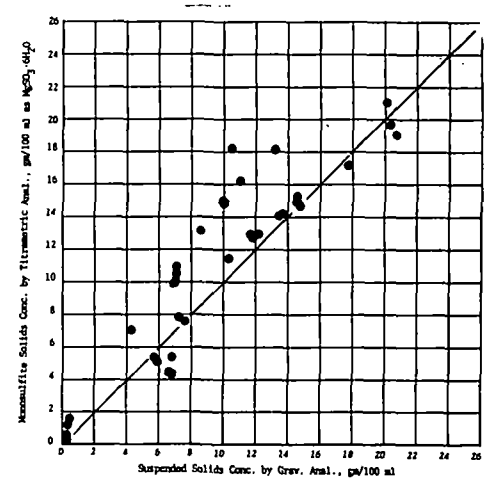

C.3.2 Sulfate Analysis Errors

The magnesium sulfate concentration was a most important measurement. The errors associated with this analysis are similar to those encountered in the SO_3 analysis with an additional source arising from potential oxidation of the 10cc slurry sample from sulfite to sulfate before analysis was completed. The maximum probable error arising from measurement deviation amounts to:

$$\frac{\Delta \text{Sulfate}}{\text{Sulfate}} = 17.05\%$$

The major contributor to this error is the vague titration endpoint. The tendency was to overtitrate, that is, to exceed the true endpoint.

As an independent check upon the sulfate analysis technique, samples were analyzed from time to time by conventional gravimetric methods. Although a qualitative comparison was exhibited, quantitative agreement was poor. This comparison is plotted in Figure C.6. On the average, the titrated sulfates are about 64% higher than the gravimetric sulfates. The 17% experimental error can explain only part of this deviation. The remainder must be due to unavoided sulfation of some of the sulfite in the titrated sample. See Section A.5 for description of titration method.

C.6. COMPARISON BETWEEN GRAVIMETRIC AND TITRAMETRIC SULFATE ANALYSES

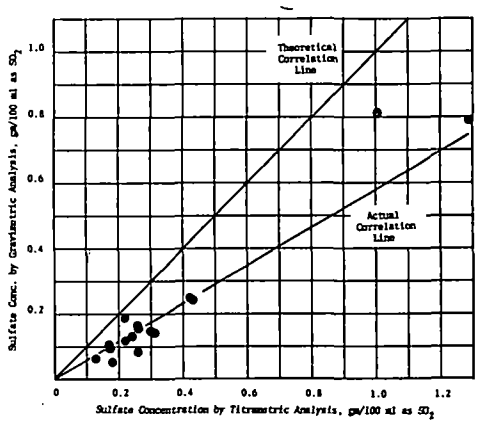

C.3.3 MgO Makeup Composition and Concentration

The concentration of the magnesia slurry whether slaked or not was determined by titration with 7 N sulfuric acid. Titration errors and representative sampling errors are the primary problems. Sampling of the slurry is a problem because the magnesia wants to settle very rapidly meaning that drawing of a representative sample into the pipette can be difficult. This was circumvented in part by cutting the capillary end off the pipette which permits rapid withdrawal of the magnesia slurry from the sample beaker. Assuming a representative sample was obtained, the maximum probable error in the magnesia concentration was:

$$\frac{\Delta(\text{XMGO})}{\text{XMGO}} = 7.2\%$$

The composition of the magnesia, i.e., the ratio of $M_g(OH)_2$ to MgO is important from the system chemistry standpoint. The method for determining the extent of

hydration of the magnesia was described in Section A.8. Errors in this analysis arise principally from the need to remove uncombined water from the sample before calcining. If all of this water is not removed, then the fraction slaked will be too high. If this drying process is too severe, some of the combined water may be released yielding fractional slaking values too low. The total maximum probable error in the magnesia conversion for a 1% error in the precalcined weight is:

$$\frac{\Delta S}{S} = 3.5\%$$

where S = The mole % magnesia converted to $Mg(OH)_2$

One final point regarding the magnesia composition is that the results indicated that preslaking was not important from an SO_2 absorption point but may have been important as a deposition consideration. As is explained in Section 5.4, even in the case of deposition, the important factor is the concentration of slowly reacting magnesia which can, if present, continue to combine with bisulfite outside of the gas-liquid contacting zone. Preslaking may or may not have a bearing on the level of this material. It may be that the magnesia used actually had a spectrum of reactivity with some very reactive material that hydrated in cold water and some relatively unreactive material which resisted efforts to preslake. What really is needed to delineate this point is an analysis method which would be sensitive enough to detect magnesia in the presence of bisulfite in the absorption slurry. If the Palmrose analysis were sufficiently accurate, it would in fact provide this information by the difference in bisulfite concentration between the filtered and unfiltered analysis. Noting Figure C.4(b), however, it is obvious that the method is not sufficiently accurate. However, an automatic titrator might be. This point was not explored.

C.4 FLOW RATE ERROR ANALYSIS

C.4.1 Coal

The feed rate of coal to the furnace was not a directly measured quantity. Rather, it was calculated based upon an assumed constant composition and upon the measured combustion air rate. It is also assumed that the combustion is complete. This last assumption will be discussed later. The assumed coal composition and the maximum expected variation in that composition are listed as follows:

	Assumed	Variation
Carbon	71.5% by weight	70 to 74%
Hydrogen	4.85%	4.5 to 5.5%
Oxygen & Nitrogen	8.17%	7 to 9%
Sulfur	3.7%	3 to 5%
Ash	7.4%	6 to 11%
Moisture	4.38%	3 to 7%
	100.00%	

Based upon the above assumptions, the coal feed rate possessed an error potential of

$$\frac{\Delta(FCOAL)}{FCOAL} = 0.10 \text{ or } 10\%$$

The major contributor to this error was not the uncertainty in the coal composition, but rather the deviation in the excess oxygen measurement.

C.4.2 Air and Flue Gas

The air to the furnace is monitored by standard ASME design orifices. The errors arising from measurements were minimal and amounted to only about 3% maximum probable error.

One air stream to the furnace however is not accounted for in the total air flow calculation. This source is the compressed air which fluidized the coal falling from the end of the screw. A rotometer indicated a constant flow of about 0.6#/min. This amounts to about 6% of the primary air and 0.6% of the total air.

The flue gas flowrate at the furnace exit was not measured but was calculated from the furnace material balance. Therefore, the deviation in this flowrate reflects the deviations in the input flows to the furnace. The only furnace input measurement which reflects a potential significant error is the combustion air flowrate. This yielded a probable error of about 3%. In addition, a condition sometime existed whereby air could leak into the furnace or duct thus diluting the flue gas. This condition existed when the static pressure at the furnace exit went strongly negative relative to the atmosphere. Normal operation called for maintaining the static pressure at this location close to neutral. However, this was not possible because at times pluggage occurred within the tube banks of the furnace cooling section. This leakage was difficult to estimate and occurred primarily around probe penetration into the furnace stack. As a check against leakage throughout the pilot plant, an Orsat analysis was

performed at various locations. These tests at no time produced any sign of air leakage.

The flue gas flowrate was measured by a standard ASME orifice in the horizontal duct between the particulate scrubber, and the gas absorber consistently indicated a gas flow about 400 to 600 pounds per hour less than the calculated flowrate at the furnace exit. This represents about a 10% difference. This difference is difficult to rationalize. The possibility of actual loss via leakage of this quantity of gas seems very unlikely. Primary opportunities for leakage include the emergency relief apparatus (See Figure 2.12) and an expansion joint. However, these sources were checked on several occasions with no leakage detected. The maximum probable error in the flowrate amounts to

$$\frac{\Delta[\text{FWDG (9)}]}{\text{FDGW (9)}} \cong 6.7\%$$

This potential error is not sufficient to account for the observed deviation. Recalling the pitot tube traverse described in Section 6.2.4, that test showed the following agreement between orifice and pilot tube traverse.

Pilot Flowrate	-	1295 ft^3/min
Orifice	-	1340 ft^3/min

This is better than 96% agreement and reduces the probability of any large errors in the orifice calibration.

The flowrate measurement at the pilot plant exit orifice indicated a flowrate consistently (400 to 600 #/hr) higher than the flowrate at the intermediate orifice (between particulate scrubber and gas absorbers as referred to above). However, good agreement was established between this orifice and the calculated dry gas flowrate at the furnace exit. A plot of this material balance is shown in Figure C.7.

Although any unbalance in flue gas flowrate is undesirable, the only really significant factor that this situation suggests is air leakage into the pilot plant and the resulting effects that might have on the sulfate formation. However, as we stated previously, upon investigation via an Orsat analysis, no leakage could be found. Thus, it is felt that the unbalance must arise from anomolies concerning the orifice location relative to bends, etc.

C.4.3 Makeup Water

The makeup water rate to all through scrubbers was established through volume displacement meters calibrated down to 0.1 gal. The makeup water which

C.7. FLUE GAS MATERIAL BALANCE

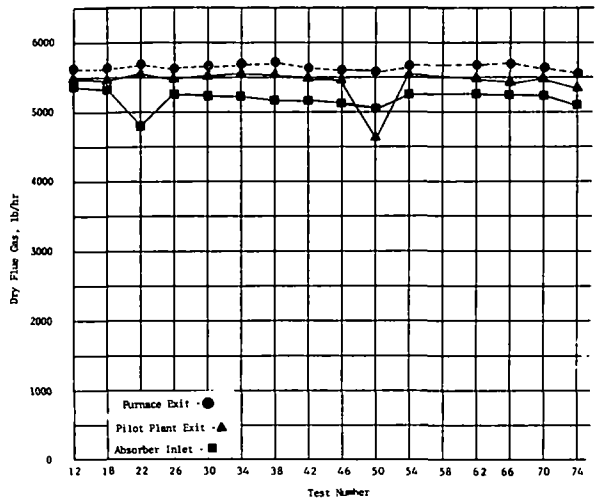

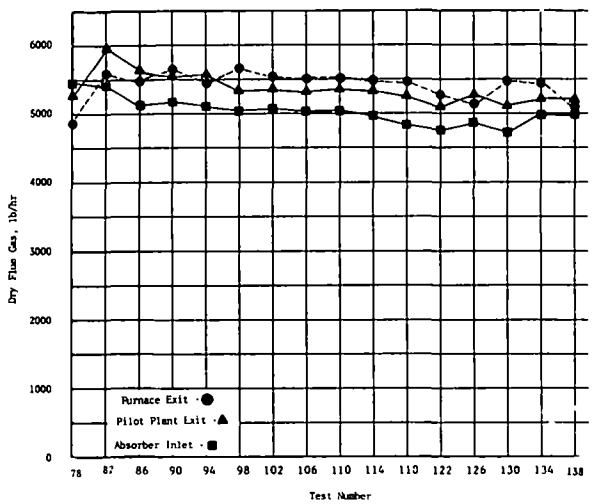

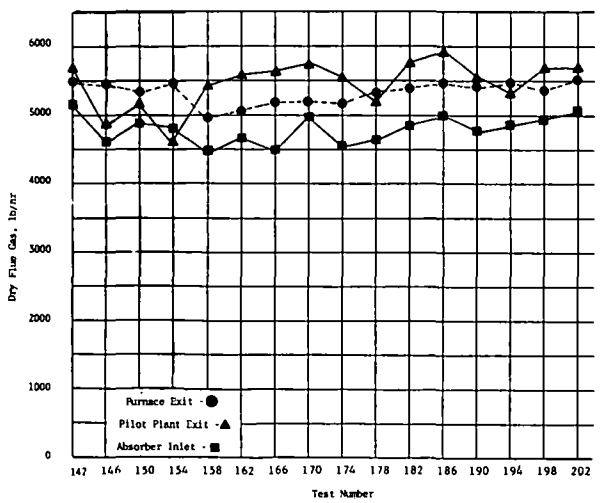

was controlled by the level controller on the scrubber sumps was therefore an unsteady flow. The average rate was established by metering the volume displaced over a period of several minutes. The degree of error in this measure was dependent upon how long the integrating period was established. The shorter the period, the greater the probable error. For the particulate scrubber, the probable maximum error was:

$$\frac{\Delta \text{Flow}}{\text{Flow}} = 0.2\% \ @ \ \Delta T = 5 \text{ min.} \quad \text{or} \quad 0.03\% \ @ \ \Delta T = 30 \text{ min.}$$

and for the gas absorbers:

$$\frac{\Delta \text{Flow}}{\text{Flow}} = 3\% \ @ \ \Delta T = 5 \text{ min.} \quad \text{or} \quad 0.5\% \ @ \ \Delta T = 30 \text{ min.}$$

C.4.4 Makeup MgO Slurry

The makeup MgO slurry was monitored by a calibrated flowrator. Although at times this flow needed careful manual control, it was normally fairly steady. The error potential of this stream is summarized as follows:

$$\frac{\Delta \text{FMGO}}{\text{FMGO}} = 0.072 \text{ or } 7.2\%$$

The major contributor is the variation in float position.

C.4.5 Venturi Absorber - FBA Product Flowrate

The method of monitoring the product flow from the SO_2 absorbers is described in Section 2.6.1 and illustrated in Figure 2.20. This system was a source of considerable error in flow measurement. The primary course of error was partial pluggage of the product nozzle. The flowrate was correlated to the nozzle pressure. Thus, as the nozzle orifice plugged, the flow was restricted but the pressure still indicated an undisturbed flow. The maximum probable error can be summarized as follows:

$$\left.\frac{\Delta \text{Flow}}{\text{Flow}}\right|_{\text{product}} \begin{array}{l} = 32.5\% \text{ with pluggage} \\ = 20\% \text{ without pluggage} \end{array}$$

The pluggage error yields an apparent flowrate higher than actual.

C.5 MATERIAL BALANCES

C.5.1 Sulfur Material Balance

The sulfur material balance variances are a reflection of all the errors involved in determining concentrations and flowrates of sulfur-containing streams. The sulfur material balance is illustrated in Figure C.8. This plot shows the total sulfur flow accounted for at the furnace inlet, leaving the furnace, and leaving the pilot plant. A good balance is evident up to test 48. From there to test 102, a large discrepancy existed between all three points. From test 102 to 128, the pilot plant exit flow continued to be in wide disagreement. From thereon, however, agreement was good. The maximum variance that would be expected at each location from measurement errors is summarized as follows:

$$\text{Furnace Input; } \frac{\Delta S}{S} = 28.8\%$$

$$\text{Furnace Exit; } \frac{\Delta S}{S} = 15.3\%$$

$$\text{Pilot Plant Exit; } \frac{\Delta S}{S} \cong 40\%$$

Examining Figure C.8, it is apparent that experimental error can account for the variance in runs 28-48 and 128-205 but not between 48 and 127. The reason for this greater variance is due to a severe pluggage condition from sulfite deposits in the product nozzle. The restriction to flow must have been higher than the 25% estimate used in calculating the expected error in the product flowrate. In fact, the sulfur balance is a good indicator in itself of the extent of deposition.

The difference between the sulfur input to and output from the furnace is a more difficult discrepancy to account for. The largest expected variances in individual measurements that can be reasonably expected cannot account for the difference evident between runs 60 and 102. The only explanation which seems plausible is as follows: During the period from about March 1 to April 1, a truck strike prevented delivery of coal to the test site. To insure continuation of the test program, coal which is stock piled in-plant was used instead. This coal was very wet (being exposed to the elements over a period of time). As such, it did not dry completely in the pulverizer. Thus, the coal lacked its usual fluidity. Therefore, when this coal was fed to the furnace, it did not disperse as well as P.C. coal normally does. The result, the

C.8. SULFUR MATERIAL BALANCE

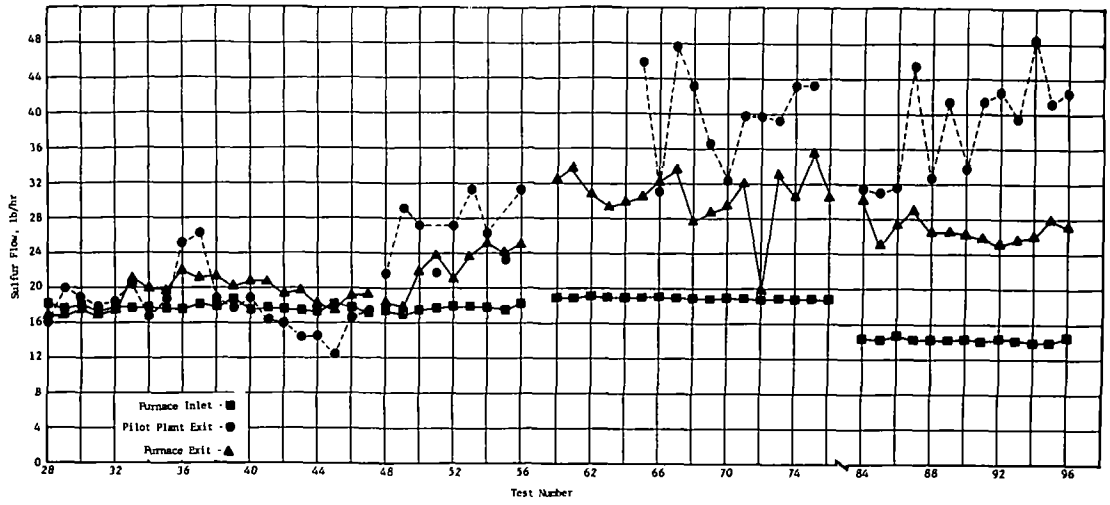

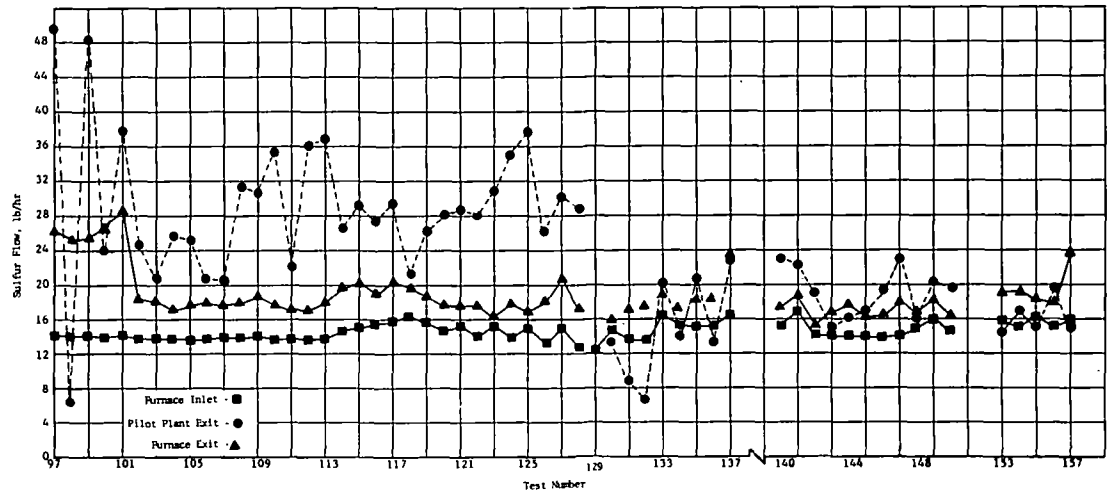

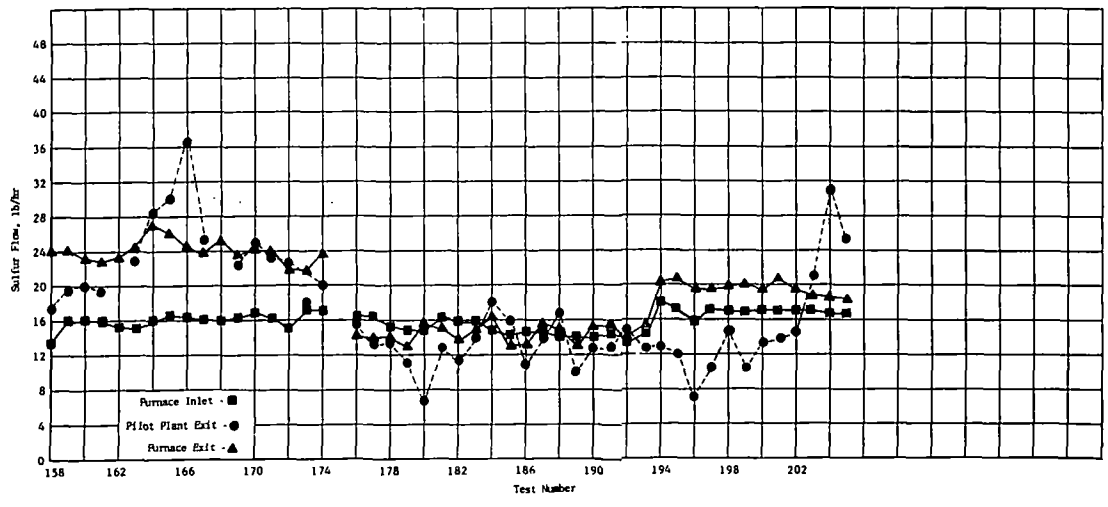

author believes, is that much of the coal fell to the furnace floor as large flakes whereupon it would slowly char liberating the more volatile sulfur constituents. In support of this hypothesis is the fact that during this period, furnace deposition was severe and rapid. The ash collected by the Thorston sampler contained as much as 20% carbon. Finally, a yellowish crystalline deposit which formed on the outer side of the P.C. hopper during this period was analyzed and found to be an iron sulfate hydrate.